8

Energy Harvesting Relaying

8.1 Introduction

8.1.1 Wireless Relaying

The relaying concept has been used in wired and wireless communications as a repeater or bridge for decades. The interest in relaying has been reignited in recent years due to the advances in electronics (Laneman et al. 2004). As such, relaying has been used in many applications recently, such as in the fourth generation (4G) standards (Hoymann et al. 2012).

A typical relaying system consists of three nodes: the source; the destination; and the relay. The source is the node that has information to deliver, the destination is the node that intends to receive this information, while the relay helps the delivery from source to destination. There are two main benefits of using a relay as an intermediate node: diversity gain; and coverage extension.

For the diversity gain, the direct link between the source and the destination still works but the relaying link provides an extra copy of the same signal at the destination. By properly combining these copies, diversity gain can be achieved to fight fading or shadowing. Thus, such a relaying system is sometimes called a distributed or virtual multiple-input-multiple-output (MIMO) system. In this case, the relay acts as a virtual antenna for the source. This increases the reliability of the system. Figure 8.1 shows a diagram of such a relaying system. There are $N + 1$ copies of the same signal available at the destination so that the destination can perform diversity combining.

For the coverage extension, the direct link between the source and the destination does not exist, due to obstacles or long transmission distances. Thus, the destination is out of the communications range of the source (Peng et al. 2011; Zhou et al. 2013a). In such a scenario, the source could increase its transmission power or deploy new infrastructure if the problem persists. However, the relay can help extend the transmission range of the source without any extra infrastructure by relaying the signal so that either the obstacle can be circumvented or the transmission distance can be reduced. This increases the capacity of the system. Figure 8.2 shows a diagram of such a relaying system. When the direct link is broken, other routes via relays can be used.

The relay could be an idle peer node in the same network. In this case, it is called peer relaying, user relaying, or mobile relaying. The relay could also be a dedicated relaying station in the network that only has the basic functions of a base station. In this case, it is called infrastructure relaying or fixed relaying. For fixed relaying, since the dedicated

Energy Harvesting Communications: Principles and Theories, First Edition. Yunfei Chen.

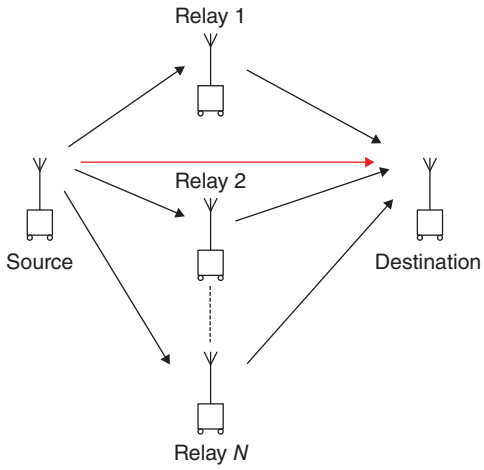

Figure 8.1 A relaying system for diversity gain.

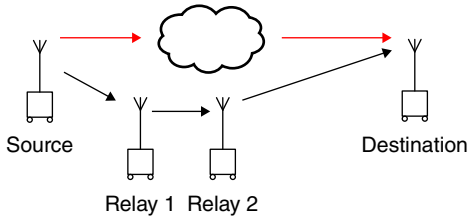

Figure 8.2 A relaying system for coverage extension.

infrastructure is shared by all nodes, it can improve the network coverage and reliability at minimal extra cost but it is not flexible. For mobile relaying, reward mechanisms must be in place to encourage idle nodes to take part in relaying. In both structures, protocols are required to complete the relaying process.

8.1.2 Relaying Protocols

There are two main protocols for relaying: amplify-and-forward (AF); and decode-and-forward (DF) (Laneman et al. 2004). In AF, the source transmits the signal to the relay and the relay simply amplifies the received signal and forwards it to the destination without any further processing. In DF, after receiving the signal from the source, the relay first decodes the signal for information and then encodes the decoded information again before forwarding it to the destination.

In terms of complexity, DF has higher complexity than AF, due to the decoding and encoding operations. In terms of performance, DF is better than AF, as DF removes the noise at the relay by performing decoding and encoding, while AF amplifies the noise along with the signal so that the received signal at the destination will be more noisy. Thus, the choice of protocol depends on the specific application that either prefers performance or simplicity.

The above protocols are also called one-way relaying, as the information is sent from the source through the relay to the destination in one direction. In this case, the transmission happens in two phases. In the first phase, the source transmits the signal to the relay, or if the direct link works to the destination too. This is called the broadcast phase.

In the second phase, the source stops transmission to avoid interference, and the relay forwards its received signal to the destination. This is called the relaying phase. Thus, the source performs one transmission, the relay performs one reception and one transmission, while the destination performs one or two receptions, depending on the existence of the direct link from the source. Compared with the direct transmission, the relaying transmission doubles the transmission time so that its data rate is only half that of the direct transmission.

To remedy the data rate issue, two-way relaying can be used. In two-way relaying, the source and the destination transmit their signals to the relay at the same time in the broadcast phase. The relay will receive a combined copy of both signals and forward the combined copy to both source and destination in the relaying phase. Since simultaneous transmission is performed, the data rate is the same as that of the direct transmission. The self-interference in the received signals at both source and destination can be removed, as they know their own transmitted signals. There is also multi-way relaying, where more than two nodes transmit their signals at the same time. Both two-way relaying and multi-way relaying belong to a wider topic of network coding. Also, the above protocols assume that the same frequency band is used during different time slots to achieve orthogonal channels. One may also achieve the orthogonality in the frequency or code domains.

8.1.3 Energy Harvesting Relaying

From the above discussion, the relay node has to use its own power and spectrum resources to deliver the information for the source. This may be acceptable for infrastructure relaying but may discourage peer nodes from participating in mobile relaying, as they will have a shorter battery life by helping others. Thus, this issue needs to be solved.

Energy harvesting is a promising solution to this problem. In energy harvesting relaying, instead of asking the relay to use its own energy, the source node transfers a certain amount of energy to the relay node as wireless power first. The relay node then uses the harvested wireless power to forward the source signal to the destination. This minimizes the extra energy cost incurred at the relay and therefore this technique holds great potential.

In a wider sense, energy harvesting relaying not only refers to the system where the source transfers energy to the relay for signal forwarding but also refers to the relaying systems where any nodes perform energy harvesting. Similar to energy harvesting cognitive radio (CR), there are also different types of energy harvesting relaying systems. For example, the relay in the above scheme harvests energy from the source. In other schemes, the relay can harvest energy from the ambient energy source or from a dedicated power transmitter or even from its own transmission. The source node can also harvest energy from the ambient energy source, from a dedicated power transmitter or from the relay.

Similar to energy harvesting CRs, energy harvesting relaying needs to satisfy the energy causality constraint. Additionally, relaying needs to satisfy the signal causality constraint that the signal forwarded by the relay must be received from the source first. Next, we will first discuss conventional relaying.

8.2 Conventional Relaying

In this section, we will first discuss AF and DF in more detail. Then, several important performance metrics are examined to measure the reliability or the capacity of a relaying system. Finally, when multiple relays are available, relay selection will be investigated. Two-way relaying will also be discussed.

8.2.1 Amplify-and-Forward Relaying

Assume that all the nodes have a single antenna and operate in the half-duplex mode. The transmission is completed in two phases. In the first broadcast phase, the source sends signals to the relay. In the second relaying phase, the relay forwards the received signal to the destination. Assume that the total transmission is T seconds and that there is no direct link between the source and the destination. The case with multiple links, including a direct link, will be discussed in Section 8.2.4.

In the first $\frac{T}{2}$ seconds, the received signal at the relay is

$$y_r = \sqrt{P_s}hs + n_r \tag{8.1}$$

where P_s is the transmission power of the source, h is the channel gain from the source to the relay, s is the transmitted information symbol with unit power $E\{|s|^2\} = 1$, and n_r is the additive white Gaussian noise (AWGN) at the relay. The fading gain h is a complex circularly symmetric Gaussian random variable with mean zero and variance $2\alpha^2$, and the noise n_r is also Gaussian with mean zero and variance $2\sigma^2$.

In the second $\frac{T}{2}$ seconds, the signal in (8.1) is simply amplified and then forwarded to the destination so that the received signal at the destination is

$$y_d = \sqrt{P_r}agy_r + n_d \tag{8.2}$$

where P_r is the transmission power of the relay, a is the amplification factor that will be discussed later, g is the channel gain from the relay to the destination, y_r is the signal forwarded, and n_d is the AWGN at the destination. Similarly, g and n_d are complex Gaussian random variables with mean zero and variance $2\alpha^2$ and $2\sigma^2$, respectively. From (8.2), the transmission power consumed by the relay is $P_r a^2 E\{|y_r|^2\}$.

The choice of the amplification factor is very important, as it determines the amplification at the relay and affects the overall performance of relaying. In Laneman et al. (2004), the amplification factor is chosen as

$$a^2 = \frac{1}{E\{|y_r|^2\}} = \frac{1}{P_s|h|^2 + 2\sigma^2} \tag{8.3}$$

to normalize the power of the received signal at the relay. As one sees, if a satisfies (8.3), $a^2 E\{|y_r|^2\} = 1$ such that the transmission power consumed by the relay becomes P_r. Since the value of a depends on the channel gain h and h varies as a random variable, one must adjust the value of a for each relaying transmission. This is called variable-gain AF. In some studies, it is also called the channel-assisted AF (Amarasuriya et al. 2011). This is the most widely used amplification factor in the literature and will be the focus of our discussion.

For variable-gain AF, one must have the knowledge of h and $2\sigma^2$ in order to calculate the amplification factor for relaying. The noise variance does not change fast and can be

estimated accurately. In channels with strong signals, $2\sigma^2$ may be negligible so that the amplification factor is given by

$$a^2 = \frac{1}{P_s|h|^2} \tag{8.4}$$

This is sometimes called ideal channel-assisted or inverting AF, as the relay always inverts the channel gain from the source to the relay (Hasna and Alouini 2003).

In both (8.3) and (8.4), the channel gain h has to be estimated for the relay. Thus, disintegrated channel estimation must be performed for variable-gain AF (Khan et al. 2012). This channel estimation incurs extra complexity at the relay. A solution to this problem is to use the average of the amplification gain in (8.3). In this case, one has

$$a^2 = E\left\{\frac{1}{P_s|h|^2 + 2\sigma^2}\right\}. \tag{8.5}$$

This average will only depend on the noise variance $2\sigma^2$ and the fading channel parameters. Thus, it is a fixed value for a homogeneous environment. This is called fixed-gain relaying.

8.2.2 Decode-and-Forward Relaying

Similar assumptions can be made for DF. In this case, the received signal at the relay is still given by (8.1) in the broadcast phase. Once the relay receives this signal, it tries to decode it. For example, if binary phase shift keying (BPSK) is used such that $s = 1$ or $s = -1$ with equal probabilities, the data decision is made as

$$\hat{s} = \begin{cases} 1, & Re\{y_r h^*\} > 0 \\ -1 & Re\{y_r h^*\} < 0 \end{cases} \tag{8.6}$$

where $Re\{y_r h^*\}$ is the decision device that multiplies the received signal y_r with the conjugate of the channel gain h and takes the real part of the product for decision. For other modulation schemes, similar decision devices can be applied to the received signal.

In the relaying phase, the decoded information $\hat{s}$ is encoded again and forwarded to the destination so that the received signal at the destination is

$$y_d = \sqrt{P_r} g\hat{s} + n_d \tag{8.7}$$

where all the symbols are defined as before. Since $\hat{s} = -1$ or $\hat{s} = 1$, one sees that the noise at the relay n_r will not appear in the received signal at the destination, unlike AF relaying. Thus, DF has a better performance than AF.

There are other variants of DF. For example, instead of decoding and encoding the signal from the source, the relay can first use the signal-to-noise ratio (SNR) in the first hop to decide if the received signal in (8.1) is of good quality. If it is, the relay will perform decoding, encoding, and then forwarding. If the SNR of the signal in (8.1) is below a threshold, an outage occurs such that the relay does not do anything. The quality check at the relay prevents the error in the first hop from propagating to the next hop. This is termed as incremental relaying in some references.

There are also other relaying protocols. For example, instead of forwarding the whole signal y_r, the relay can forward a quantized version of this signal. This is particularly useful in digital communications systems, where the signal will be quantized anyway. This is

termed quantize-and-forward relaying. Also, if the received signal at the relay is sparse, it can be compressed before being forwarded. This is termed compress-and-forward relaying. These relaying protocols are useful in different applications but in general are not as widely used as AF and DF.

8.2.3 Performance Metrics

Next, we define several performance metrics that are commonly used in relaying systems to measure their performances.

8.2.3.1 Amplify-and-Forward

For AF, using (8.1) and (8.2), one has

$$y_d = \sqrt{P_r}ag(\sqrt{P_s}hs + n_r) + n_d = \sqrt{P_rP_s}aghs + \sqrt{P_r}agn_r + n_d. \tag{8.8}$$

The first term is the signal part, while the last two terms are the noise parts. One sees that the noise at the relay n_r has also been amplified to make y_d more noisy. This is the disadvantage of AF relaying. From (8.8), the end-to-end SNR or the overall SNR can be derived as

$$\gamma = \frac{P_rP_sa^2|g|^2|h|^2}{2\sigma^2P_ra^2|g|^2 + 2\sigma^2} \tag{8.9}$$

If the variable gain in (8.3) is used, the overall SNR can be rewritten as

$$\gamma = \frac{\gamma_r\gamma_d}{\gamma_r + \gamma_d + 1} \tag{8.10}$$

where $\gamma_r = \frac{P_s|h|^2}{2\sigma^2}$ is the SNR of the first hop from the source to the relay and $\gamma_d = \frac{P_r|g|^2}{2\sigma^2}$ is the SNR of the second hop from the relay to the destination. The overall SNR is determined by the weaker hop. For example, when γ_d is much smaller than γ_r, $\gamma \approx \gamma_d$, and when γ_r is much smaller than γ_d, $\gamma \approx \gamma_r$. The exact result in (8.10) is not mathematically tractable in many design problems. Hence, approximations can be used. One such approximation is

$$\gamma \approx \frac{\gamma_r\gamma_d}{\gamma_r + \gamma_d} \tag{8.11}$$

when the ideal channel-assisted AF is used or when the SNR is very large so that $\gamma_r + \gamma_d + 1 \approx \gamma_r + \gamma_d$. This is called the harmonic mean (Hasna and Alouini 2004). Other approximations are also possible, for example, by choosing the maximum or the minimum of γ_r and γ_d. They are not discussed here as they are less frequently used.

Using the end-to-end SNR, we can define the probability of power outage or the outage probability as

$$P_o(\gamma_0) = Pr\{\gamma < \gamma_0\} = F_\gamma(\gamma_0) \tag{8.12}$$

where γ_0 is the threshold SNR below which the receiver at the destination cannot detect any signal, and $F_\gamma(\cdot)$ is the cumulative distribution function (CDF) of γ. Thus, the outage probability is essentially the value of the CDF of γ at γ_0.

Also, using the end-to-end SNR, the error rates for different modulation schemes can be derived (Simon and Alouini 2005). For example, for M-ary square quadrature

amplitude modulation, the symbol error rate is

$$P_e(\gamma) = 4\frac{\sqrt{M}-1}{\sqrt{M}}Q\left(\sqrt{\frac{3\gamma}{M-1}}\right) - 4\left(\frac{\sqrt{M}-1}{\sqrt{M}}\right)^2 Q^2\left(\sqrt{\frac{3\gamma}{M-1}}\right) \tag{8.13}$$

and for M-ary phase shift keying,

$$P_e(\gamma) = \frac{1}{\pi}\int_0^{(M-1)\pi/M} e^{-\gamma\frac{\sin^2(\pi/M)}{\sin^2\theta}}d\theta \tag{8.14}$$

where M is the constellation size, and $Q(\cdot)$ is the Gaussian Q function. In all cases, the error rate is a function of the end-to-end SNR. Since γ is random, the average error rate is calculated as

$$\bar{P}_e = \int_0^\infty P_e(x)f_\gamma(x)dx \tag{8.15}$$

where $f_\gamma(x)$ is the probability density function (PDF) of γ.

The above two measures, outage and error rate, determine the reliability of the relaying communications system. Next, we define the achievable rate or the capacity of the system. For delay-tolerant applications, the achievable rate can vary. Thus, from the Shannon's limit, one has

$$R(\gamma) = \frac{1}{2}\log_2(1+\gamma) \tag{8.16}$$

where $\frac{1}{2}$ takes the rate penalty of relaying into account. The average or ergodic capacity in a fading channel is given by

$$\bar{R} = \int_0^\infty R(x)f_\gamma(x)dx. \tag{8.17}$$

In other applications, delay is constrained so that the data rate must be larger than a certain value R_0. In this case, using (8.16), one has

$$R(\gamma) = \frac{1}{2}\log_2(1+\gamma) \geq R_0. \tag{8.18}$$

This gives $\gamma \geq 2^{2R_0} - 1$. Thus, the achievable rate in delay-constrained applications is given by

$$R = \frac{R_0}{2}[1 - P_o(2^{2R_0} - 1)] \tag{8.19}$$

where the outage probability P_o is given in (8.15).

8.2.3.2 Decode-and-Forward

For DF, we cannot define the end-to-end SNR in the same way as for AF but we can derive the equivalent end-to-end SNR. We start from the hop performances. From (8.1) and (8.7), the achievable rates of the source-to-relay link and the relay-to-destination link are (Nasir et al. 2014)

$$R_r = \log_2(1+\gamma_r) \tag{8.20}$$

and

$$R_d = \log_2(1+\gamma_d) \tag{8.21}$$

respectively. However, the rates on both sides of the relay must be balanced. If R_r is larger than R_d, a buffer will be required at the relay. Without a buffer, some data have to be discarded. Similarly, if R_d is larger than R_r, a rate outage occurs, as the relay does not have enough data to forward. Thus, the overall rate of the relaying link is the minimum of R_r and R_d, given by

$$R(\gamma) = \frac{1}{2}\min\{R_r, R_d\} = \frac{1}{2}\log_2(1 + \min\{\gamma_r, \gamma_d\}) = \frac{1}{2}\log_2(1 + \gamma) \tag{8.22}$$

where γ is the equivalent end-to-end SNR for DF in terms of rate given by

$$\gamma = \min\{\gamma_r, \gamma_d\} \tag{8.23}$$

and $\frac{1}{2}$ again takes the rate penalty of relaying into account.

For the error rate, the end-to-end SNR is not straightforward to obtain either. We only consider the case when BPSK is used. In this case, the error rate in the source-to-relay link is given by

$$P_e^r(\gamma_r) = Q(\sqrt{2\gamma_r}) \tag{8.24}$$

and the error rate in the relay-to-destination link is given by

$$P_e^d(\gamma_d) = Q(\sqrt{2\gamma_d}) \tag{8.25}$$

where $Q(\cdot)$ is the Gaussian Q function defined as before. The overall error rate of the relaying link from the source to the relay and then to the destination is given by

$$P_e(\gamma) = P_e^r(\gamma_r)[1 - P_e^d(\gamma_d)] + P_e^d(\gamma_d)[1 - P_e^r(\gamma_r)] \tag{8.26}$$

as the bit error only occurs when there is an error either in the source-to-relay link or in the relay-to-destination link, but not in both links. Thus, the equivalent end-to-end SNR γ can be found by solving the following equation

$$Q(\sqrt{2\gamma}) = Q(\sqrt{2\gamma_r})[1 - Q(\sqrt{2\gamma_d})] + Q(\sqrt{2\gamma_d})[1 - Q(\sqrt{2\gamma_r})] \tag{8.27}$$

for γ. This is a non-linear equation and is generally difficult to solve. It has been reported in Wang et al. (2007) that

$$\min\{\gamma_r, \gamma_d\} - 1.62 \leq \gamma \leq \min\{\gamma_r, \gamma_d\}. \tag{8.28}$$

When the hop SNRs are much larger than 1.62, roughly, the equivalent end-to-end SNR can be approximated as $\gamma \approx \min\{\gamma_r, \gamma_d\}$, which is the same as that from the achievable rate in (8.23). Figure 8.3 examines the accuracy of this approximation. One sees that when both γ_d and γ_r are small, there is some noticeable difference between the accurate bit error rate (BER) and the approximated BER. However, when γ_r is larger than 4 dB, this difference is negligible. For other modulation schemes, the equivalent end-to-end SNR can also be derived by solving $P_e(\gamma) = P_e^r(\gamma_r)[1 - P_e^d(\gamma_d)] + P_e^d(\gamma_d)[1 - P_e^r(\gamma_r)]$ but this is not a trivial problem.

In summary, the end-to-end SNR for DF is not as straightforward as that for AF but one may use (8.23) as either an exact result for achievable rate or an approximate result for error rate. Using this end-to-end SNR, the outage probability for DF can also be defined as

$$P_o(\gamma_0) = Pr\{\gamma < \gamma_0\} = F_\gamma(\gamma_0) \tag{8.29}$$

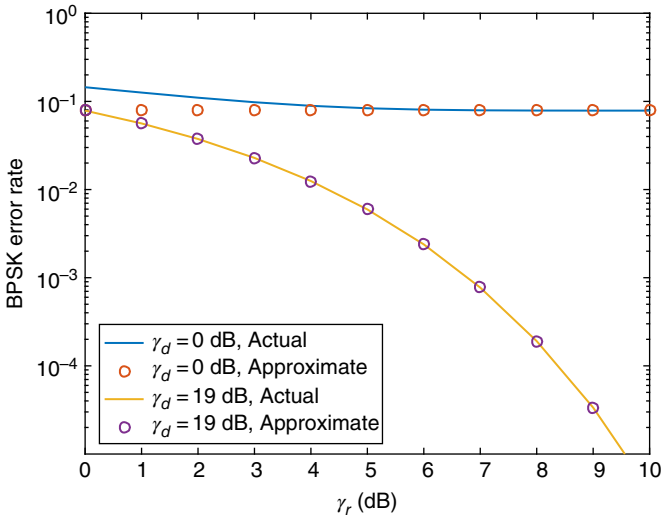

Figure 8.3 Accuracy of the equivalent end-to-end SNR for the BER of DF.

where $F_\gamma(\cdot)$ is the CDF of γ. Using (8.23), it can be derived that

$$F_\gamma(\gamma_0) = 1 - [1 - F_{\gamma_r}(\gamma_0)][1 - F_{\gamma_d}(\gamma_0)] \tag{8.30}$$

where $F_{\gamma_r}(\cdot)$ and $F_{\gamma_d}(\cdot)$ are the CDFs of γ_r and γ_d, respectively.

Also, for delay-constrained applications when the data rate must be larger than a threshold R_0, the achievable rate can be shown as

$$R = \frac{1}{2} R_0 [1 - P_o(2^{2R_0} - 1)]. \tag{8.31}$$

Finally, γ in (8.23) is also a random variable. Its CDF is given by

$$F_\gamma(x) = 1 - [1 - F_{\gamma_r}(x)][1 - F_{\gamma_d}(x)]. \tag{8.32}$$

The average error rate is given by

$$\bar{P}_e = \int_0^\infty P_e(x) f_\gamma(x) dx \tag{8.33}$$

and the average achievable rate or ergodic capacity is given by

$$\bar{R} = \int_0^\infty R(x) f_\gamma(x) dx \tag{8.34}$$

where $f_\gamma(x) = \frac{dF_\gamma(x)}{dx}$ is the PDF of γ.

Figure 8.4 compares the ergodic capacities of AF and DF, where $\bar{\gamma}_r$ and $\bar{\gamma}_d$ are the average hop SNRs and Rayleigh fading is used. One sees that DF always has a higher capacity than AF. The performance metrics discussed above will be used in the following discussion.

8.2.4 Relay Selection

In the previous discussion, we have assumed that there is only one relaying node and that the direct link between the source and the destination is broken, in order to focus on

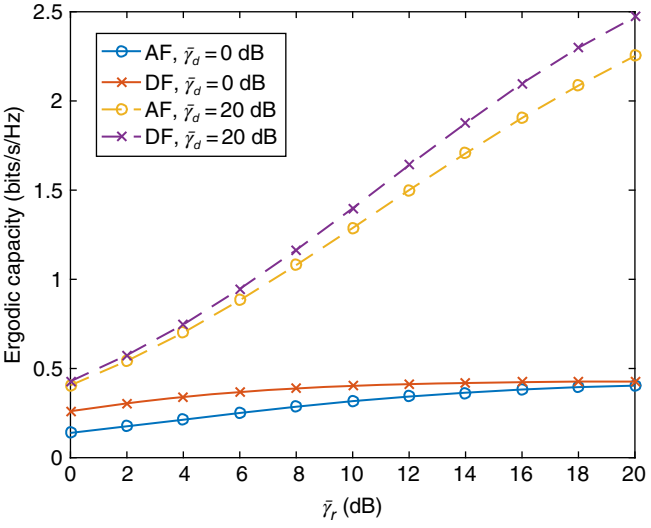

Figure 8.4 Comparison of ergodic capacities for AF and DF.

the relaying process from the source to the relay and then to the destination. In practical communications systems, the direct link may still work. Also, several peer nodes might be idle at the same time so that multiple relays are available. Consequently, the signal from the source can arrive at the destination through different routes. At the destination, all these copies can be coherently combined to achieve high diversity gain. However, the complexity of such a network increases with the number of relays. In some applications, such as wireless sensor networks, complexity is more of a concern than performance. In these applications, to reduce the network complexity, relay selection can be implemented that often chooses one out of all available links for the best tradeoff between complexity and performance.

It has been reported in Jing and Jafarkhani (2009) that, with properly designed schemes, the diversity order of relay selection is the same as the combination of all available links. Several relay selection schemes can be used. We use AF as an example. Consider an AF relaying system with one source, one destination, and N relays. Similarly, a two-phase transmission is assumed. In the first phase, the source broadcasts its signal to all the relays such that the received signal at the nth relay can be expressed as

$$y_{nr} = h_n\sqrt{P_s}s + w_n \tag{8.35}$$

where $n = 1, 2, \cdots, N$ is the relay index, h_n is the complex fading gain in the channel between the source and the nth relay, P_s is the transmission power of the source, s is the transmitted symbol with unit power, and w_n is the AWGN at the nth relay with variance $2\sigma^2$. In the second phase, the received signals at the relays are amplified and forwarded such that the received signal from the nth relay at the destination is

$$y_{nd} = \sqrt{P_{nr}}a_n g_n y_{nr} + z_n \tag{8.36}$$

where P_{nr} is the transmission power of the nth relay, g_n is the complex fading gain in the channel from the nth relay to the destination, $a_n = \sqrt{\frac{1}{P_s|h_n|^2+2\sigma^2}}$ is the amplification

factor, and z_n is the complex Gaussian noise in the channel between the nth relay and the destination with the noise power $2\sigma^2$.

The end-to-end SNR of the nth relaying link can be shown as

$$\gamma_n = \frac{\gamma_{rn}\gamma_{dn}}{\gamma_{rn} + \gamma_{dn} + 1} \tag{8.37}$$

where $\gamma_{rn} = \frac{P_s|h_n|^2}{2\sigma^2}$ and $\gamma_{dn} = \frac{P_{nr}|g_n|^2}{2\sigma^2}$ are the instantaneous SNRs of the first hop and the second hop, respectively.

8.2.4.1 Full Selection

In the full selection scheme, the relay is selected according to

$$\hat{n} = \max_{n=1,2,\cdots,N} \{\gamma_n\} \tag{8.38}$$

that is, the relay that can provide the largest end-to-end SNR is selected. This is intuitively the best, because the achievable rate increases with the end-to-end SNR, while the error rate decreases with the end-to-end SNR. Thus, the largest end-to-end SNR will lead to the largest data rate or the smallest error rate. Denote this scheme as the $\max\{\gamma_n\}$ scheme.

For the full selection, the error rate can be derived as $P_e = \int_0^\infty P_e(x) dF_{\gamma_{\hat{n}}}(x)$, where $P_e(x)$ is the conditional error rate, conditioned on $\gamma_{\hat{n}}$, and $F_{\gamma_{\hat{n}}}(x) = F^N_{\gamma_n}(x)$ is the CDF of $\gamma_{\hat{n}}$ with $F_{\gamma_n}(x)$ given in Tsiftsis et al. (2006) for Nakagami-m fading channels.

8.2.4.2 Partial Selection

The performance of the full selection scheme should be the best, as it maximizes the end-to-end SNR. However, this means that, in order to make this selection, the source requires knowledge of the channel state information of both the source-to-relay link and the relay-to-destination link for all relays. This may incur a huge amount of overhead. To reduce this overhead, partial relay selection can be performed by using the hop SNR instead. For example, one can choose the link with the largest first hop SNR as

$$\hat{n} = \max_{n=1,2,\cdots,N} \{\gamma_{rn}\}. \tag{8.39}$$

In this case, only the channel state information of the first hops is required for selection. Denote this scheme as the $\max\{\gamma_{rn}\}$ scheme. This scheme reduces the complexity of relaying greatly. The error rate in this case is given by $P_e = \int_0^\infty P_e(x) dF_{\gamma_{\hat{n}}}(x)$, where $F_{\gamma_{\hat{n}}}(x)$ is the CDF of $\gamma_{\hat{n}}$ given by Chen et al. (2011a)

Another partial selection scheme is to choose the relaying link with the strongest second-hop SNR as

$$\hat{n} = \max_{n=1,2,\cdots,N} \{\gamma_{dn}\}. \tag{8.40}$$

Denote this scheme as the $\max\{\gamma_{dn}\}$ scheme. Its probability of error can be derived in a similar way and is given by Chen et al. (2011a).

The above two partial selection schemes use the hop SNRs for selection. This requires channel estimators for h_n or g_n or both, $n = 1, 2, \cdots, N$. To remove this complexity in the relaying system, it is also possible to use the received signal amplitude for selection directly. Thus, two other partial selection schemes are

$$\hat{n} = \max_{n=1,2,\cdots,N} \{|y_{nr}|\} \tag{8.41}$$

and

$$\hat{n} = \max_{n=1,2,\cdots,N} \{|y_{nd}|\}. \tag{8.42}$$

denoted as the $\max\{|y_{nr}|\}$ scheme and the $\max\{|y_{nd}|\}$ scheme, respectively.

The selection of the relaying link is made at the base station in a centralized network or at the group leader in a distributed network. The decision will be broadcast by the base station or the group leader to the source, the destination and all the relays before relaying. Thus, although there are N links, when the relaying starts, only one relaying link will be active and the relaying process is still the same as the two-phase transmission discussed before. On the other hand, if one wants to use all available relays, in order to avoid interference in the relaying phase, the relays have to forward their signals one by one, to achieve orthogonality in the time domain causing significant delay. This is another advantage of performing relay selection.

Next, we compare the performances of these schemes. In the comparison, BPSK is used. Also, consider Rayleigh fading channels with unit average fading power and unit noise power, while $UE = \frac{P_m}{P_s}$, which is also the ratio of $E\{\gamma_{nr}\}$ to $E\{\gamma_{nd}\}$. Figure 8.5 compares different relay selection schemes when $N = 2$ and $UE = 0.1$. One sees that the $\max\{\gamma_n\}$ scheme performs the best, as expected, as it uses the SNRs in both hops. Among the partial selection schemes, the $\max\{\gamma_{nd}\}$ and $\max\{|y_{nd}|\}$ schemes outperform the $\max\{\gamma_{nr}\}$ and $\max\{|y_{nr}|\}$ schemes. For example, at a BER of 10^{-2}, the $\max\{\gamma_{nd}\}$ and $\max\{|y_{nd}|\}$ schemes have performance gains of around 5 dB. Comparing the partial selection schemes, one sees that the $\max\{|y_{nd}|\}$ scheme performs the best. Its performance is indistinguishable from the performance of the full selection $\max\{\gamma_n\}$ scheme when the SNR is less than 20 dB. Figure 8.6 compares them when $N = 2$ and $UE = 10$. In this case, the $\max\{\gamma_{nr}\}$ and $\max\{|y_{nr}|\}$ schemes outperform the $\max\{\gamma_{nd}\}$ and $\max\{|y_{nd}|\}$ schemes. Among the partial selection schemes, the $\max\{|y_{nr}|\}$ scheme performs the best. One concludes that one should choose the best idle node for

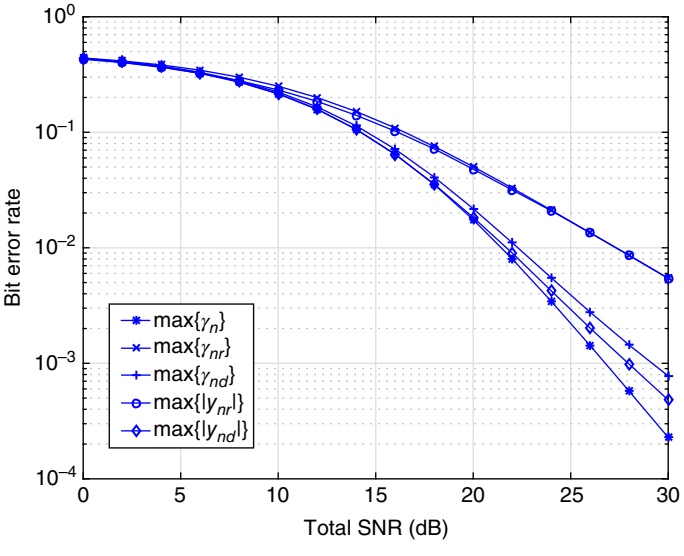

Figure 8.5 Different relay selection schemes when $N = 2$ and $UE = 0.1$.

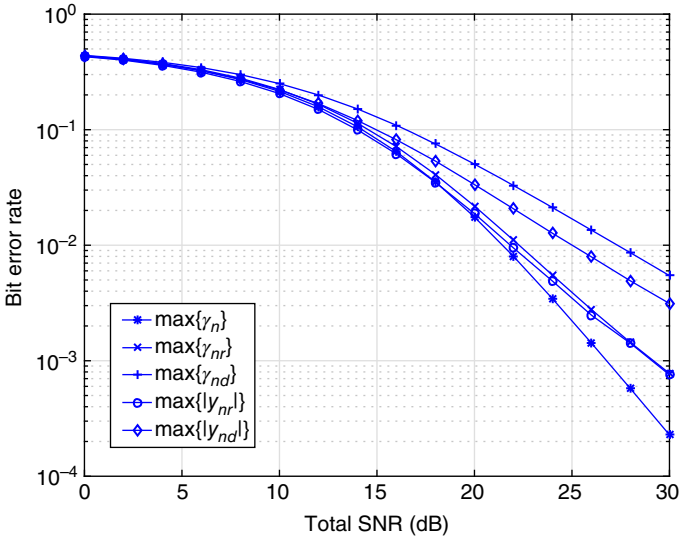

Figure 8.6 Different relay selection schemes when $N = 2$ and $UE = 10$.

the hop with smaller average SNR in order to achieve the best BER performance in partial selection.

8.2.5 Two-Way Relaying

Next, we discuss two-way relaying that was mentioned before. Both AF and DF in the previous discussion perform one-way relaying, where the source transmits data to the destination through the relay in one direction. In this scheme, the data rate is only half of that of the direct transmission, as the source has to stop for $\frac{T}{2}$ seconds to avoid interference. On the other hand, in two-way relaying, the source node and the destination node have data to exchange so that they transmit to the relay at the same time in the same channel to maintain the data rate. Figure 8.7 shows the frame structure and a diagram of two-way relaying.

In two-way relaying, there are also two phases. In the multiple-access phase, both the source node and the destination node send their data to the relaying node. In the broadcasting phase, the relaying node sends its received signal to both source and destination.

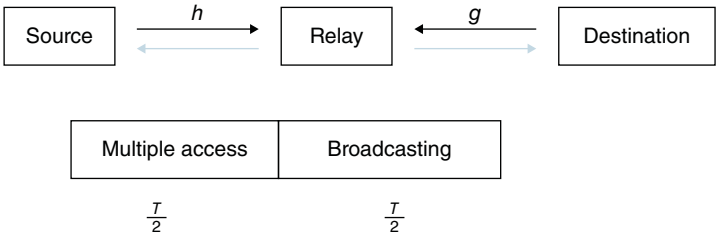

Figure 8.7 Diagram of two-way relaying.

Thus, in the multiple-access phase of the first $\frac{T}{2}$ seconds, the received signal at the relay can be given by

$$y_r = \sqrt{P_2}hs_1 + \sqrt{P_1}gs_2 + n_r \tag{8.43}$$

where P_1 and P_2 are the transmission power of the source node and the destination node, respectively, h and g are the fading channel gains from the source node and the destination node, respectively, and s_1 and s_2 are the transmitted symbols of the source node and the destination node, respectively, and they follow BPSK modulation in this case, while n_r is the AWGN defined as before. In this case, the symbols s_1 and s_2 are mixed in one received signal.

In the broadcasting phase of the second $\frac{T}{2}$ seconds, if AF is used, the relay simply amplifies the received signal and broadcasts it to both source and destination. Use the source node as an example. The received signal at the source node is given by

$$y_{d1} = \sqrt{P_r}ahy_r + n_d \tag{8.44}$$

where P_r, a, and h are transmission power, the amplification factor, and the channel gain from relay to source, respectively. In this equation, we have assumed channel reciprocity. Thus, one has

$$y_{d1} = \sqrt{P_rP_1}ah^2s_1 + \sqrt{P_rP_2}aghs_2 + \sqrt{P_r}ahn_r + n_d. \tag{8.45}$$

In this equation, the first term is the self-interference caused by the transmission of the source's own signal s_1, the second term is the desired signal from the destination node that needs to be decoded, and the last two terms are the noise. Before decoding, the self-interference will be removed, as s_1 is known to the source node. Assuming perfect removal, that is, the first source knows a and h perfectly, one has

$$y'_{d1} = y_{d1} - \sqrt{P_rP_{s1}}ah^2s_1 = \sqrt{P_rP_{s2}}aghs_2 + \sqrt{P_r}ahn_r + n_d \tag{8.46}$$

which is then used to decode s_2 from the destination node. Similar operations will be performed at the destination node to decode the information from the source node.

If DF is used, the relay tries to decode s_1 and s_2 using its received signal. This is usually difficult as s_1 and s_2 are mixed in the same received signal. However, when the two channels from the source and the destination are not balanced, or one is stronger than the other, decoding can still be performed. In this case, the received signal is used to decode the signal from the stronger node, while treating the signal from the other node as interference. After this decoding, the signal from the stronger node will be subtracted from the received signal to decode the signal from the weaker node. Assume that the signal from the source node is the stronger one. One has

$$\hat{s}_1 = \begin{cases} 1, & Re\{y_rh^*\} > 0 \\ -1 & Re\{y_rh^*\} < 0 \end{cases} \tag{8.47}$$

where y_r is the received signal at the relay. Then, to decode the signal from the weaker node, one has

$$\hat{s}_2 = \begin{cases} 1, & Re\{y'_rg^*\} > 0 \\ -1 & Re\{y'_rg^*\} < 0 \end{cases} \tag{8.48}$$

where

$$y'_r = y_r - \sqrt{P_1}h\hat{s}_1. \tag{8.49}$$

Once $\hat{s}_1$ and $\hat{s}_2$ are available, the relay forms a function of $x = \hat{s}_1 \bigoplus \hat{s}_2$ using network coding and then broadcasts it to both source and destination. The received signal at the source node is

$$y_{d1} = \sqrt{P_r} h x + n_d \tag{8.50}$$

This signal will be used to decode x and the effect of the self symbol s_1 can be easily removed by performing $\hat{x} \bigoplus s_1$, where $\hat{x}$ is the decoded symbol of x.

In one-way relaying, one symbol s is transmitted during T seconds, as the source has to stop transmission in the second $\frac{T}{2}$ seconds to avoid interference. On the other hand, in two-way relaying, two symbols s_1 and s_2 are transmitted during T seconds, using simultaneous transmission and network coding. Thus, two-way relaying has the same data rate as the direct transmission from source to destination.

The above two-way relaying is also called bi-directional relaying and it has to be combined with network coding for effective operation. As one can see from the above discussion, the success of this relaying protocol depends on accurate knowledge of all channel state information at all nodes, and the relay also consumes more power than that in one-way relaying. In the following, we only focus on one-way relaying.

8.3 Types of Energy Harvesting Relaying

From this section on, we focus on energy harvesting relaying. In general, energy harvesting relaying is different from conventional relaying in that at least one of the nodes in the relaying process harvests energy from either an ambient source, the other nodes, or a dedicated power transmitter. There are different types of energy harvesting relaying. For example, one can categorize them based on the relaying protocols: energy harvesting AF relaying; and energy harvesting DF relaying. One can also categorize them based on the energy harvesting methods: time switching energy harvesting relaying; and power splitting energy harvesting relaying.

We categorize different energy harvesting relaying systems based on the energy source, as the energy source has more fundamental impact than the relaying protocol or energy harvesting method on the relaying system designs. For example, if the relay harvests energy from the source, the source has to either increase its transmission power or increase its frame length for power transfer. If the relay harvests energy from the ambient source, the energy causality constraint applies such that the relay must accumulate enough energy before forwarding the signal. In all cases, either the energy causality constraint or the signal causality constraint or both need to be considered in the optimization of one of the performance metrics discussed in Section 8.2.3.

In some energy harvesting relaying systems, both the source and the relay harvest energy from the ambient sources, such as in Huang et al. (2013), Minasian et al. (2014), and Orhan and Erkip (2015). This is the most general case. In this case, optimal scheduling or power allocation algorithms can be formulated, as the energy arrival rate varies and hence the transmission time and power should be adapted to it. For example, in Minasian et al. (2014), assuming that both source and relay harvest energies from the ambient source, the optimal transmission policy was designed to maximize the achievable rate. The energy causality was considered in the optimization, along with the constraint on a finite battery. In Orhan and Erkip (2015) the optimal transmission

policy was also obtained by maximizing the achievable rates of four different setups with respect to the transmission power of the source and the transmission power of the relay. In this optimization, both energy and signal causality constraints were accounted for. The battery has an infinite size but the buffer at the relay is finite so that overflow must be dealt with. In Huang et al. (2013) a similar optimization problem that maximizes the achievable rate over the transmission power of the source and the relay was formulated but the energy arrival follows a deterministic model with known arrival time and amount. Also, in Moradian and Ashtiani (2015), the relay has a fixed power supply as well as harvesting energy from the ambient source, while in Kashef and Ephremides (2016) the data traffic or the data arrival were studied along with the energy arrival in the optimization.

In some energy harvesting relaying systems, the source harvests energy from the ambient source, while the relay does not harvest (Luo et al. 2013). In this case, the relay could be an infrastructure relay and the randomness in the energy availability comes from the source. For example, in Luo et al. (2013) the throughput and the transmission time were optimized with respect to the transmission power of the source and the relay. They are adaptive to the energy harvested by the source. The problem is similar to that in Minasian et al. (2014) and Orhan and Erkip (2015) and other studies due to the randomness of the energy at the source, but it is simpler due to the fixed power at the relay.

In some energy harvesting systems, unlike Luo et al. (2013), the source does not harvest, while the relay harvests energy from the ambient source (Medepally and Mehta 2010; Qian et al. 2016). Then, the randomness in the energy availability comes from the relay, not from the source. One can also optimize the transmission policy in terms of transmission time and transmission power for the relay. Again, the energy causality, the battery size and the buffer size at the relay will affect the design problem.

In some energy harvesting relaying systems, both the source and the relay harvest energy from the hybrid access point (HAP) during its power transmission (Chen et al. 2015). The difference between this system and the HAP wireless powered system discussed in Chapter 6 is that, in this system, the uplink information delivery is completed via a relaying process, while in Chapter 6, it is a direct transmission to the HAP. A similar system was also considered in Liang et al. (2017). In another energy harvesting system, both the source and the relay harvest energy from the power beacon (Zhong et al. 2015b). These systems are similar to the wireless powered systems discussed in Chapter 6, except that the direct transmission there has been replaced by a relaying transmission. In another variant, the relay harvests energy from the HAP and uses this energy to forward signals from the user equipment to the HAP or from the HAP to the user equipment (Hwang et al. 2017; Ramezani and Jamalipour 2017). The source does not harvest in this case. In these problems, energy causality is often not a problem as there is dedicated wireless power supply.

In another interesting study, the relay first harvests energy from the source for relay transmission but during the relay transmission, the source also harvests energy from the relay for extra energy (Chen et al. 2017c). This is possible if the source and the relay are peer nodes of similar transmission power. This is part of a wider topic on energy self-recycling for the full-duplex node (Hwang et al. 2017) or for the whole network (Xie et al. 2017).

In most energy harvesting relaying systems, however, the relay node harvests energy from the source node and the source node has a fixed power supply (Nasir et al. 2013) as

Table 8.1 Energy harvesting relaying systems with different energy sources.

Reference	Source energy	Relay energy
Minasian et al. (2014)	Ambient environment	Ambient environment
Luo et al. (2013)	Ambient environment	Fixed supply
Qian et al. (2016)	Fixed supply	Ambient environment
Chen et al. (2015)	HAP	HAP
Zhong et al. (2015b)	PB	PB
Hwang et al. (2017)	Fixed supply	HAP
Chen et al. (2017c)	Relay node	Source node
Nasir et al. (2013)	Fixed supply	Source node

HAP, hybrid access point; PB, power beacon.

this removes the relay's concern on its battery life and therefore encourages idle nodes to participate in relaying.

Table 8.1 summarizes the different energy harvesting relaying systems based on their energy sources. These references are meant to be examples, not an exhaustive list of all the relevant studies. Also, in the literature, there are other terms, such as wireless powered relaying, relaying with wireless energy harvesting or radio frequency (RF) energy harvesting, and so on. In the following, we will mainly use some examples to discuss the system where both source and relay harvest energy from the ambient environment, the system where both source and relay harvest energy from a dedicated power transmitter, and the system where the relay harvests energy from the source only.

8.4 From the Ambient Environment

Figure 8.8 shows a diagram of the energy harvesting system where both source and relay harvest energy from the ambient environment. In this case, the energy uncertainty appears at both the source and the relay. Thus, energy causality must be considered for both the source and the relay. We aim to find the optimum transmission power that maximizes the achievable rate.

Consider AF. The instantaneous achievable rate for one relaying transmission with a duration of T is given by (8.16). Over a time horizon of N relaying transmissions, the total achievable rate is

$$R = \frac{1}{2}\sum_{i=1}^{N}\log_2\left[1+\frac{\gamma_r(i)\gamma_d(i)}{\gamma_r(i)+\gamma_d(i)+1}\right] \tag{8.51}$$

where

$$\gamma_r(i) = \frac{P_s(i)|h(i)|^2}{2\sigma^2} \tag{8.52}$$

$$\gamma_d(i) = \frac{P_r(i)|g(i)|^2}{2\sigma^2}. \tag{8.53}$$

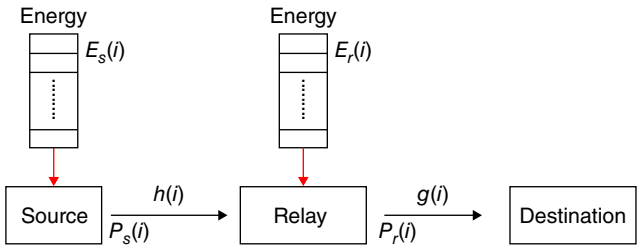

Figure 8.8 Both source and relay harvest energy from the ambient environment.

In these equations, $P_s(i)$, $h(i)$, $P_r(i)$, and $g(i)$ represent the transmission power of the source, the channel gain from the source to the relay, the transmission power of the relay, and the channel gain from the relay to the destination, respectively, during the ith transmission. This assumes a block fading channel.

We are going to optimize $P_s(i)$ and $P_r(i)$ for $i = 1, 2, \cdots, N$ to maximize R. This means that the data rate during each transmission varies due to the changes in the transmission power. There is no direct link between the source and the destination. It is quite easy to extend the results to the case with direct link by replacing the end-to-end SNR in (8.51) with the overall SNR using either relay selection or combination. For example, if relay selection is used and the direct link has a channel gain of $f(i)$, $\frac{\gamma_r(i)\gamma_d(i)}{\gamma_r(i)+\gamma_d(i)+1}$ can be replaced by $\max\left\{\frac{P_s(i)|f(i)|^2}{2\sigma^2}, \frac{\gamma_r(i)\gamma_d(i)}{\gamma_r(i)+\gamma_d(i)+1}\right\}$. If relay combination is used, $\frac{\gamma_r(i)\gamma_d(i)}{\gamma_r(i)+\gamma_d(i)+1}$ can be replaced by $\frac{P_s(i)|f(i)|^2}{2\sigma^2} + \frac{\gamma_r(i)\gamma_d(i)}{\gamma_r(i)+\gamma_d(i)+1}$. Other derivations are similar.

The source harvests $E_s(i)$ energy from the ambient environment at the beginning of the ith transmission. The relay harvests $E_r(i)$ energy from the ambient environment at the beginning of the ith transmission. Also, at the beginning of the ith transmission, the source has $S_s(i)$ energy in the battery and the relay has $S_r(i)$ energy in the battery. The battery has a finite size of S_{max} at both the source and the relay. The buffer size at the relay is infinite. This implies that the relay can always take as much data from the source as needed without any overflow. Putting all the conditions together, one has the optimization problem as

$$\max_{\mathbf{P_s},\mathbf{P_r}} R \tag{8.54}$$

$$T\sum_{i=1}^{k} P_s(i) \le \sum_{i=1}^{k} E_s(i),\ k = 1, 2, \cdots, N, \tag{8.55}$$

$$T\sum_{i=1}^{k} P_r(i) \le \sum_{i=1}^{k} E_r(i),\ k = 1, 2, \cdots, N, \tag{8.56}$$

$$\sum_{i=1}^{k+1} E_s(i) - T\sum_{i=1}^{k} P_s(i) \le S_{max},\ k = 1, 2, \cdots, N-1, \tag{8.57}$$

$$\sum_{i=1}^{k+1} E_r(i) - T\sum_{i=1}^{k} P_r(i) \le S_{max},\ k = 1, 2, \cdots, N-1, \tag{8.58}$$

$$P_s(i) \ge 0, P_r(i) \ge 0,\ i = 1, 2, \cdots, N \tag{8.59}$$

where $\mathbf{P_s} = [P_s(1)P_s(2)\cdots P_s(N)]$ and $\mathbf{P_r} = [P_r(1)P_r(2)\cdots P_r(N)]$. The first two constraints in (8.55) and (8.56) come from the energy causality that the consumed energy

must be smaller than the harvested energy. If the source or the relay do not harvest, one of these two constraints can be removed to have another optimization problem. The second two constraints in (8.57) and (8.58) come from the limited capacity of the battery. However, they are not necessary, as the battery overflow will not affect the transmission.

One sees from (8.54) that all of $E_s(i)$, $E_r(i)$, $h(i)$, and $g(i)$, $i = 1, 2, \cdots, N$, need to be known in order to calculate the optimum values. This knowledge is not causal, as the values for $i = k+1, k+2, \cdots, N$ are not available in the kth transmission. Thus, the optimization must be performed offline. For online optimization, one must remove or replace values of $E_s(i)$, $E_r(i)$, $h(i)$, and $g(i)$ for $i > k$ during the ith transmission.

To solve the optimization in (8.54), a two-step iterative procedure can be used. In the first step during the first iteration, $\mathbf{P_r} = \left[\frac{E_r(1)}{T} \frac{E_r(2)}{T} \cdots \frac{E_r(N)}{T}\right]$ can be assigned as initial values to optimize $\mathbf{P_s}$ only as

$$\max_{\mathbf{P_s}} R \tag{8.60}$$

$$T \sum_{i=1}^{k} P_s(i) \leq \sum_{i=1}^{k} E_s(i), \ k = 1, 2, \cdots, N, \tag{8.61}$$

$$\sum_{i=1}^{k+1} E_s(i) - T \sum_{i=1}^{k} P_s(i) \leq S_{max}, \ k = 1, 2, \cdots, N-1, \tag{8.62}$$

$$P_s(i) \geq 0, \ i = 1, 2, \cdots, N. \tag{8.63}$$

The optimized $\mathbf{P_s}$ can then be used in the second step to optimize $\mathbf{P_r}$ only as

$$\max_{\mathbf{P_r}} R \tag{8.64}$$

$$T \sum_{i=1}^{k} P_r(i) \leq \sum_{i=1}^{k} E_r(i), \ k = 1, 2, \cdots, N, \tag{8.65}$$

$$\sum_{i=1}^{k+1} E_r(i) - T \sum_{i=1}^{k} P_r(i) \leq S_{max}, \ k = 1, 2, \cdots, N-1, \tag{8.66}$$

$$P_r(i) \geq 0, \ i = 1, 2, \cdots, N. \tag{8.67}$$

Then another iteration starts where the first step uses the value of $\mathbf{P_r}$ from (8.64). The iteration stops when the achievable rate using the optimized values of $\mathbf{P_s}$ and $\mathbf{P_r}$ does not change above an accuracy threshold. This process converges, but sometimes not to a global optima. It was shown in Minasian et al. (2014) that performance gains can be achieved by using the proposed optimization. More details can be found in Minasian et al. (2014).

The above optimization problem does not consider the signal causality. When there is not enough data buffer at the relay, this constraint needs to be considered. In this case, the optimization problem in (8.54) can be modified as

$$\max_{\mathbf{P_s}, \mathbf{P_r}} R \tag{8.68}$$

$$T \sum_{i=1}^{k} P_s(i) \leq \sum_{i=1}^{k} E_s(i), \ k = 1, 2, \cdots, N, \tag{8.69}$$

$$T \sum_{i=1}^{k} P_r(i) \leq \sum_{i=1}^{k} E_r(i), \ k = 1, 2, \cdots, N, \tag{8.70}$$

$$\sum_{i=1}^{k+1} E_s(i) - T\sum_{i=1}^{k} P_s(i) \le S_{max},\ k = 1, 2, \cdots, N-1, \tag{8.71}$$

$$\sum_{i=1}^{k+1} E_r(i) - T\sum_{i=1}^{k} P_r(i) \le S_{max},\ k = 1, 2, \cdots, N-1, \tag{8.72}$$

$$P_s(i) \ge 0, P_r(i) \ge 0,\ i = 1, 2, \cdots, N \tag{8.73}$$

$$\sum_{i=1}^{k} \log_2[1+\gamma_r(i)] \le \sum_{i=1}^{k} \log_2[1+\gamma_d(i)],\ k = 1, 2, \cdots, N, \tag{8.74}$$

$$\sum_{i=1}^{k} \log_2[1+\gamma_r(i)] - \sum_{i=1}^{k} \log_2[1+\gamma_d(i)] \le B_{max},\ k = 1, 2, \cdots, N \tag{8.75}$$

where (8.74) is the new constraint on the signal causality, that is, the amount of data forwarded by the relay to the destination cannot be larger than the amount of data received by the relay from the source. Also, (8.75) is a constraint on the buffer size at the relay, that is, the extra data from the source cannot be larger than the capacity of the buffer B_{max}.

The optimization in (8.68) is also an offline optimization. It can be solved by using a similar two-step iterative procedure as in Minasian et al. (2014). Several special cases can be obtained. If the source node does not harvest, the constraints on the source node (8.69) and (8.71) can be dropped. This corresponds to the case discussed in Medepally and Mehta (2010) and Qian et al. (2016). If the relay node does not harvest, the constraints on the relay node (8.70) and (8.72) can be dropped. This corresponds to the case discussed in Luo et al. (2013). In all these cases, if the battery and the buffer are large enough, the optimization can be simplified as

$$\max_{\mathbf{P_s},\mathbf{P_r}} R \tag{8.76}$$

$$T\sum_{i=1}^{k} P_s(i) \le \sum_{i=1}^{k} E_s(i),\ k = 1, 2, \cdots, N, \tag{8.77}$$

$$T\sum_{i=1}^{k} P_r(i) \le \sum_{i=1}^{k} E_r(i),\ k = 1, 2, \cdots, N, \tag{8.78}$$

$$P_s(i) \ge 0, P_r(i) \ge 0,\ i = 1, 2, \cdots, N \tag{8.79}$$

$$\sum_{i=1}^{k} \log_2[1+\gamma_r(i)] \le \sum_{i=1}^{k} \log_2[1+\gamma_d(i)],\ k = 1, 2, \cdots, N \tag{8.80}$$

where only the energy causality and the signal causality need to be considered.

One can also consider the DF case by replacing R with (8.22). It is not discussed here. In Orhan and Erkip (2015), the transmission time has also been optimized. Instead of using a fixed time duration of T, they proposed to adjust the time duration as t_i for the ith transmission and optimize them. This makes the optimization more complicated. In all these optimizations, the amount of harvested energy $E_s(i)$ and $E_r(i)$ needs to be known at both the source and the relay. This is the deterministic model discussed in Chapter 3. However, they can also be random values that follow the stochastic models

discussed in Chapter 3. In this case, since the optimized transmission power is a function of the harvested energy, the optimized transmission power is also random and needs to be adjusted from transmission to transmission. To overcome this problem, one may use the average constraints or the outage constraints in the optimization.

8.5 From the Power Transmitter

In this case, both the source and the relay harvest energy from a dedicated power transmitter. Since the energy is supplied as wireless power by the dedicated power transmitter, the uncertainty in the energy supply has been greatly reduced. In this case, the time allocation between power transfer and information delivery is more important, similar to the discussion in Chapter 6.

8.5.1 One User and Single Antenna

We start from the simplest case with one user and a single antenna. Figure 8.9 shows a diagram of the considered system. In this case, the signal is sent from the source to the relay and then to the HAP. Assume that the direct link is broken due to obstacles. In this case, there is a HAP, a user terminal and a relay node in the network. All nodes work in the half-duplex mode. In the downlink, the HAP transmits power for τT seconds so that the relay and the user terminal can harvest this signal for energy. The user terminal and the relay rely completely on the harvested energy without any other energy source. After harvesting the energy, in the next $\frac{1-\tau}{2}T$ seconds, the user terminal uses the harvested energy to send the signal to the HAP and the relay in the uplink. In this case, the user terminal is the source, and the HAP is the destination. In the last $\frac{1-\tau}{2}T$ seconds, the relay uses the harvested energy to forward the signal to the HAP using AF.

One sees that this system is similar to the HAP wireless powered system discussed in Chapter 6, except that the signal is now relayed via two hops. Following similar procedures to those in Section 6.4, the harvested energy at the relay and at the source can be given by

$$E_r = \eta_r P_a |h_r|^2 \tau \tag{8.81}$$

and

$$E_s = \eta_s P_a |h_s|^2 \tau \tag{8.82}$$

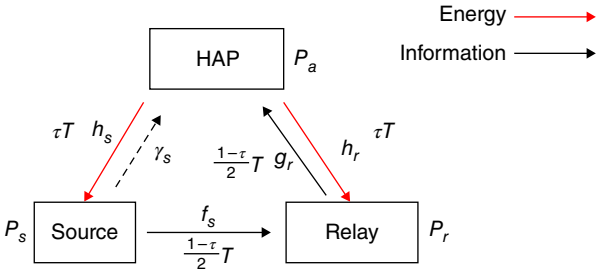

Figure 8.9 Both source and relay harvest from a dedicated power transmitter with one user.

where η_r and η_s are the conversion efficiencies of the harvesters at the relay and the source, respectively, P_a is the transmission power of the HAP, h_r is the channel gain from the HAP to the relay, h_s is the channel gain from the HAP to the source, and $T = 1$ has been assumed for convenience. Using them, the transmission power at the relay and the source can be derived as

$$P_r = \frac{E_r}{(1-\tau)/2} = \frac{2\eta_r \tau}{1-\tau} P_a |h_r|^2 \tag{8.83}$$

and

$$P_s = \frac{E_s}{(1-\tau)/2} = \frac{2\eta_s \tau}{1-\tau} P_a |h_s|^2 \tag{8.84}$$

respectively. Thus, from Section 8.2.3, one has the hop SNRs as

$$\gamma_r = \frac{P_s |f_s|^2}{2\sigma^2} = \frac{2\eta_s \tau}{(1-\tau)2\sigma^2} |f_s|^2 P_a |h_s|^2 \tag{8.85}$$

and

$$\gamma_d = \frac{P_r |g_r|^2}{2\sigma^2} = \frac{2\eta_r \tau}{(1-\tau)2\sigma^2} P_a |h_r|^2 |g_r|^2 \tag{8.86}$$

where f_s is the channel gain from the source to the relay and g_r is the channel gain from the relay to the HAP. Thus, if only the relaying link is used, the achievable rate at the HAP in the uplink is given by

$$\begin{aligned} R &= \frac{1-\tau}{2} \log_2 \left(1 + \frac{\gamma_r \gamma_d}{\gamma_r + \gamma_d + 1} \right) \\ &= \frac{1-\tau}{2} \log_2 \left[1 + \frac{\frac{2\eta_s \tau}{(1-\tau)2\sigma^2} |f_s|^2 P_a |h_s|^2 \frac{2\eta_r \tau}{(1-\tau)2\sigma^2} P_a |h_r|^2 |g_r|^2}{\frac{2\eta_s \tau}{(1-\tau)2\sigma^2} |f_s|^2 P_a |h_s|^2 + \frac{2\eta_r \tau}{(1-\tau)2\sigma^2} P_a |h_r|^2 |g_r|^2 + 1} \right]. \end{aligned} \tag{8.87}$$

Thus, the optimization problem is

$$\max_{\tau} \{R\} \tag{8.88}$$

$$0 \le \tau \le 1. \tag{8.89}$$

Figure 8.10 shows R versus τ. For simplicity, we set $\eta_r = \eta_s = 0.5$, and $f_s = h_s = h_r = g_r = 2\sigma^2 = 1$. As expected, the rate first increases and then decreases when τ increases. An optimum value of τ exists that maximizes the rate. The rate also increases with P_a. A single-variable equation can also be obtained by taking the first-order derivative of R with respect to τ and then solving the equation for the optimum τ.

The above result assumes that only the relaying link is used. If the direct link from the source to the HAP exists with a SNR of γ_s and is also used, one can either perform relay selection or combination. In the case when relay selection is used, the performance was obtained and optimized in Chen et al. (2015).

8.5.2 Multiple Users and Single Antenna

Next, we consider the more practical case when multiple user terminals exist. Figure 8.11 shows a diagram of the considered system. In this case, relays and sources form pairs.

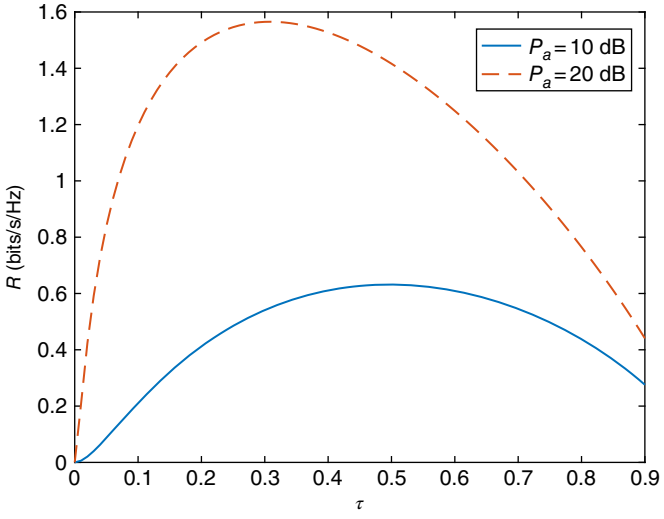

Figure 8.10 R versus τ.

Figure 8.11 Both source and relay harvest from a dedicated power transmitter with multiple users and multiple relays.

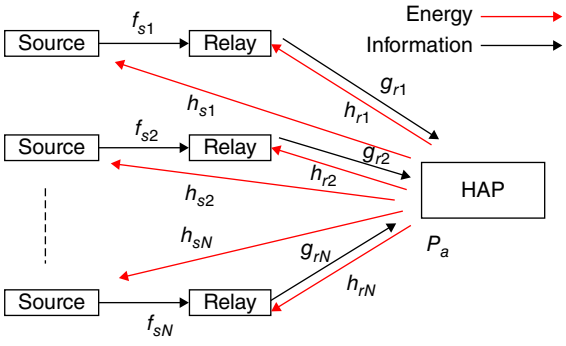

Assume that there are N pairs of user terminals and relays. Each user terminal is helped by the nearest relay. In the first $\tau_0 T$ seconds, the HAP broadcasts signals in the downlink for harvesting. In the next $\frac{\tau_1}{2}T$ seconds, user terminal 1 uses the harvested energy to transmit the signal to relay 1, and in the next $\frac{\tau_1}{2}T$ seconds, the relay uses the harvested energy to forward the signal to the HAP. Then, user terminal 2 uses the harvested energy to transmit to relay 2 for $\frac{\tau_2}{2}T$ seconds, and relay 2 forwards the signal to the HAP for the next $\frac{\tau_2}{2}T$ seconds, and so on.

Following the similar procedures, the achievable rate from the kth user terminal to the HAP is

$$R_k = \frac{\tau_k}{2}\log_2\left(1 + \frac{\frac{2\eta_s\tau_0}{\tau_k 2\sigma^2}|f_{sk}|^2 P_a |h_{sk}|^2 \frac{2\eta_r\tau_0}{\tau_k 2\sigma^2} P_a |h_{rk}|^2 |g_{rk}|^2}{\frac{2\eta_s\tau_0}{\tau_k 2\sigma^2}|f_{sk}|^2 P_a |h_{sk}|^2 + \frac{2\eta_r\tau_0}{\tau_k 2\sigma^2} P_a |h_{rk}|^2 |g_{rk}|^2 + 1}\right) \tag{8.90}$$

where $k = 1, 2, \cdots, N$, and f_{sk}, h_{sk}, h_{rk}, and g_{rk} are the channel gains from the kth source to the kth relay, from the HAP to the kth source, from the HAP to the kth relay, and

from the kth relay to the HAP, respectively. Thus, one has the sum rate

$$R_t = \sum_{k=1}^{N} \frac{\tau_k}{2} \log_2 \left(1 + \frac{\frac{2\eta_s \tau_0}{\tau_k 2\sigma^2} |f_{sk}|^2 P_a |h_{sk}|^2 \frac{2\eta_r \tau_0}{\tau_k 2\sigma^2} P_a |h_{rk}|^2 |g_{rk}|^2}{\frac{2\eta_s \tau_0}{\tau_k 2\sigma^2} |f_{sk}|^2 P_a |h_{sk}|^2 + \frac{2\eta_r \tau_0}{\tau_k 2\sigma^2} P_a |h_{rk}|^2 |g_{rk}|^2 + 1} \right) \tag{8.91}$$

which can be optimized with respect to τ_0 and $\tau_k, k = 1, 2, \cdots, N$, subject to $\sum_{k=0}^{N} \tau_k = 1$ and $\tau_k \geq 0$. This is very similar to the optimization problem in Chapter 6, except that we use the end-to-end SNR of the kth link now.

In Ramezani and Jamalipour (2017) the system was simplified by considering energy harvesting at the relay only. In this case,

$$R_t = \sum_{k=1}^{N} \frac{\tau_k}{2} \log_2 \left(1 + \frac{\frac{P_s}{\sigma^2} |f_{sk}|^2 \frac{2\eta_r \tau_0}{\tau_k 2\sigma^2} P_a |h_{rk}|^2 |g_{rk}|^2}{\frac{P_s}{2\sigma^2} |f_{sk}|^2 + \frac{2\eta_r \tau_0}{\tau_k 2\sigma^2} P_a |h_{rk}|^2 |g_{rk}|^2 + 1} \right). \tag{8.92}$$

The closed-form expressions for the optimum values of τ_k were obtained in Ramezani and Jamalipour (2017) as

$$\tau_0^{opt} = \frac{1}{1 + \sum_{i=1}^{N} \frac{1}{a_i}} \tag{8.93}$$

$$\tau_k^{opt} = \frac{1}{a_k \left(1 + \sum_{i=1}^{N} \frac{1}{a_i} \right)}, \; k = 1, 2, \cdots, N \tag{8.94}$$

where a_k is the solution to

$$\log \left(1 + \frac{A_k a_k}{B_k a_k + C_k} \right) - \frac{A_k C_k a_k}{(B_k a_k + C_k)(A_k a_k + B_k a_k + C_k)} = \sum_{i=1}^{N} \frac{A_i C_i}{(B_i a_i + C_i)(A_i a_i + B_i a_i + C_i)} \tag{8.95}$$

and $A_k = \frac{P_s}{\sigma^2} |f_{sk}|^2 \frac{2\eta_r}{2\sigma^2} P_a |h_{rk}|^2 |g_{rk}|^2$, $B_k = \frac{2\eta_r}{2\sigma^2} P_a |h_{rk}|^2 |g_{rk}|^2$, and $C_k = \frac{P_s}{2\sigma^2} |f_{sk}|^2 + 1$, for $k = 1, 2, \cdots, N$. The optimization in (8.91) may be solved in a similar way by using the Lagrange multiplier. It can lead to an equation similar to (8.95) but will be more complicated. Figure 8.12 compares (8.91) and (8.92) for the case of two users, when $P_a = P_s = 10$ dB and all the channel gains have been set to 1 with $\eta_r = \eta_s = 0.5$. From this figure, one can clearly see a global maximum of R_t for certain values of τ_1 and τ_2. Also, (8.92) has a slightly higher rate than (8.91).

Other optimization problems can also be formulated. For example, instead of having a one-to-one pair for the relays and the sources, one source can use all relays to have diversity gain. Also, direct links can be added to further complicate the end-to-end SNR. Finally, one can assume that the source receives energy from the HAP while the relay does not.

8.5.3 One User and Multiple Antennas

Next, consider the case when multiple antennas are used. In this case, the HAP is equipped with K antennas, while the user terminal and the relay has a single antenna.

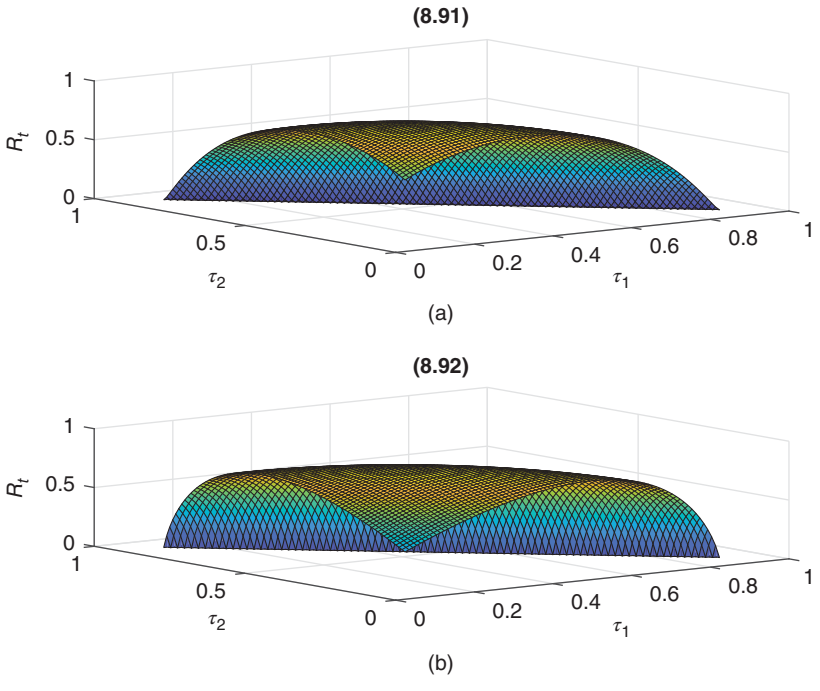

Figure 8.12 Comparison of (a) (8.91) and (b) (8.92) for the case of two users.

The system diagram is similar to Figure 8.9, except that there are multiple channels between the HAP and other nodes.

Similarly, the energy harvested at the relay and the energy harvested at the source can be given by

$$E_r = \eta_r P_a |\mathbf{h_r}^T \mathbf{w}|^2 \tau \tag{8.96}$$

and

$$E_s = \eta_s P_a |\mathbf{h_s}^T \mathbf{w}|^2 \tau \tag{8.97}$$

where $\mathbf{h_r}$ is the $K \times 1$ channel vector from the HAP to the relay, $\mathbf{h_s}$ is the $K \times 1$ channel vector from the HAP to the source, $\mathbf{w}$ is the energy beamforming vector at the HAP, and other symbols are defined as before. Using the harvested energy, the transmission power at the relay and the source can be derived as

$$P_r = \frac{E_r}{(1-\tau)/2} = \frac{2\eta_r \tau}{1-\tau} P_a |\mathbf{h_r}^T \mathbf{w}|^2 \tag{8.98}$$

and

$$P_s = \frac{E_s}{(1-\tau)/2} = \frac{2\eta_s \tau}{1-\tau} P_a |\mathbf{h_s}^T \mathbf{w}|^2 \tag{8.99}$$

respectively, where the source transmits the signal for the first $\frac{(1-\tau)}{2}$ seconds and the relay forwards the signal for the next $\frac{(1-\tau)}{2}$ seconds.

Assume that the channel gain from the source to the relay is still f_s but the $K \times 1$ channel vector from the relay to the HAP becomes $\mathbf{g_r}$. Using these assumptions and following

a similar procedure to Section 8.2.3, the end-to-end SNR and then the achievable rate can be derived as

$$\begin{aligned}\gamma &= \frac{\gamma_r \gamma_d}{\gamma_r + \gamma_d + 1} \\ &= \frac{\frac{2\eta_s \tau}{(1-\tau)2\sigma^2}|f_s|^2 P_a |\mathbf{h_s}^T \mathbf{w}|^2 \frac{2\eta_r \tau}{(1-\tau)2\sigma^2} P_a |\mathbf{h_r}^T \mathbf{w}|^2 ||\mathbf{g_r}||^2}{\frac{2\eta_s \tau}{(1-\tau)2\sigma^2}|f_s|^2 P_a |\mathbf{h_s}^T \mathbf{w}|^2 + \frac{2\eta_r \tau}{(1-\tau)2\sigma^2} P_a |\mathbf{h_r}^T \mathbf{w}|^2 ||\mathbf{g_r}||^2 + 1}\end{aligned} \tag{8.100}$$

$$R = \frac{1-\tau}{2}\log_2(1+\gamma) \tag{8.101}$$

respectively. Hence, the optimization problem becomes

$$\max_{\tau, \mathbf{w}} \{R\} \tag{8.102}$$

$$0 \leq \tau \leq 1, ||\mathbf{w}||^2 = 1. \tag{8.103}$$

This optimization problem can be converted into an iterative two-step optimization as

$$\begin{aligned}&\max_{\mathbf{w}} \{\gamma\} \\ &||\mathbf{w}||^2 = 1\end{aligned} \tag{8.104}$$

and then

$$\begin{aligned}&\max_{\tau} \left\{ \frac{1-\tau}{2}\log_2(1+\gamma) \right\} \\ &0 \leq \tau \leq 1.\end{aligned} \tag{8.105}$$

The optimization problem can also be simplified by assuming that the source or the relay does not harvest energy. Instead of AF, one can also use DF. In this case, the end-to-end SNR becomes

$$\gamma = \min \left\{ \frac{2\eta_s \tau}{(1-\tau)2\sigma^2}|f_s|^2 P_a |\mathbf{h_s}^T \mathbf{w}|^2, \frac{2\eta_r \tau}{(1-\tau)2\sigma^2} P_a |\mathbf{h_r}^T \mathbf{w}|^2 ||\mathbf{g_r}||^2 \right\} \tag{8.106}$$

and the achievable rate to be optimized becomes

$$R = \frac{1-\tau}{2}\log_2 \left[1 + \frac{2\tau}{(1-\tau)2\sigma^2} \min\{\eta_s |f_s|^2 P_a |\mathbf{h_s}^T \mathbf{w}|^2, \eta_r P_a |\mathbf{h_r}^T \mathbf{w}|^2 ||\mathbf{g_r}||^2\} \right]. \tag{8.107}$$

The optimization of (8.107) with respect to τ and $\mathbf{w}$ has closed-form expressions for the optimum values of τ and $\mathbf{w}$. The derivation for DF can be found in Zhong et al. (2015a).

One can also extend the above results to the case when multiple user terminals and multiple antennas are used. The derivation is similar. In summary, when the source and the relay harvest energy from a dedicated power transmitter, the optimization is performed for the achievable rate with respect to the time allocation and other relevant parameters. The energy causality and the signal causality in this case are not the main concerns. Next, we consider another important energy harvesting relaying system where the relay harvests energy from the source for forwarding.

8.6 From the Source

Figure 8.13 shows a diagram and the time structure of the energy harvesting system where the relay harvests energy from the source and the source has fixed power supply.

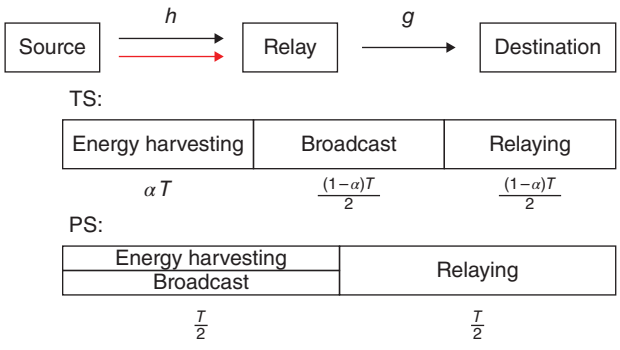

Figure 8.13 The relay harvests energy from the source.

In this system, both the source and the destination have fixed power supply but the relay either does not have enough energy or is not willing to use its own energy. For such a system, the source must provide the wireless power required for relaying and the relay can harvest this wireless power for forwarding. Next, we discuss AF relaying, followed by DF relaying.

8.6.1 Amplify-and-Forward Relaying

There are two energy harvesting methods, time switching (TS) and power splitting (PS), as discussed in Chapter 6 for SWIPT. If TS is used for AF relaying, the source first transmits the signal for αT seconds and the relay harvests energy during this period of time, where $0 \leq \alpha \leq 1$. Then, the source transmits the information for $\frac{1-\alpha}{2}T$ seconds to the relay, and the relay uses all the harvested energy to forward this signal to the destination for $\frac{1-\alpha}{2}T$ seconds. All nodes have a single antenna and operate in the half-duplex mode. One can see that if α increases, more energy can be harvested by the relay and hence, the transmission power of the relay increases for a larger achievable rate. On the other hand, since T is fixed, when α increases, the time used for information transmission will decrease to reduce the achievable rate. Thus, an optimum value of α exists.

Similar to (8.81), the amount of harvested energy is given by

$$E_r = \eta P_s |h|^2 \alpha \tag{8.108}$$

where η is the conversion efficiency of the harvester, P_s is the transmission power of the source, h is the channel gain between the source and the relay, and α is the harvesting time with $T = 1$ for simplicity. If this harvested energy is used for signal forwarding, the transmission power of the relay is given by

$$P_r = \frac{E_r}{(1-\alpha)/2} = \frac{2\eta\alpha}{1-\alpha} P_s |h|^2. \tag{8.109}$$

Thus, one has

$$\gamma_r = \frac{P_s |h|^2}{2\sigma^2} \tag{8.110}$$

and

$$\gamma_d = \frac{P_r |g|^2}{2\sigma^2} = \frac{2\eta\alpha}{2\sigma^2(1-\alpha)} P_s |h|^2 |g|^2 \tag{8.111}$$

where g is the channel gain from the relay to the destination.

For AF, the end-to-end SNR is then derived as

$$\gamma = \frac{\frac{P_s|h|^2}{2\sigma^2}\frac{2\eta\alpha}{2\sigma^2(1-\alpha)}P_s|h|^2|g|^2}{\frac{2\eta\alpha}{2\sigma^2(1-\alpha)}P_s|h|^2|g|^2 + \frac{P_s|h|^2}{2\sigma^2} + 1}. \tag{8.112}$$

Using (8.112), the outage probability can be derived as (Nasir et al. 2013)

$$P_o(\gamma_0) = 1 - \frac{1}{e_h}\int_{d\gamma_0/c}^{\infty} e^{-\frac{x}{e_h} - \frac{a\gamma_0 x + b\gamma_0}{(cx^2 - d\gamma_0 x)e_g}} dx \tag{8.113}$$

where Rayleigh fading channels are assumed so that $|h|^2$ and $|g|^2$ follow exponential distributions with parameters e_h and e_g, respectively, $a = 2\sigma^2 P_s(1-\alpha)$, $b = 4\sigma^4(1-\alpha)$, $c = 2\eta P_s^2\alpha$, and $d = 4\eta P_s\sigma^2\alpha$. Thus, in delay-constrained applications, the information rate is

$$R = \frac{1-\alpha}{2}R_0[1 - P_o(2^{2R_0} - 1)] \tag{8.114}$$

where R_0 is the minimum rate that needs to be achieved and γ_0 has been replaced by $2^{2R_0} - 1$.

Also, using (8.112), the ergodic capacity can be derived for delay-tolerant applications as (Nasir et al. 2013)

$$C = \frac{1-\alpha}{2}\int_0^{\infty}\int_{dx/c}^{\infty} \frac{(axy + bx)cy^2}{(cy^2 - dxy)^2 e_g e_h x} e^{-\frac{y}{e_h} - \frac{axy+bx}{(cy^2-dxy)e_g}} \log_2(1+x)dydx \tag{8.115}$$

by averaging the instantaneous rate over the random variables $|h|^2$ and $|g|^2$. Figure 8.14 shows R and C versus α for TS AF, where $P_s = 10$ dB, $e_h = e_g = 2\sigma^2 = 1$, and $R_0 = 2$. One sees that there is an optimum value of α for both R and C. These optimum values are different for R and C, showing that the choice of performance measure is relevant in optimum designs. Details of the derivations regarding TS and AF can be found in Section 6.3.2.1 and Section 8.2, respectively.

If PS is used, the source transmits the signal to the relay during the first $\frac{T}{2}$ seconds, and the relay forwards the signal to the destination in the second $\frac{T}{2}$ seconds. However, before the signal forwarding, the relay splits the received signal from the source into two parts: ρ part of the power is used for energy harvesting; and $(1-\rho)$ part of the power is used for information forwarding.

In this case, the amount of harvested energy is

$$E_r = \frac{1}{2}\eta\rho P_s|h|^2 \tag{8.116}$$

where ρ is the PS factor and $0 \le \rho \le 1$. Since the relaying time is $\frac{1}{2}$ (again $T = 1$ has been used for simplicity.), the transmission power of the relay is

$$P_r = \frac{E_r}{1/2} = \eta\rho P_s|h|^2. \tag{8.117}$$

It turns out that the hop SNRs are given by

$$\gamma_r = \frac{(1-\rho)P_s|h|^2}{(1-\rho)2\sigma_a^2 + 2\sigma_d^2} \tag{8.118}$$

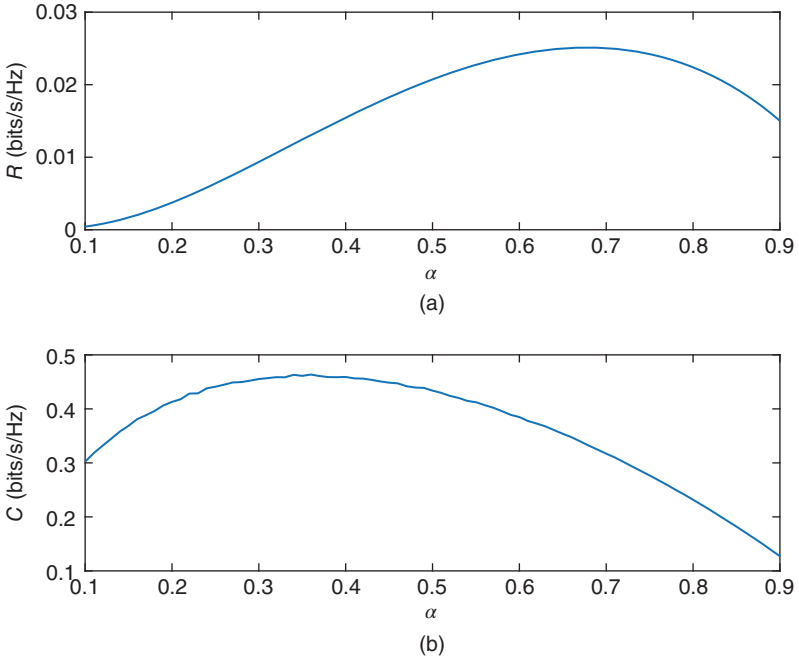

Figure 8.14 (a) R and (b) C versus α for TS AF.

and

$$\gamma_d = \frac{P_r|g|^2}{2\sigma^2} = \frac{\eta\rho}{2\sigma^2}P_s|h|^2|g|^2 \tag{8.119}$$

where g is the channel gain from the relay to the destination, $2\sigma_a^2$ is the noise power at the RF part, $2\sigma_d^2$ is the noise power at the baseband, and $2\sigma^2 = 2\sigma_a^2 + 2\sigma_d^2$. Section 6.3.2.2 explains how PS works and the associated noise power.

It can be shown that PS AF has the same outage probability as (8.113), except that $a = 2\sigma^2 P_s(1-\rho)$, $b = 2\sigma^2[(1-\rho)2\sigma_a^2 + 2\sigma_d^2]$, $c = \eta P_s^2\rho(1-\rho)$, and $d = [(1-\rho)2\sigma_a^2 + 2\sigma_d^2]\eta P_s\rho$. The rate and the ergodic capacity are given by

$$R = \frac{R_0}{2}[1 - P_o(2^{2R_0} - 1)] \tag{8.120}$$

and

$$C = \frac{1}{2}\int_0^\infty \int_{dx/c}^\infty \frac{(axy+bx)cy^2}{(cy^2-dxy)^2 e_g e_h x} e^{-\frac{y}{e_h} - \frac{axy+bx}{(cy^2-dxy)e_g}} \log_2(1+x)dydx \tag{8.121}$$

respectively. Figure 8.15 shows R and C versus ρ for PS AF, where $P_s = 10$ dB, $e_h = e_g = 1$, $2\sigma_a^2 = 2\sigma_d^2 = 0.5$, and $R_0 = 2$. Again, there exists an optimum ρ for both R and C, and these optimum values are different. Compared with TS AF, the optimum ρ for R for PS is smaller than the optimum α for R, while the optimum ρ for C for PS is larger than the optimum α for C.

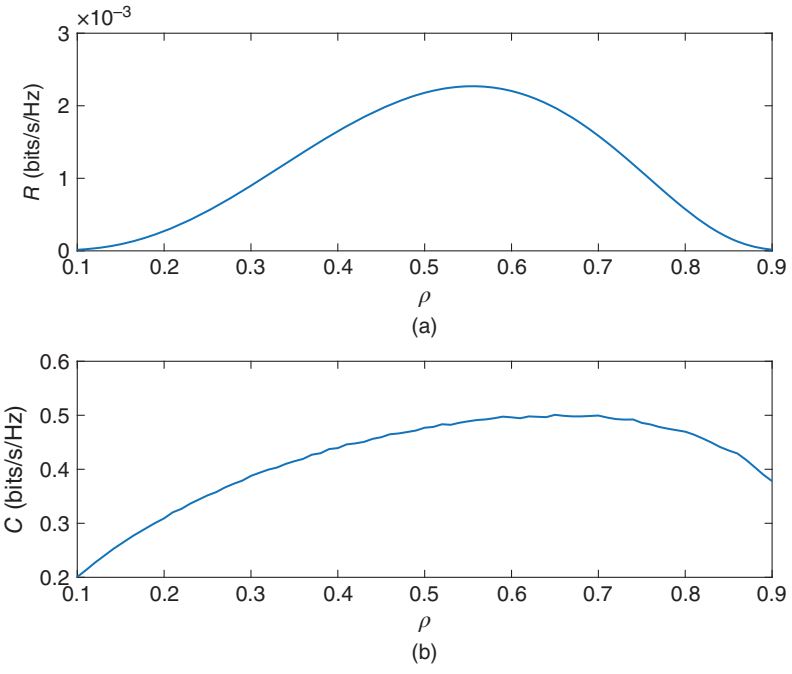

Figure 8.15 (a) R and (b) C versus ρ for PS AF.

8.6.2 Decode-and-Forward Relaying

In this section, we will discuss a DF relaying system where the relay node harvests energy from the source node to decode its received information before forwarding it to the destination node. In the discussion, the exact BER and throughput performances of DF relaying using PS energy harvesting are analyzed. Three different scenarios are considered: instantaneous transmission where the channel state information is fixed and known; delay- or error-constrained transmission where the source transmission rate or the error rate is restricted with a minimum requirement; and delay- or error-tolerant transmission where throughput or error rate is averaged over the channel state.

Again, a typical three-node system is considered. In this case, the source node transmits a signal to the relay node. The relay node splits the received signal into two parts. One part is used for energy harvesting and the other part is used for information decoding. The decoded information is then encoded again and forwarded to the destination by using the harvested energy. Assume a total relaying time of T, where $\frac{T}{2}$ is used in the broadcasting phase and $\frac{T}{2}$ is used in the relaying phase.

Using the above assumptions, the energy harvested at the relay node is

$$E_h = \eta\rho P_s|h|^2\frac{T}{2} \tag{8.122}$$

and the transmission power of the relay is therefore

$$P_r = \frac{E_h}{T/2} = \eta\rho P_s|h|^2. \tag{8.123}$$

The symbols are defined the same as before. Also, for the later derivation, one has the PDF of the channel power as

$$f_{|h|^2}(x) = \frac{1}{\Omega_h} e^{-\frac{x}{\Omega_h}}, x > 0. \tag{8.124}$$

Thus, Rayleigh fading is assumed. The hop SNR for the source-to-relay link and the hop SNR for the relay-to-destination link can be derived as

$$\gamma_r = \frac{(1-\rho)P_s|h|^2}{2(1-\rho)\sigma_a^2 + 2\sigma_d^2} \tag{8.125}$$

$$\gamma_d = \frac{\eta\rho P_s|h|^2|g|^2}{2\sigma_a^2 + 2\sigma_d^2} \tag{8.126}$$

as before, where the fading power of the relay-to-destination link follows

$$f_{|g|^2}(x) = \frac{1}{\Omega_g} e^{-\frac{x}{\Omega_g}}, x > 0. \tag{8.127}$$

For later use, the CDFs of $|h|^2$ and $|g|^2$ are given by

$$F_{|h|^2}(y) = 1 - e^{\frac{y}{\Omega_h}}, y > 0 \tag{8.128}$$

and

$$F_{|g|^2}(y) = 1 - e^{\frac{y}{\Omega_g}}, y > 0, \tag{8.129}$$

respectively. Using the hop SNRs, the BERs for BPSK signals at the relay and at the destination, respectively, can be derived as

$$BER_r = \frac{1}{2}\text{erfc}(\sqrt{\gamma_r}) \tag{8.130}$$

and

$$BER_d = \frac{1}{2}\text{erfc}(\sqrt{\gamma_d}) \tag{8.131}$$

where erfc(·) is the complementary error function [Gradshteyn and Ryzhik 2000, eq. (8.250.4)]. Similarly, the throughput of the source-to-relay link and the relay-to-destination link can be derived as

$$C_r = \ln(1 + \gamma_r) \tag{8.132}$$

and

$$C_d = \ln(1 + \gamma_d), \tag{8.133}$$

respectively.

8.6.2.1 Instantaneous Transmission

In this scenario, the channel state information is known via channel estimation. The end-to-end BER of the whole relaying link from source to destination can be calculated as

$$BER = BER_r(1 - BER_d) + BER_d(1 - BER_r). \tag{8.134}$$

An error occurs only when either the source-to-relay link or the relay-to-destination link are erroneous but not both. Using (8.130) and (8.131), one has for BPSK

$$BER = \frac{1}{2}\text{erfc}\left(\sqrt{\frac{(1-\rho)P_s|h|^2}{2(1-\rho)\sigma_a^2+2\sigma_d^2}}\right) + \frac{1}{2}\text{erfc}\left(\sqrt{\frac{\eta\rho P_s|h|^2|g|^2}{2\sigma_a^2+2\sigma_d^2}}\right) - \frac{1}{2}\text{erfc}\left(\sqrt{\frac{(1-\rho)P_s|h|^2}{2(1-\rho)\sigma_a^2+2\sigma_d^2}}\right)\text{erfc}\left(\sqrt{\frac{\eta\rho P_s|h|^2|g|^2}{2\sigma_a^2+2\sigma_d^2}}\right). \quad (8.135)$$

When the hop SNRs in the two links are reasonably large, the third term in (8.135) is very small. In this case, the first two terms are dominant. One sees that, when the value of ρ increases, the first term in (8.135) increases while the second term in (8.135) decreases. Thus, there exists an optimum value of ρ that minimizes the BER.

By taking the differentiation of (8.135) with respect to ρ and setting the derivative to zero, after some mathematical manipulations, the optimum value of ρ satisfies

$$\begin{aligned} & e^{-\frac{\eta\rho_{opt}^B P_s|h|^2|g|^2}{2\sigma_a^2+2\sigma_d^2}} \frac{1}{\sqrt{\rho_{opt}^B}} \sqrt{\frac{\eta P_s|h|^2|g|^2}{2\sigma_a^2+2\sigma_d^2}} \left[1-\text{erfc}\left[\sqrt{\frac{(1-\rho_{opt}^B)P_s|h|^2}{2(1-\rho_{opt}^B)\sigma_a^2+2\sigma_d^2}}\right]\right] \\ &= e^{-\frac{(1-\rho_{opt}^B)P_s|h|^2}{2(1-\rho_{opt}^B)\sigma_a^2+2\sigma_d^2}} \frac{1}{\sqrt{1-\rho_{opt}^B}} \frac{\sqrt{P_s|h|^2}2\sigma_d^2}{[2(1-\rho_{opt}^B)\sigma_a^2+2\sigma_d^2]^{1.5}} \\ &\quad \times \left[1-\text{erfc}\left(\sqrt{\frac{\eta\rho_{opt}^B P_s|h|^2|g|^2}{2\sigma_a^2+2\sigma_d^2}}\right)\right]. \end{aligned} \quad (8.136)$$

This equation could be further simplified when the SNRs in the two links are large such that the two complementary error functions can be approximated as zero. However, due to the non-linear exponential functions in the equation, there is still no closed-form expression for the optimum value of ρ. Nevertheless, the single-variable equation can be numerically solved using standard mathematical software.

On the other hand, the end-to-end throughput of the DF relaying system can be derived as

$$C = \min\{C_r, C_d\} = \ln\left(1+\min\left\{\frac{(1-\rho)P_s|h|^2}{2(1-\rho)\sigma_a^2+2\sigma_d^2}, \frac{\eta\rho P_s|h|^2|g|^2}{2\sigma_a^2+2\sigma_d^2}\right\}\right). \quad (8.137)$$

There also exists an optimum value of ρ. The optimum value of ρ can be derived as (Gao et al. 2017)

$$\rho_{opt}^C = \frac{(\sigma_a^2+\sigma_d^2+\eta|g|^2\sigma_d^2+\eta|g|^2\sigma_a^2)-\sqrt{\Delta}}{2\eta|g|^2\sigma_a^2} \quad (8.138)$$

where $\Delta = [\eta|g|^2\sigma_a^2]^2 + (\eta|g|^2\sigma_a^2)(2\sigma_a^2+2\sigma_d^2+2\eta|g|^2\sigma_a^2) + (\sigma_a^2+\sigma_d^2-\eta|g|^2\sigma_a^2)^2$. One sees from (8.138) that the optimum value of ρ does not depend on $|h|^2$, the channel power of the source-to-relay link. Also, when $\frac{|g|^2}{2\sigma_a^2+2\sigma_d^2}$ is large and goes to infinity, ρ_{opt}^C approaches zero.

8.6.2.2 Delay- or Error-Constrained Transmission

In this scenario, the transmission rate of the source or the BER are restricted by a minimum requirement. Specifically, for the delay-constrained case, one has $C = R_0$ such that the throughput is constrained by

$$\hat{C} = \frac{R_0}{2}(1 - p_{out}^C) \tag{8.139}$$

where $\frac{1}{2}$ takes the throughput penalty of relaying into account and the outage probability is

$$p_{out}^C = Pr\{\gamma < \gamma_{th}^C\} \tag{8.140}$$

with

$$\gamma = \min\{\gamma_r, \gamma_d\} = \min\left\{\frac{(1-\rho)P_s|h|^2}{2(1-\rho)\sigma_a^2 + 2\sigma_d^2}, \frac{\eta\rho P_s|h|^2|g|^2}{2\sigma_a^2 + 2\sigma_d^2}\right\} \tag{8.141}$$

being the end-to-end SNR of the DF relaying system and $\gamma_{th}^C = 2^{R_0} - 1$ is the threshold of γ.

Similarly, for the error-constrained case, one has $BER = BER_r(1 - BER_d) + BER_d(1 - BER_r) = BER_0$. However, this form is not very convenient to use. We can define an equivalent end-to-end SNR as

$$BER = \frac{1}{2}\text{erfc}(\sqrt{\gamma_{eq}}) \tag{8.142}$$

where γ_{eq} is bounded as (Wang et al. 2007)

$$\gamma - 1.62 < \gamma_{eq} \leq \gamma \tag{8.143}$$

where γ is given by (8.141). When γ is large, the upper and lower bounds will converge such that $\gamma_{eq} \approx \gamma$. Thus, one has $\frac{1}{2}\text{erfc}(\sqrt{\gamma_{eq}}) < BER_0$ such that $\gamma_{eq} > \gamma_{th}^B$, where $\gamma_{th}^B = [\text{erfc}^{-1}(2BER_0)]^2$ and $\text{erfc}^{-1}(\cdot)$ is the inverse function of the complementary error function. We use the bit correct rate (BCR) to be constrained as

$$B\hat{C}R = (1 - BER_0)(1 - p_{out}^B) \tag{8.144}$$

where the outage probability in this case is given by

$$p_{out}^B = Pr\{\gamma < \gamma_{th}^B\} \tag{8.145}$$

when the upper bound of γ_{eq} is used or

$$p_{out}^B = Pr\{\gamma < \gamma_{th}^B + 1.62\} \tag{8.146}$$

when the lower bound of γ_{eq} is used.

Thus, the derivations of the constrained throughput and BCR boil down to the calculation of the CDF of γ. This CDF can be derived as (Gao et al. 2017)

$$F_\gamma(y) = F_{|g|^2}\left(\frac{\sigma_a^2 + \sigma_d^2}{(1-\rho)\sigma_a^2 + \sigma_d^2}\frac{1-\rho}{\eta\rho}\right) + F_{|h|^2}\left(\frac{2(1-\rho)\sigma_a^2 + 2\sigma_d^2}{(1-\rho)P_s}y\right)$$
$$-F_{|g|^2}\left(\frac{\sigma_a^2 + \sigma_d^2}{(1-\rho)\sigma_a^2 + \sigma_d^2}\frac{1-\rho}{\eta\rho}\right)F_{|h|^2}\left(\frac{2(1-\rho)\sigma_a^2 + 2\sigma_d^2}{(1-\rho)P_s}y\right)$$

$$-\frac{1}{\Omega_g}\int_0^{\frac{\sigma_a^2+\sigma_d^2}{(1-\rho)\sigma_a^2+\sigma_d^2}\frac{1-\rho}{\eta\rho}} e^{-\frac{1}{\Omega_2}t-\frac{(2\sigma_a^2+2\sigma_d^2)y}{\Omega_h\eta\rho P_s t}}\,dt \tag{8.147}$$

where $F_{|h|^2}(\cdot)$ and $F_{|g|^2}(\cdot)$ are the CDFs of $|h|^2$ and $|g|^2$ given before. The one-dimensional integral in (8.147) cannot be solved and has to be evaluated numerically. Using (8.147), one has

$$\hat{C} = \frac{R_0}{2}[1 - F_\gamma(\gamma_{th}^C)] \tag{8.148}$$

and

$$\begin{aligned} B\hat{C}R &= (1 - BER_0)[1 - F_\gamma(\gamma_{th}^B)], \\ B\hat{C}R &= (1 - BER_0)[1 - F_\gamma(\gamma_{th}^B + 1.62)]. \end{aligned} \tag{8.149}$$

It is difficult to find an explicit expression for the optimum value of ρ from (8.148) and (8.149). They will be found numerically.

8.6.2.3 Delay- or Error-Tolerant Transmission

In this scenario, one has to calculate the ergodic capacity and the average BER by averaging them over the channel gains such that only the channel statistics are needed.

In the case of delay-tolerant transmission, the ergodic capacity can be calculated as

$$\bar{C} = \int_0^\infty \int_0^\infty \ln\left(1 + \min\left\{\frac{(1-\rho)P_s x}{2(1-\rho)\sigma_a^2 + 2\sigma_d^2}, \frac{\eta\rho P_s xy}{2\sigma_a^2 + 2\sigma_d^2}\right\}\right) f_{|h|^2}(x) f_{|g|^2}(y)\,dxdyz$$

by averaging the throughput over the fading gains. This integration can be derived as (Gao et al. 2017)

$$\begin{aligned} \bar{C} = \frac{1}{\Omega_h}&\left[1 - F_{|g|^2}\left(\frac{\sigma_a^2+\sigma_d^2}{(1-\rho)\sigma_a^2+\sigma_d^2}\frac{1-\rho}{\eta\rho}\right)\right] W\left(\frac{(1-\rho)P_s}{2(1-\rho)\sigma_a^2+2\sigma_d^2}, \frac{1}{\Omega_h}\right) \\ &+\frac{1}{\Omega_h\Omega_g}\int_0^{\frac{\sigma_a^2+\sigma_d^2}{(1-\rho)\sigma_a^2+\sigma_d^2}\frac{1-\rho}{\eta\rho}} W\left(\frac{\eta\rho P_s y}{2\sigma_a^2+2\sigma_d^2}, \frac{1}{\Omega_h}\right) e^{-\frac{y}{\Omega_g}}\,dy \end{aligned} \tag{8.150}$$

where $W(a,b) = \int_0^\infty \ln(1+ax)e^{-bx}dx$.

In the case of error-tolerant transmission, the average BER can be calculated as

$$\begin{aligned} B\bar{E}R = \int_0^\infty \int_0^\infty &\left[\frac{1}{2}\mathrm{erfc}\left(\sqrt{\frac{(1-\rho)P_s x}{2(1-\rho)\sigma_a^2+2\sigma_d^2}}\right) + \frac{1}{2}\mathrm{erfc}\left(\sqrt{\frac{\eta\rho P_s xy}{2\sigma_a^2+2\sigma_d^2}}\right)\right. \\ &\left. -\frac{1}{2}\mathrm{erfc}\left(\sqrt{\frac{(1-\rho)P_s x}{2(1-\rho)\sigma_a^2+2\sigma_d^2}}\right)\mathrm{erfc}\left(\sqrt{\frac{\eta\rho P_s xy}{2\sigma_a^2+2\sigma_d^2}}\right)\right] f_{|h|^2}(x) f_{|g|^2}(y)\,dxdy \end{aligned}$$

This can be solved as (Gao et al. 2017)

$$\begin{aligned} B\bar{E}R = \frac{1}{2\Omega_h}U\left(\frac{(1-\rho)P_s}{2(1-\rho)\sigma_a^2+2\sigma_d^2}, \frac{1}{\Omega_h}\right) + \frac{1}{2\Omega_h\Omega_g}V\left(\frac{\eta\rho P_s}{2\sigma_a^2+2\sigma_d^2}, \frac{1}{\Omega_h}, 1, \frac{1}{\Omega_g}\right) \\ -\frac{1}{2\Omega_h\Omega_g}\int_0^\infty \mathrm{erfc}\left(\sqrt{\frac{(1-\rho)P_s x}{2(1-\rho)\sigma_a^2+2\sigma_d^2}}\right) e^{-\frac{1}{\Omega_h}x} U\left(\frac{\eta\rho P_s x}{2\sigma_a^2+2\sigma_d^2}, \frac{1}{\Omega_g}\right) dx \end{aligned}$$

where

$$U(a,b) = \frac{1}{b} - \frac{2\sqrt{a}\Gamma(1.5)}{\sqrt{\pi}(\sqrt{b})^3}\, {}_2F_1(0.5, 1.5; 1.5; -\frac{a}{b}) \tag{8.151}$$

and

$$V(a,b,c) = \frac{1}{bc} - \frac{2\sqrt{a/\pi}}{b^{1.5}c^{1.5}} \frac{E(0.5, 1.5; 1.5, 1.5; \frac{bc}{a})}{\Gamma(0.5)} \tag{8.152}$$

with ${}_2F_1(\cdot,\cdot;\cdot;\cdot)$ being the hypergeometric function and $E(\cdot,\cdot;\cdot,\cdot;\cdot)$ is the MacRobert's E function (Gradshteyn and Ryzhik 2000).

8.6.2.4 Numerical Examples

We show some numerical examples for the expressions derived. Without loss of generality, in the examples, $P_s = 1$, $2\sigma_a^2 = 2\sigma_d^2 = 1$, while $|h|^2$ and $|g|^2$ in the instantaneous transmission change with $\beta_h = \frac{|h|^2}{2\sigma_a^2+2\sigma_d^2}$ and $\beta_g = \frac{|g|^2}{2\sigma_a^2+2\sigma_d^2}$ and Ω_h and Ω_g in the delay- and error-tolerant or -constrained transmissions change with $\beta_h = \frac{\Omega_h}{2\sigma_a^2+2\sigma_d^2}$ and $\beta_g = \frac{\Omega_g}{2\sigma_a^2+2\sigma_d^2}$. The value of β_h and β_g can be considered as the quality indicators of the source-to-relay and relay-to-destination links and for fixed noise variances are proportional to the fading power or the average fading power of the links.

Figures 8.16–8.19 show the performances of instantaneous transmission using DF relaying with PS. In particular, Figure 8.16 shows the throughput versus ρ for different values of β_g and η. Several observations can be made. First, there does exist an optimum

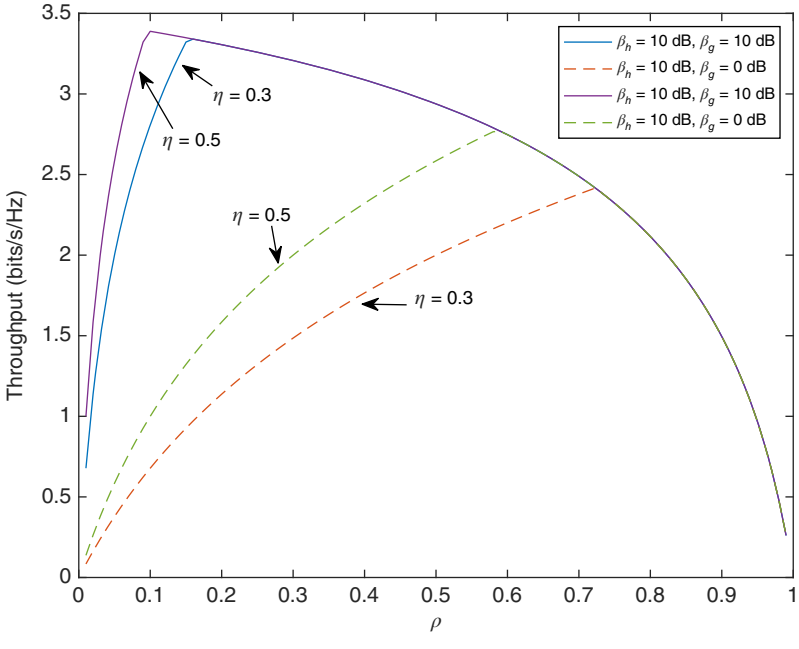

Figure 8.16 Throughput versus ρ for different values of η, β_h and β_g using instantaneous transmission.

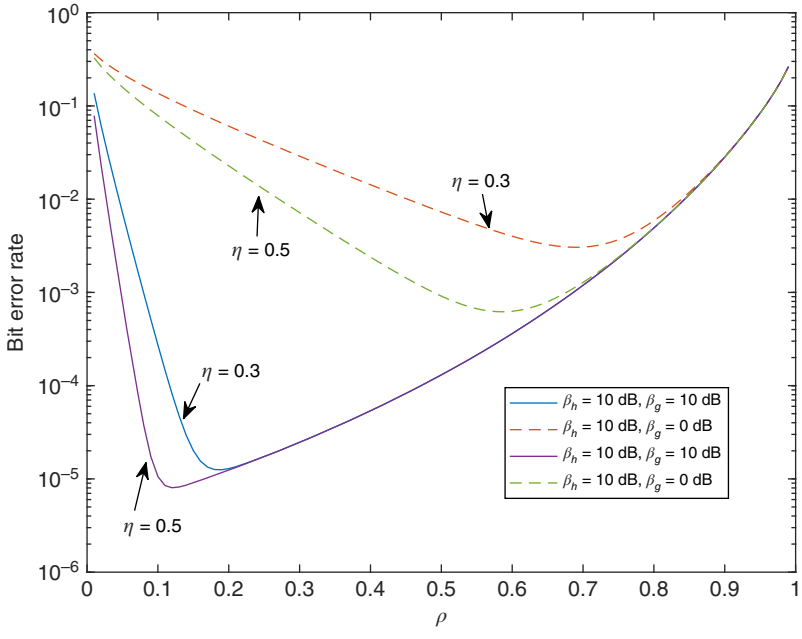

Figure 8.17 BER versus ρ for different values of η, β_h and β_g using instantaneous transmission.

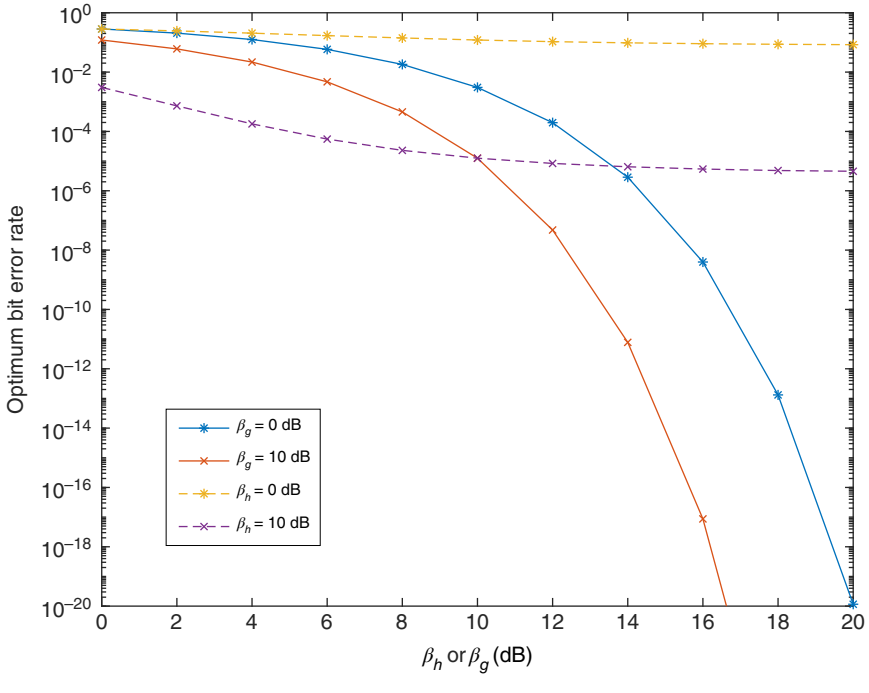

Figure 8.18 Optimum BER versus β_h or β_g when $\eta = 0.3$ using instantaneous transmission.

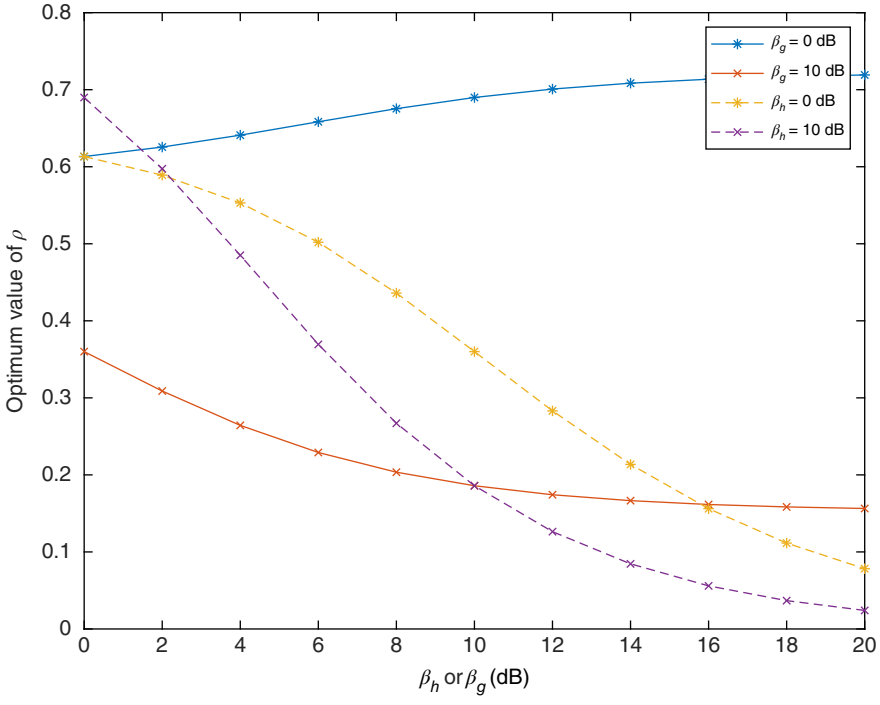

Figure 8.19 The optimum ρ achieving minimum BER versus β_h or β_g when $\eta = 0.3$ using instantaneous transmission.

value of ρ that maximizes the throughput, in all the cases considered. The optimum value of ρ lies at the only discontinuity of the throughput. This optimum value can also be calculated using (8.138). Secondly, when the value of η increases, the throughput increases and the optimum value of ρ decreases, but a large part of the throughput curves overlap with each other on the right side of the peak, indicating that the throughput performance is not sensitive to the value of η in this part. Thirdly, when β_g increases, the throughput increases. Specifically, when β_g increases from 0 to 10 dB, the throughput increases from around 2.4 to 3.3 bits/s/Hz. Figure 8.17 shows the BER versus ρ for different values of β_g and η. In this case, there exists an optimum value of ρ that minimizes the BER as well. The BER decreases when η or β_g increases, as expected. Again, on the right side of the peak, there is a large part of the BER curves that overlap with each other for different η, showing that the BER is not sensitive to η in this part either.

Figure 8.18 shows the optimum minimum BER using the optimized ρ for different values of β_h and β_g. When β_h is fixed in the legend, the x axis corresponds to β_g, and when β_g is fixed in the legend, the x axis corresponds to β_h. In this case, one sees that the optimized BER decreases significantly with β_h, when β_g is fixed to 0 and 10 dB, while the optimized BER remains almost the same when β_g increases and β_h is fixed to 0 and 10 dB. Thus, the BER is more sensitive to β_h. Figure 8.19 shows the optimized ρ used to calculate the minimum BER in Figure 8.18. When β_g is fixed to 0 or 10 dB, the optimum ρ only changes slightly with β_h. When β_h is fixed to 0 or 10 dB, the optimum ρ decreases with an increase of β_g, as less power needs to be harvested when the channel condition of the relay-to-destination link improves, under the same other conditions.

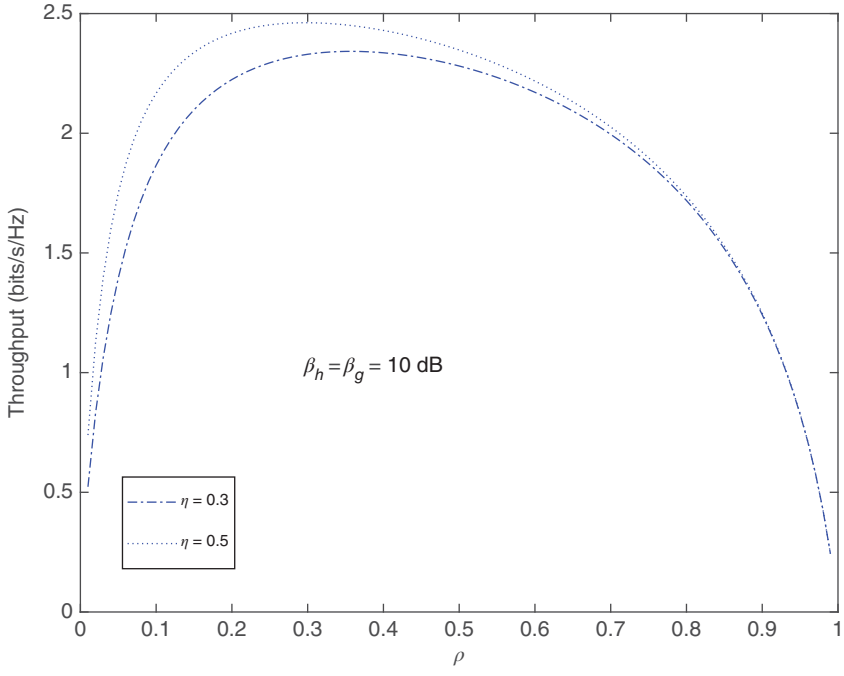

Figure 8.20 Throughput versus ρ for different values of η using delay-tolerant transmission.

Figures 8.20 and 8.21 show the performances of delay- and error-tolerant transmissions where the ergodic capacity or average BER are considered, respectively. Again, an optimum value of ρ exists that either maximizes the throughput or minimizes the BER. The value of η changes the performance slightly. In this case, the BER is less sensitive to η than the throughput.

Figures 8.22 and 8.23 show the performances of delay- or error-constrained transmissions. One sees that there exists an optimum value of ρ that maximizes the throughput or the BCR. The throughput increases quickly with ρ, when ρ is small, and decreases slowly with ρ, when ρ keeps increasing. The right sides of the peak of the throughput curves largely overlap with each other for different values of η. This shows that the throughput is not sensitive to η in delay-constrained transmission. Figure 8.23 shows the BCR versus ρ for different values of η. In general, the lower bound leads to higher BCR but the optimum value of ρ is approximately the same for both bounds.

In Ju et al. (2015), an initial amount of energy was added at the relay to derive the performances. The direct link was also considered. In Gao et al. (2017), the results were extended to Nakagami-m fading channels. One can obtain the above results by setting $m = 1$ in Gao et al. (2017) or by removing the direct link and setting the initial energy to zero in Ju et al. (2015). Recently, light energy harvesting was also studied, where the first hop uses visible light and the relay harvests the direct current from the light for forwarding signal in the second hop using RF (Rakia et al. 2016). In summary, these studies focus on the optimization of achievable rate with respect to the TS coefficient or the PS factor. In some cases, power allocation can be jointly considered. Since the energy is supplied by the source, the energy causality at the relay is not a constraint any more.

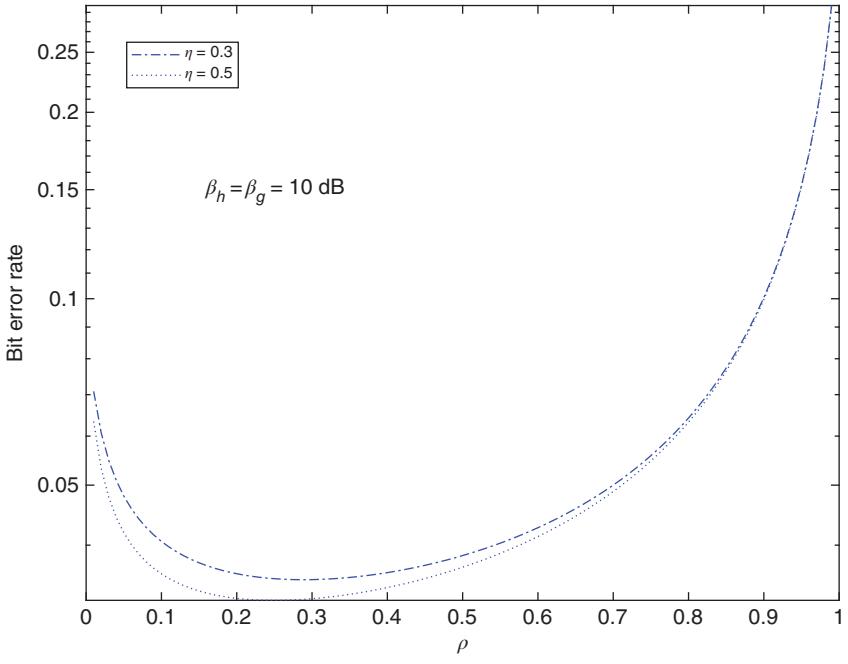

Figure 8.21 BER versus ρ for different values of η using error-tolerant transmission.

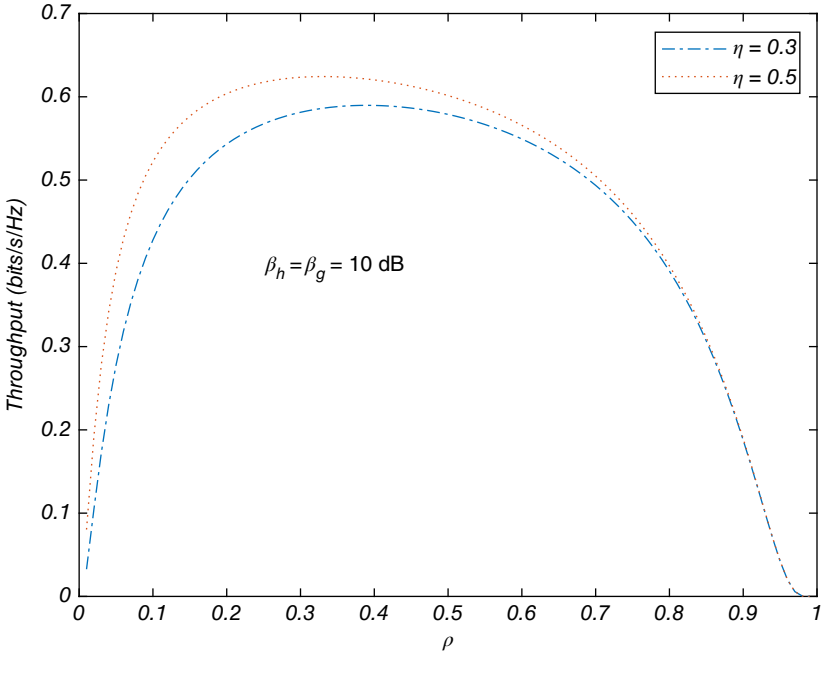

Figure 8.22 Throughput versus ρ for different values of η using delay-constrained transmission.

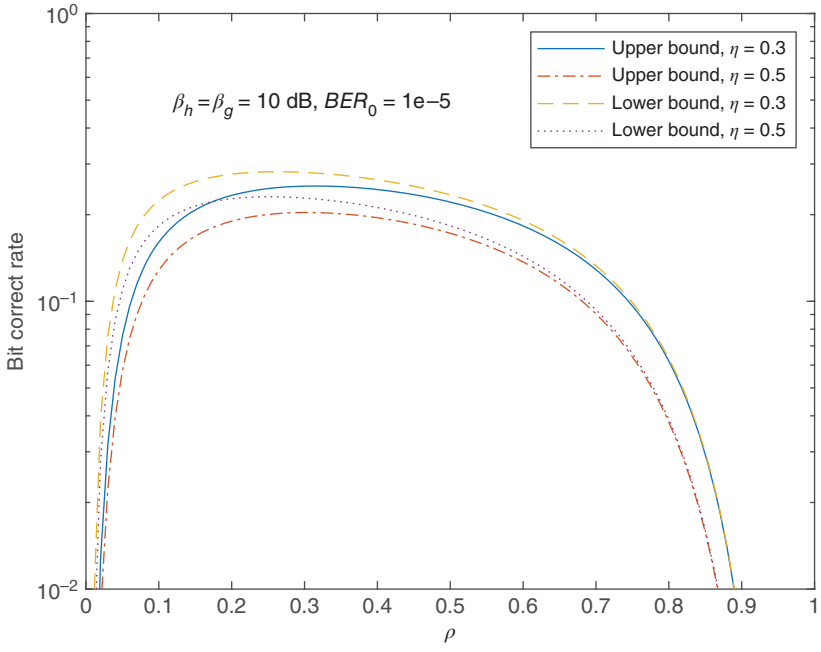

Figure 8.23 BCR versus ρ for different values of η using error-constrained transmission.

Also, since these studies only consider transmissions in blocks, the signal causality is not a concern either.

8.6.3 Energy Harvesting Source

An interesting improvement of the energy relaying system discussed in Section 8.6.1 and Section 8.6.2 is that, when the relay forwards the signal to the destination, the source node can also harvest energy from this transmission, as the wireless medium is of broadcast nature. The extra energy harvested by the source node may allow the source to perform more or better transmissions. In this system, the relay node harvests energy from the source node, and the source node harvests energy from the relay node.

This subsection studies such an improved energy harvesting relaying system. In the study, we consider a typical three-node AF relaying system. Again, all nodes have a single antenna and work in a half-duplex mode, and there is no direct link between the source and the destination. Assume that both the source node and the relay node are equipped with energy harvesters and thus, can harvest energies from the relevant radio-frequency (RF) signals. Consider static AWGN channels. Also, assume that there are E_t joules of total energy initially available at the source node and that one complete relaying transmission takes T seconds that includes broadcasting, relaying and energy harvesting phases.

If the TS strategy is used, we assume that the TS coefficient is α. Then, the relay node harvests energy from the source node for αT seconds and receives information from the

source node for $\frac{1-\alpha}{2}T$ seconds in the broadcasting phase. The received signal at the relay can be given by

$$y_r = \sqrt{P_s}\frac{h}{\sqrt{d_{sr}^{\upsilon}}}s + n_{ra} + n_{rc} \tag{8.153}$$

where P_s is the transmission power of the source, h is the fixed channel gain of the source-to-relay link, d_{sr} is the distance between source and relay, υ is the path loss exponent, $s = \pm 1$ is the transmitted symbol, n_{ra} is the AWGN incurred at the RF front as a Gaussian random variable with mean zero and variance $2\sigma_a^2$, and n_{rc} is the AWGN incurred in the RF-to-baseband conversion as a Gaussian random variable with mean zero and variance $2\sigma_d^2$. Thus, the harvested energy at the relay can be shown as

$$E_{hr} = \eta P_s \frac{h^2}{d_{sr}^{\upsilon}}\alpha T \tag{8.154}$$

where η is the conversion efficiency of the energy harvester and all other symbols are defined as before.

In the relaying phase, the relay node transmits y_r to the destination for $\frac{1-\alpha}{2}T$ seconds such that the received signal at the destination is

$$y_d = \frac{g}{\sqrt{d_{rd}^{\upsilon}}}\sqrt{P_r}by_r + n_{da} + n_{dc} \tag{8.155}$$

where g is the fixed channel gain of the relay-to-destination link, d_{rd} is the distance between relay and destination, $P_r = \frac{E_{hr}}{\frac{1-\alpha}{2}T} = \frac{2\alpha\eta}{1-\alpha}P_s\frac{h^2}{d_{sr}^{\upsilon}}$ is the transmission power of the relay, by_r is the normalized transmitted signal, normalized with respect to the average power of y_r, $b = \frac{1}{\sqrt{P_s\frac{h^2}{d_{sr}^{\upsilon}}+2\sigma_a^2+2\sigma_d^2}}$ is the amplification factor, n_{da} is the AWGN at the destination incurred by the RF front as a Gaussian random variable with mean zero and variance $2\sigma_a^2$, and n_{dc} is the AWGN at the destination from RF-to-baseband conversion with mean zero and variance $2\sigma_d^2$.

Unlike the conventional relaying protocol, in the new protocol, the source node also harvests energy from the transmitted signal of the relay node during the broadcasting phase so that the received signal at the source node during relaying is

$$y_s = \frac{h}{\sqrt{d_{sr}^{\upsilon}}}\sqrt{P_r}by_r + n_{sa} \tag{8.156}$$

where the channel gain h and the distance d_{sr} are used due to channel reciprocity and n_{sa} is the AWGN at the source. Further, the received signal at the source node can be expanded as

$$y_s = \frac{\sqrt{P_rP_s}bh^2}{d_{sr}^{\upsilon}}s + \frac{\sqrt{P_r}bh}{\sqrt{d_{sr}^{\upsilon}}}(n_{ra} + n_{rc}) + n_{sa}. \tag{8.157}$$

In this case, the harvested energy at the source is

$$E_{hs} = \eta\frac{P_rP_sb^2h^4}{d_{sr}^{2\upsilon}} \cdot \frac{(1-\alpha)T}{2}. \tag{8.158}$$

Using $b = \frac{1}{\sqrt{P_s \frac{h^2}{d_{sr}^v} + 2\sigma_a^2 + 2\sigma_d^2}}$ and $P_r = \frac{E_{hr}}{\frac{1-\alpha}{2}T} = \frac{2\alpha\eta}{1-\alpha} P_s \frac{h^2}{d_{sr}^v}$ one has

$$E_{hs} = \eta^2 \alpha \frac{P_s^2 (h^2/d_{sr}^v)^3 T}{P_s h^2/d_{sr}^v + 2\sigma_a^2 + 2\sigma_d^2}. \tag{8.159}$$

For the conventional relaying protocol using TS, without energy harvesting at the source node, the source node transmits the signal for a duration of $\alpha T + \frac{1-\alpha}{2}T$ with a transmission power of P_s, where the first part is the energy transfer time and the second part is the information delivery time from the source to the relay. Thus, each transmission costs the source node an energy of

$$E_i = \left(\alpha T + \frac{1-\alpha}{2} T\right) P_s. \tag{8.160}$$

Using the total energy, the total number of transmissions the source can make in the conventional protocol using TS is

$$K_{TS}^{Con} = \frac{E_t}{E_i} = \frac{E_t}{P_s T} \frac{2}{1+\alpha}. \tag{8.161}$$

In the case of TS, the end-to-end SNR at the destination can be derived from its received signal in (8.155) as

$$\gamma_{TS} = \frac{P_s \gamma_d \gamma_r b^2}{\gamma_d b^2 + \frac{(1-\alpha) d_{sr}^v}{2\alpha\eta P_s h^2 (2\sigma_a^2 + 2\sigma_d^2)}} \tag{8.162}$$

where $\gamma_d = \frac{g^2}{d_{rd}^v (2\sigma_a^2 + 2\sigma_d^2)}$ and $\gamma_r = \frac{h^2}{d_{sr}^v (2\sigma_a^2 + 2\sigma_d^2)}$. Thus, the overall throughput in all transmissions using an initial energy of E_t at the source node is derived as

$$C_{TS}^{Con} = K_{TS}^{Cov} \cdot \log_2(1 + \gamma_{TS}) \frac{1-\alpha}{2}. \tag{8.163}$$

For the new protocol, each relaying transmission generates an additional energy of E_{hs} at the source, which could be used for later transmissions. Two strategies are considered. In the first strategy, all the harvested energies at the source node will be stored until the K_{TS}^{Cov} transmissions are finished. Then, they will be used to make more transmissions. In this case, one has the new total number of relay transmissions as

$$K_{TS}^{New} = \left\lfloor \frac{E_t/(P_s T)}{\frac{1+\alpha}{2} - \eta^2 \alpha \frac{P_s^2 (h^2/d_{sr}^v)^3 T}{P_s h^2/d_{sr}^v + 2\sigma_a^2 + 2\sigma_d^2}} \right\rfloor \tag{8.164}$$

where $[\cdot]$ is the rounding function and $\frac{1+\alpha}{2} > \eta^2 \alpha \frac{P_s^2 (h^2/d_{sr}^v)^3 T}{P_s h^2/d_{sr}^v + 2\sigma_a^2 + 2\sigma_d^2}$. Thus, one has the total throughput in the first strategy as (Chen et al. 2017c)

$$C_{TS}^{New1} = K_{TS}^{New} \cdot \log_2(1 + \gamma_{TS}) \frac{1-\alpha}{2}. \tag{8.165}$$

One sees that $C_{TS}^{New1} > C_{TS}^{Con}$, as $K_{TS}^{New} > K_{TS}^{Cov}$. Thus, the new protocol has throughput gain over the conventional protocol and this gain comes from using the extra energy

harvested at the source node to make more transmissions. More specifically, the gain can be calculated as

$$Gain_1 = \frac{C_{TS}^{New1} - C_{TS}^{Con}}{C_{TS}^{Con}} = \frac{1}{1 - \eta^2 \frac{2\alpha}{1-\alpha} P_s \left(\frac{h^2}{d_{sr}^v}\right)^3 b^2} - 1 \tag{8.166}$$

which depends on P_s, η, $\frac{h^2}{d_{sr}^v}$, α, and b.

In the second strategy, instead of storing all harvested energy until the K_{TS}^{Cov} transmissions are finished, the harvested energy will be used immediately in the next transmission to increase its transmission power. This strategy has the advantages of requiring smaller energy storage at the source node as well as improving the quality of each relay transmission. In particular, one has the following iterative relationships (Chen et al. 2017c)

$$\begin{aligned} P_s^{(i+1)} &= \frac{E_t / K_{TS}^{Con} + E_{hs}^{(i)}}{T} \frac{2}{1+\alpha} \\ \gamma_{TS}^{i+1} &= \frac{P_s^{(i+1)} \gamma_d \gamma_r}{\gamma_d + \frac{(1-\alpha) d_{sr}^v (P_s^{(i+1)} \frac{h^2}{d_{sr}^v} + 2\sigma_a^2 + 2\sigma_d^2)}{2\alpha\eta P_s^{(i+1)} h^2 (2\sigma_a^2 + 2\sigma_d^2)}} \\ E_{hs}^{(i+1)} &= \eta^2 \alpha \frac{(P_s^{(i)})^2 (h^2 / d_{sr}^v)^3 T}{P_s^{(i)} h^2 / d_{sr}^v + 2\sigma_a^2 + 2\sigma_d^2}. \end{aligned} \tag{8.167}$$

where $i = 1, 2, \cdots, K_{TS}^{Con}$, $E_{hs}^1 = 0$, and $P_s^1 = P_s$. In this case, the total throughput is derived as (Chen et al. 2017c)

$$C_{TS}^{New2} = \sum_{i=1}^{K_{TS}^{Con}} \log_2(1 + \gamma_{TS}^{(i)}) \frac{1-\alpha}{2}. \tag{8.168}$$

There is no direction calculation of the gain in this strategy.

If the PS strategy is used, we assume that ρ is the PS factor. In this case, the source transmits the signal to the relay for $\frac{T}{2}$ seconds. Part of this signal is received at the relay for information delivery as

$$y_r = \sqrt{(1-\rho)P_s} \frac{h}{\sqrt{d_{sr}^v}} s + \sqrt{1-\rho} n_{ra} + n_{rc} \tag{8.169}$$

and part of this signal is harvested by the relay as

$$E_{hr} = \eta \rho P_s \frac{h^2}{d_{sr}^v} \frac{T}{2}. \tag{8.170}$$

In the relaying phase, the relay uses the harvested energy to forward the signal to the destination such that the received signal at the destination is

$$y_d = \frac{g}{\sqrt{d_{rd}^v}} \sqrt{P_r} b y_r + n_{da} + n_{dc} \tag{8.171}$$

where $P_r = \frac{E_{hr}}{T/2} = \eta \rho P_s \frac{h^2}{d_{sr}^v}$ in this case and all other symbols are defined as before.

Also, unlike the conventional relaying protocol, in the relaying phase of the new system, the source node also harvests energy from the relay transmission with a received signal of

$$y_s = \frac{h}{\sqrt{d_{sr}^v}}\sqrt{P_r}by_r + n_{sa} \tag{8.172}$$

and the harvested energy is obtained as

$$E_{hs} = \eta^2\rho(1-\rho)\frac{P_s^2(h^2/d_{sr}^v)^3T/2}{P_sh^2/d_{sr}^v + 2\sigma_a^2 + 2\sigma_d^2}. \tag{8.173}$$

For PS, in the conventional protocol, each relay transmission costs the source node an energy of

$$E_i = \frac{T}{2}P_s \tag{8.174}$$

and the total number of transmissions is then

$$K_{PS}^{Con} = \frac{2E_t}{P_sT}. \tag{8.175}$$

Also, using PS, the end-to-end SNR at the destination is

$$\gamma_{PS} = \frac{P_s\gamma_d\gamma_pb^2}{\gamma_db^2 + \frac{d_{sr}^v}{(1-\rho)[2\sigma_a^2+2\sigma_d^2/(1-\rho)]\eta\rho P_sh^2}} \tag{8.176}$$

where $\gamma_p = \frac{h^2}{d_{sr}^v[2\sigma_a^2+2\sigma_d^2/(1-\rho)]}$ and other symbols are defined as before. This gives the total throughput of the conventional protocol using PS as (Chen et al. 2017c)

$$C_{PS}^{Con} = \frac{K_{PS}^{Con}}{2}\log_2(1+\gamma_{PS}). \tag{8.177}$$

In the new protocol where the source node harvests energy during the relaying phase, using the first strategy, the number of total transmissions is calculated as

$$K_{PS}^{New} = \left\lceil \frac{2E_t/(P_sT)}{1-\eta^2\rho(1-\rho)\frac{P_s^2(h^2/d_{sr}^v)^3T/2}{P_sh^2/d_{sr}^v+2\sigma_a^2+2\sigma_d^2}} \right\rceil. \tag{8.178}$$

where $1 > \eta^2\rho(1-\rho)\frac{P_s^2(h^2/d_{sr}^v)^3T/2}{P_sh^2/d_{sr}^v+2\sigma_a^2+2\sigma_d^2}$ and the total throughput is (Chen et al. 2017c)

$$C_{PS}^{New1} = \frac{K_{PS}^{New}}{2}\log_2(1+\gamma_{PS}). \tag{8.179}$$

The performance gain in this case is given by

$$Gain_2 = \frac{1}{1-\eta^2\rho(1-\rho)P_s\left(\frac{h^2}{d_{sr}^v}\right)^3b^2} - 1. \tag{8.180}$$

On the other hand, using the second strategy for the new protocol, one has

$$P_s^{(i+1)} = \frac{2(E_t/K_{PS}^{Con} + E_{hs}^{(i)})}{T}$$

$$\gamma_{PS}^{i+1} = \frac{P_s^{(i+1)}\gamma_d\gamma_p}{\gamma_d + \frac{d_{sr}^{\upsilon}(P_s^{(i+1)}\frac{h^2}{d_{sr}^{\upsilon}}+2\sigma_a^2+2\sigma_d^2)}{[2(1-\rho)\sigma_a^2+2\sigma_d^2]\eta\rho P_s^{(i+1)}h^2}}$$

$$E_{hs}^{(i+1)} = \eta^2\rho(1-\rho)\frac{(P_s^{(i)})^2(h^2/d_{sr}^{\upsilon})^3T/2}{P_s^{(i)}h^2/d_{sr}^{\upsilon}+2\sigma_a^2+2\sigma_d^2}. \tag{8.181}$$

and the total throughput is (Chen et al. 2017c)

$$C_{PS}^{New2} = \sum_{i=1}^{K_{PS}^{Con}} \log_2(1+\gamma_{PS}^{(i)})\frac{1}{2}. \tag{8.182}$$

Next, we use some numerical examples to show the gain of using the new energy harvesting relaying system where the source node and the relay node harvest energy from each other. The parameters of α and ρ are first calculated by finding their optimum values that maximize the throughput of a single transmission $\log_2(1+\gamma_{TS})\frac{1-\alpha}{2}$ and $\log_2(1+\gamma_{PS})\frac{1}{2}$, respectively, as is often the case in practice. We examine the effects of P_s, η, d_{sr}, and $2\sigma_a^2+2\sigma_d^2$ on the performance gain. Other parameters are set as $E_t = 100\ J$, $T = 1\ s$, $2\sigma_a^2 = 2\sigma_d^2 = \sigma^2$, $\upsilon = 2.7$, and $h = g = 1$. The path loss exponent $\upsilon = 2.7$ corresponds to an urban cellular environment. The channel gains $h = g = 1$ is chosen such that the operating SNR will be from 10 to 20 dB without any path loss, when σ^2 is from 0.01 to 0.1 as examined in this study. These are all realistic setups. The choices of distances are for illustration purposes only. Other choices of parameters can also be made, depending on the applications considered. The gain examined in the figures is calculated as the difference between the throughput of the new system and the throughput of the conventional system normalized by that of the conventional system, as given in (8.166) and (8.180).

Figure 8.24 shows the performance gain versus P_s. Several observations can be made. First, since the gain is always positive, the new scheme with energy harvesting source outperforms the conventional scheme without energy harvesting source, as expected, as the source node harvests extra energy in the relaying phase. Secondly, the new scheme using the first strategy has a larger performance gain than that using the second strategy at the cost of requiring a larger capacity for energy storage. Thirdly, the TS energy harvesting has a larger gain than the PS energy harvesting, as PS normally harvests less energy than TS.

Figure 8.25 shows the gain versus η. One sees that the performance gain increases when η increases. Figure 8.26 shows the gain versus d_{sr}. In this case, the performance gain decreases when d_{sr} increases. Also, the rate of change in Figure 8.26 is much higher than that in Figure 8.25. Again, the first strategy using TS has the largest gain. Figure 8.27 shows the gain versus σ^2. In this case, the gain increases when σ^2 increases, except when the first strategy is used with PS.

From these figures, for variable-gain AF relaying, one concludes that the distance d_{sr} has the largest effect on the performance gain, followed by the conversion efficiency η. To increase the performance gain of the new protocol, one needs to choose a large η or a small d_{sr}. Also, TS is preferred to PS, as it produces larger gains.

Figures 8.28–8.31 show the corresponding results for fixed-gain AF relaying, where $b = 1$ is used instead of $b = \frac{1}{\sqrt{P_s\frac{h^2}{d_{sr}^{\upsilon}}+2\sigma_a^2+2\sigma_d^2}}$ in (8.155). Again, the performance gain

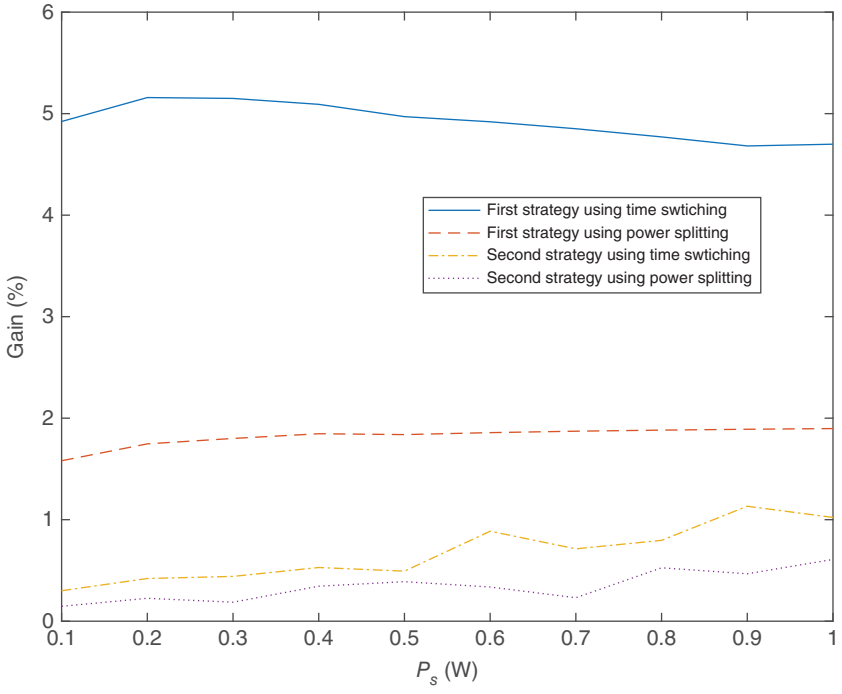

Figure 8.24 Performance gain versus P_s when $d_{sr} = 1.2$ m, $d_{rd} = 1.2$ m, $\eta = 0.5$ and $\sigma^2 = 0.01$ for variable-gain AF.

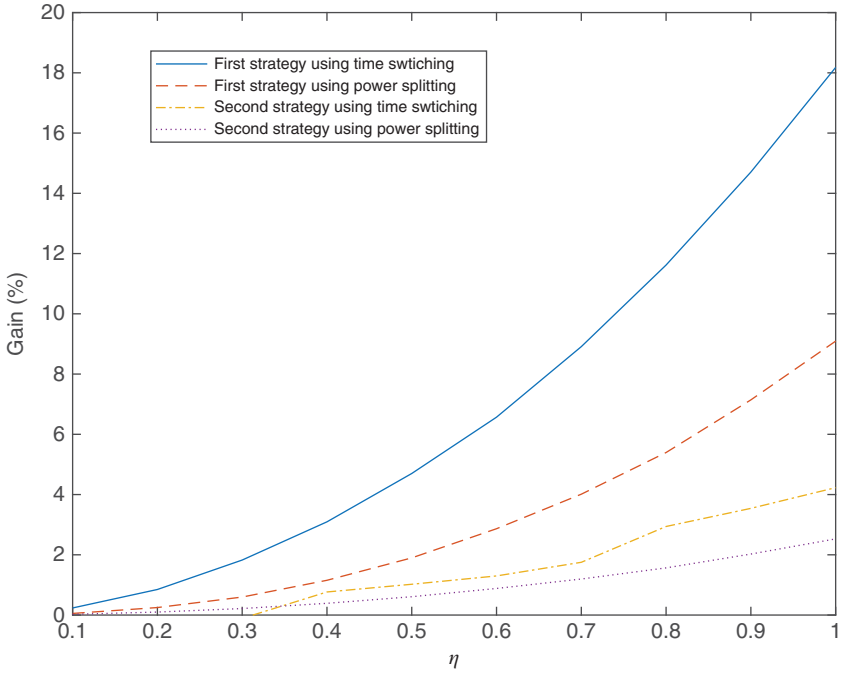

Figure 8.25 Performance gain versus η when $P_s = 1$ W, $d_{sr} = 1.2$ m, $d_{rd} = 1.2$ m, and $\sigma^2 = 0.01$ for variable-gain AF.

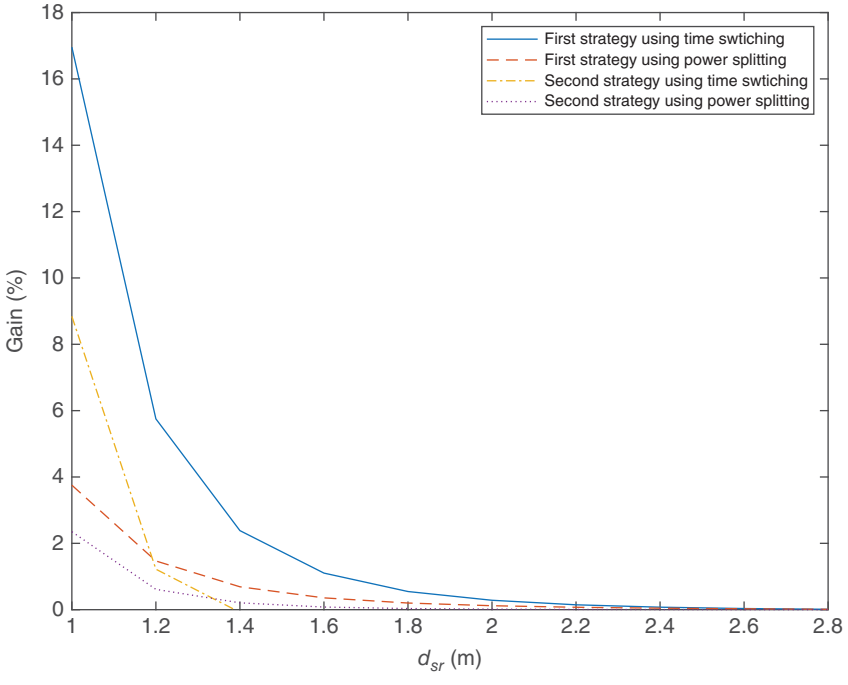

Figure 8.26 Performance gain versus d_{sr} when $P_s = 1$ W, $d_{rd} = 3 - d_{sr}$, $\eta = 0.5$, and $\sigma^2 = 0.01$ for variable-gain AF.

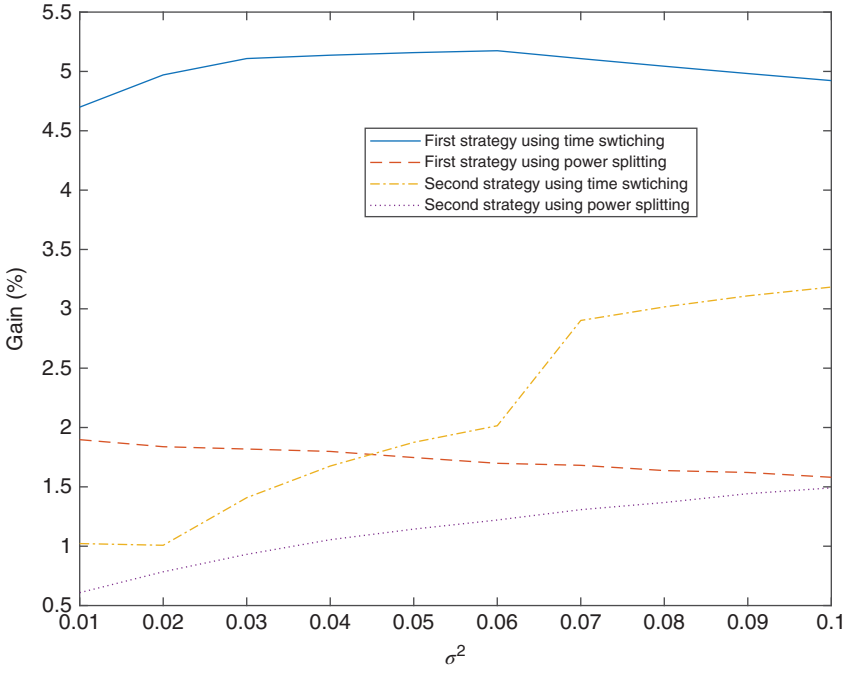

Figure 8.27 Performance gain versus σ^2 when $P_s = 1$ W, $d_{sr} = 1.2$ m, $d_{rd} = 1.2$ m, and $\eta = 0.5$ for variable-gain AF.

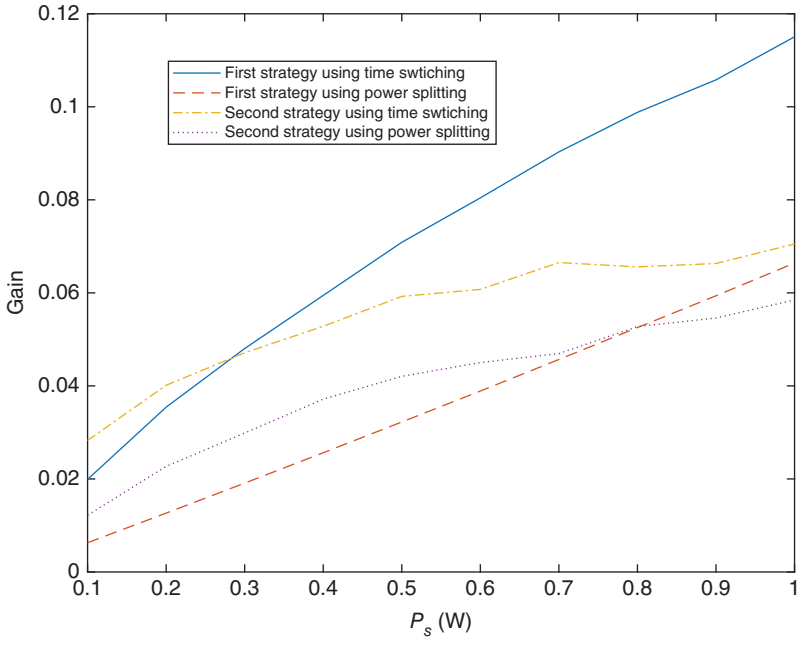

Figure 8.28 Performance gain versus P_s when $d_{sr} = 1.2$ m, $d_{rd} = 1.2$ m, $\eta = 0.5$, and $\sigma^2 = 0.01$ for fixed-gain AF, where $b = 1$.

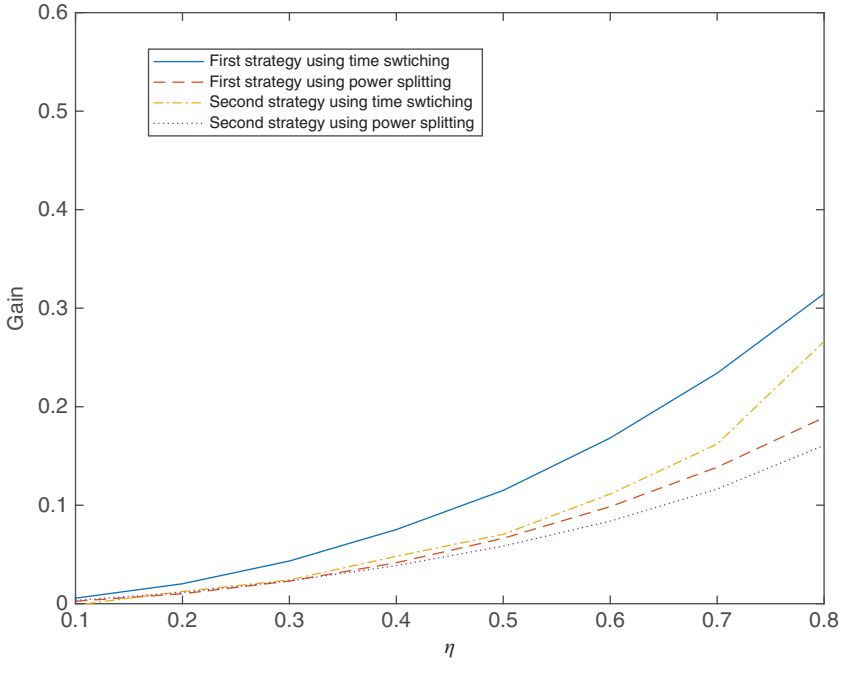

Figure 8.29 Performance gain versus η when $P_s = 1$ W, $d_{sr} = 1.2$ m, $d_{rd} = 1.2$ m, and $\sigma^2 = 0.01$ for fixed-gain AF, where $b = 1$.

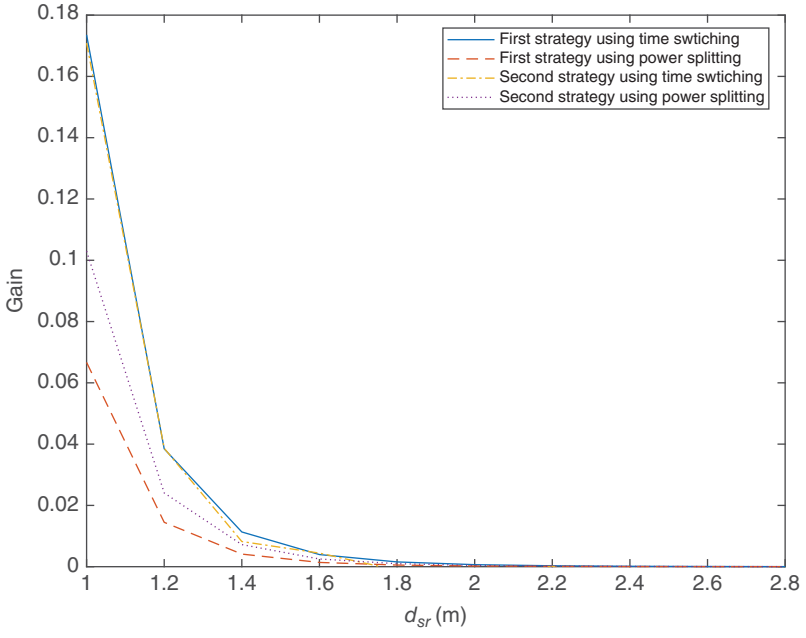

Figure 8.30 Performance gain versus d_{sr} when $P_s = 1$ W, $d_{rd} = 3 - d_{sr}$, $\eta = 0.5$, and $\sigma^2 = 0.01$ for fixed-gain AF, where $b = 1$.

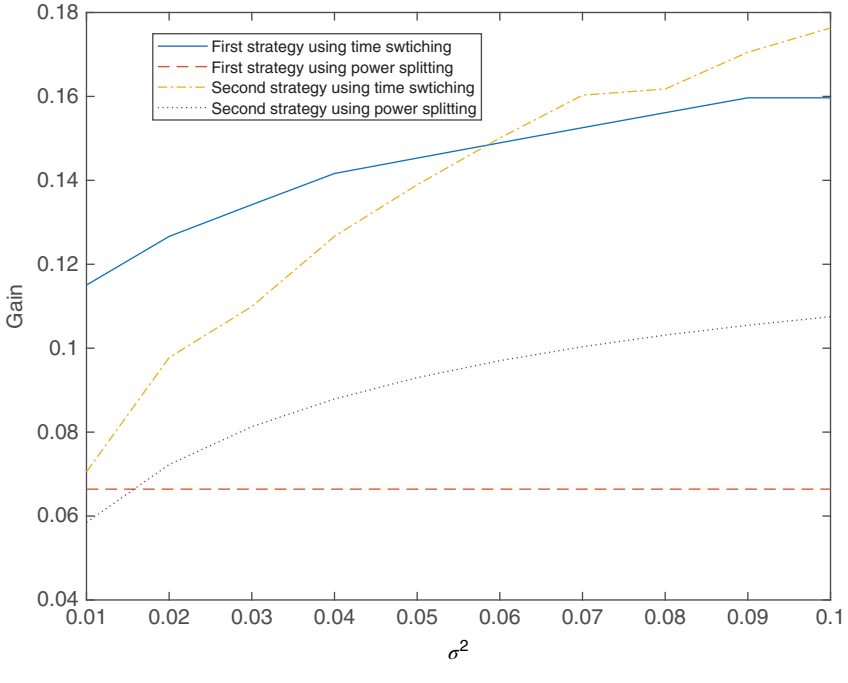

Figure 8.31 Performance gain versus σ^2 when $P_s = 1$ W, $d_{sr} = 1.2$ m, $d_{rd} = 1.2$ m, and $\eta = 0.5$ for fixed-gain AF, where $b = 1$.

increases with P_s. The first strategy is still better than the second strategy but PS outperforms TS when the value of P_s is small. The performance gain also increases with η, as expected, as more harvested energy always leads to better system performance. In Figure 8.29, the first strategy is always better than the second strategy and TS is always better than PS. On the other hand, from Figure 8.30, the performance gain drops quickly when the distance d_{sr} increases. There is little difference between the first strategy and the second strategy for TS but TS is still better than PS. Finally, from Figure 8.31, for fixed-gain AF relaying, the performance gain also increases with σ^2, except for the first strategy using PS. Again, TS is better than PS but the first strategy is better than the second strategy only when σ^2 is small.

Note that the above result considers a static AWGN channel for simplicity. In this case, channel estimation can be performed for each transmission, and the estimated channel information can then be used at the source node for rate adaptation. Alternatively, one can also average the instantaneous throughput derived above and use the average throughput at the source node. Note also that energy harvesting is used to encourage the nodes to be involved in relaying but this does not necessarily mean that the relay transmits very weak signals to the destination. In fact, the relay needs to transmit signals comparable with what is transmitted by the source in order for the destination to decode them correctly. Also, due to channel reciprocity, the channel attenuation from the source to the relay will be the same as that from the relay to the source. Thus, it is practically meaningful for the source to recycle the energy transmitted by the relay. More results on energy harvesting source node can be found in Chen et al. (2017c).

8.7 Other Important Issues

In the previous section, we have discussed several different energy harvesting relaying systems based on their sources of energy. As can be seen, the source of energy is one of the most important factors that has a fundamental impact on the designs of these systems. For systems harvesting energy from the ambient source, the energy causality and the signal causality must be accounted for. For systems with dedicated source or systems where only the relay harvests from the source, the time allocation or the harvesting parameter is more important. In all these problems, fixed resources are assumed so that one must find the best tradeoff between energy and information. This is very similar to the problems in Chapter 6, where the same signal or link is used for both energy and information and hence its use needs to be optimized.

Next, we will discuss several important issues in energy harvesting relaying. These issues occur in all types of energy harvesting relaying systems. In the discussion, we may assume only one specific type of those systems to make the discussion concise, but readers can easily extend them to other types of energy harvesting relaying systems.

8.7.1 Interference

As mentioned in Chapter 6, interference has been an important issue in almost all wireless communications systems. This is mainly due to the limited spectral resource in wireless systems such that most frequency bands are shared by all users in the communications system. However, as discussed in Chapter 6, for energy harvesting wireless

communications, interference could actually be beneficial, as it provides an extra source of energy. The overall effect of interference depends on whether it provides more energy or reduces the signal-to-interference-plus-noise ratio (SINR) more.

Next, we analyze the effect of co-channel interference on energy harvesting relaying. In the analysis, consider a three-node AF relaying system where the source transmits signal and energy to the relay and the relay uses the harvested energy to forward the signal to the destination. All nodes have a single antenna and operate in half-duplex mode.

8.7.1.1 Time Switching

Using TS, the source transmits energy to the relay for αT seconds, followed by $\frac{1-\alpha}{2}T$ seconds during which the source transmits the information to the relay, and another $\frac{1-\alpha}{2}T$ seconds during which the relay uses the harvested energy to forward the information to the destination. The model is very similar to that in Section 8.6, except that there is interference so that the received signal at the relay is given by

$$y_r = \sqrt{P_s}hs + \sum_{i=1}^{N} \sqrt{P_i}h_i s_i + n_{ra} + n_{rd} \tag{8.183}$$

where P_s, h, and s are the same as defined before, P_i is the transmission power of the ith interferer, h_i is the channel gain from the ith interferer to the relay, s_i is the symbol transmitted by the ith interferer, n_{ra} is the antenna noise with mean zero and variance $2\sigma_a^2$, and n_{rd} is the baseband noise with mean zero and variance $2\sigma_d^2$. Together one has $n_{ra} + n_{rd} = n$ with mean zero and variance $2\sigma^2 = 2\sigma_a^2 + 2\sigma_d^2$. One sees that the only difference between (8.183) and the previous model is the second term that represents the interference.

From (8.183), the harvested energy is given by

$$E_r = \eta \left(P_s|h|^2 + \sum_{i=1}^{N} P_i|h_i|^2 \right) \alpha \tag{8.184}$$

where $T = 1$ and $E\{|s|^2\} = E\{|s_i|^2\} = 1$ have been used for simplicity. The extra energy from the interference is evident in (8.184). The transmission power of the relay is given by

$$P_r = \frac{E_r}{(1-\alpha)/2} = \frac{2\alpha\eta}{1-\alpha} \left(P_s|h|^2 + \sum_{i=1}^{N} P_i|h_i|^2 \right). \tag{8.185}$$

Using this energy for relaying, the received signal at the destination is

$$y_d = \sqrt{P_r}agy_r + \sum_{j=1}^{N} \sqrt{Q_j}g_j s_j' + n_{da} + n_{dd} \tag{8.186}$$

where $a = \frac{1}{\sqrt{P_s|h|^2 + 2\sigma_{ra}^2 + 2\sigma_{rc}^2}}$ is the amplification factor, P_r, g, and y_r are defined as before, Q_j is the transmission power of the ith interferer, g_j is the channel gain from the ith interferer to the destination, s_j' is its transmitted symbol, and n_{da} is the antenna noise and n_{dd} is the baseband noise at the destination with means zero and variances $2\sigma_a^2$ and $2\sigma_d^2$, respectively. Note that the amplification factor is determined by the noise power and the signal power only. The reason that it does not include the interference power is

because, in practice, the relay will only have knowledge of the channel gain and the noise power through estimation processes but will not be able to estimate the interference power due to its variability.

Using (8.186), the end-to-end SNR in this case can be derived as

$$\gamma = \frac{\gamma_r \gamma_d}{\gamma_d + \frac{(1-\alpha)(P_s|h|^2+2\sigma_{ra}^2+2\sigma_{rd}^2)/(2\alpha\eta)}{(\sum_{i=1}^{N} P_i|h_i|^2+2\sigma_{ra}^2+2\sigma_{rd}^2)(P_s|h|^2+\sum_{i=1}^{N} P_i|h_i|^2)}} \tag{8.187}$$

where

$$\gamma_r = \frac{P_s|h|^2}{\sum_{i=1}^{N} P_i|h_i|^2 + 2\sigma_{ra}^2 + 2\sigma_{rd}^2} \tag{8.188}$$

and

$$\gamma_d = \frac{|g|^2}{\sum_{j=1}^{N} Q_j|g_j|^2 + 2\sigma_{da}^2 + 2\sigma_{dd}^2} \tag{8.189}$$

are the hop SINR of the source-to-relay and relay-to-destination links, respectively. If one lets $N = 0$, the case without interference, as discussed before, can be obtained.

Using (8.187), the outage probability for Nakagami-m fading channels was derived in Chen (2016) as

$$\begin{aligned} P_o(\gamma_0) = 1 - &\left(\frac{m_{I1}}{P_{I1}\Omega_{I1}}\right)^{Nm_{I1}} \left(\frac{m_1}{P_s\Omega_1}\right)^{m_1} \left(\frac{m_{I2}}{P_{I2}\Omega_{I2}}\right)^{Nm_{I2}} \\ &\times \sum_{l=0}^{m_2-1} \sum_{l'=0}^{l} \frac{(m_2/\Omega_2)^l \binom{l'}{l} (2\sigma_{da}^2 + 2\sigma_{dd}^2)^{l-l'} (Nm_{I2} + l' - 1)!}{\Gamma(Nm_{I1})\Gamma(m_1)\Gamma(Nm_{I2})l!} \\ &\times \int_0^{\infty} \int_{\gamma_0 z + 2\gamma_0\sigma_{ra}^2 + 2\gamma_0\sigma_{rd}^2}^{\infty} e^{-\frac{m_2(2\sigma_{da}^2+2\sigma_{dd}^2)}{\Omega_2} X(y,z) - \frac{m_1}{P_s\Omega_1} y - \frac{m_{I1}}{P_{I1}\Omega_{I1}} z} \\ &\times \frac{[X(y,z)]^l y^{m_1-1} z^{Nm_{I1}-1}}{\left[\frac{m_{I2}}{Q_{I2}\Omega_{I2}} + \frac{m_2 X(y,z)}{\Omega_2}\right]^{Nm_{I2}+l'}} dydz \end{aligned} \tag{8.190}$$

where $X(y,z) = \frac{1-\alpha}{2\alpha\eta} \frac{\gamma_0(y+2\sigma_{ra}^2+2\sigma_{rd}^2)}{(y+z)(y-\gamma_0 z-2\gamma_0\sigma_{ra}^2-2\gamma_0\sigma_{rd}^2)}$, m_{I1} and Ω_{I1} are the m parameter and the average fading power of the interferer at the relay, m_{I2} and Ω_{I2} are the m parameter and the average fading power of the interferer at the destination, m_1 and Ω_1 are the m parameter and the average fading power of h, and m_2 and Ω_2 are the m parameter and the average fading power of g. Details of this derivation can be found in Chen (2016).

Using (8.190), the achievable rate for delay-constrained applications can be shown as

$$R = \frac{(1-\alpha)R_0}{2}[1 - P_o(2^{2R_0} - 1)]. \tag{8.191}$$

Figures 8.32 and 8.33 show R for TS versus α in a Nakagami-m fading channel with Rayleigh interferer under different conditions, when $2\sigma_{ra}^2 = 2\sigma_{rd}^2 = 2\sigma_{da}^2 = 2\sigma_{dd}^2 = 1$ and $P_s = P_{I1} = Q_{I2} = \Omega_{I1} = \Omega_{I2} = 1$, while Ω_1 and Ω_2 vary with the average SINRs $\Delta_1 = \frac{\Omega_1}{NP_{I1}\Omega_{I1}+2\sigma_{ra}^2+2\sigma_{rd}^2}$ and $\Delta_2 = \frac{\Omega_2}{NQ_{I2}\Omega_{I2}+2\sigma_{ra}^2+2\sigma_{rd}^2}$, respectively. One can see that the rate increases when η increases, N increases, R_0 increases, or the m parameter increases,

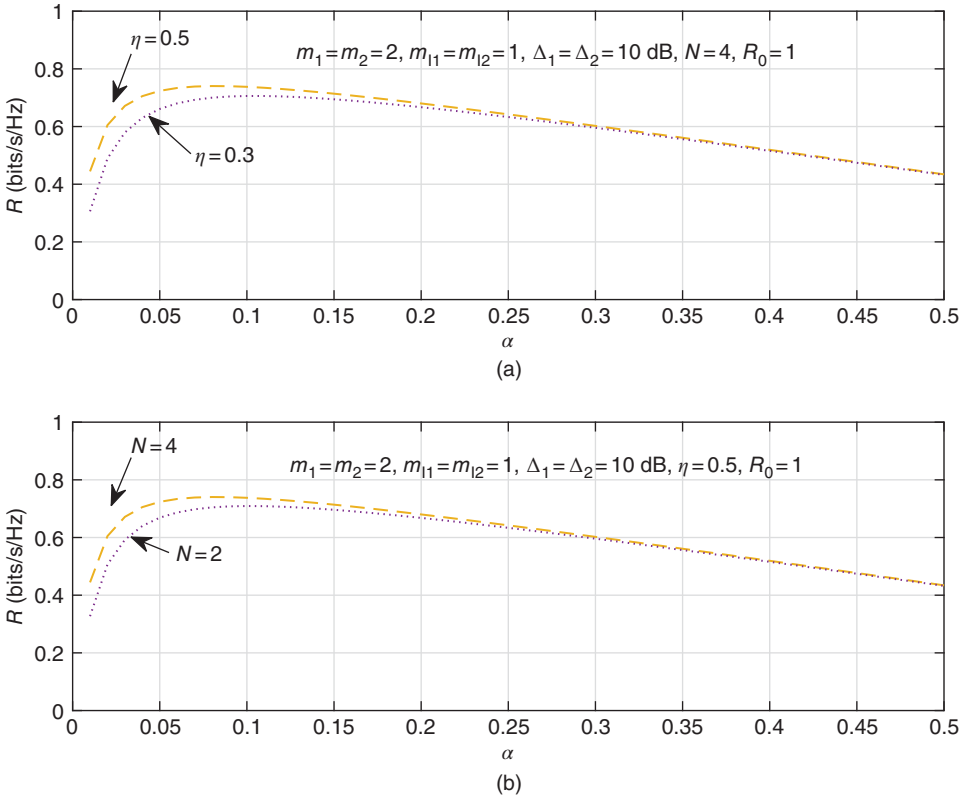

Figure 8.32 R versus α for different values of (a) η and (b) N in TS.

as more energy can be harvested with larger η or N or when channel conditions are better. Also, similar to before, an optimum α exists in all cases, and the optimum value changes with η, N, R_0, or the m parameter. The observation that the rate increases with N implies that, in these cases, the interference is beneficial, or the benefit of harvesting the interference outweighs the degradation caused by the interference.

8.7.1.2 Power Splitting

If PS is used, the source transmits the signal to the relay for $\frac{T}{2}$ seconds, followed by $\frac{T}{2}$ seconds during which the relay forwards the information to the destination. In the first $\frac{T}{2}$ seconds, the signal will be split into two parts, one part for information decoding and the other part for energy harvesting. The received signal at the relay for information decoding is given by

$$y_r = \sqrt{(1-\rho)P_s}hs + \sqrt{1-\rho}\sum_{i=1}^{N}\sqrt{P_i}h_i s_i + \sqrt{1-\rho}n_{ra} + n_{rd} \tag{8.192}$$

where ρ is the PS factor and all other symbols are defined as before. In this case, the antenna noise n_{ra} is split, because PS is performed at the RF part, while the baseband noise n_{rd} is not split.

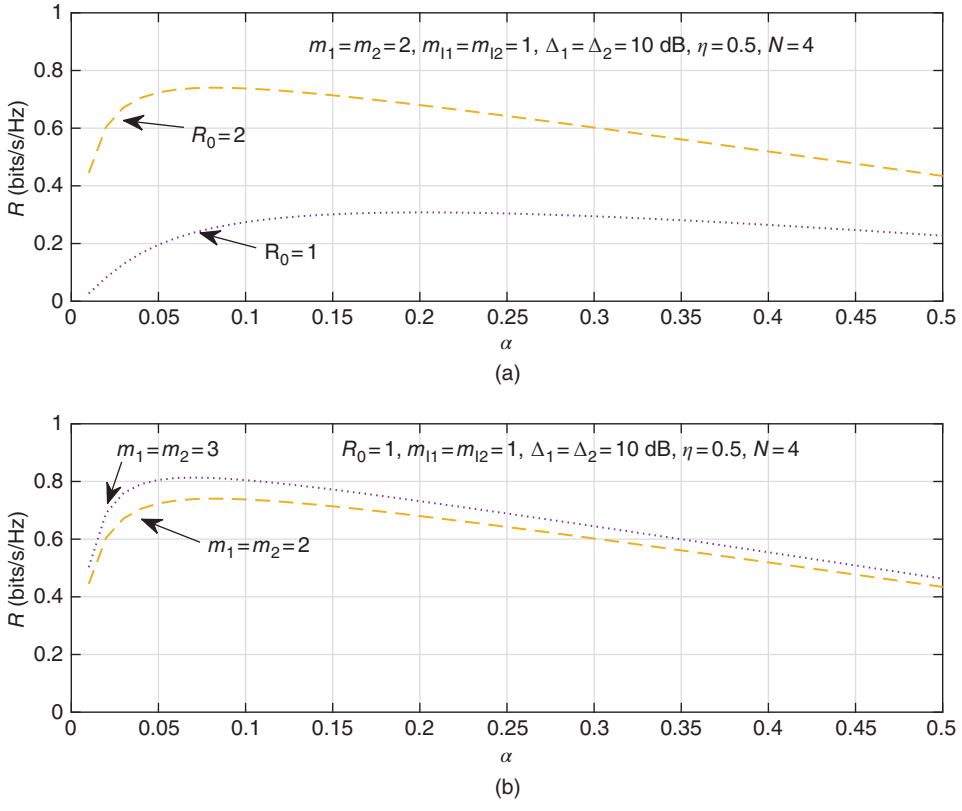

Figure 8.33 R versus α for different values of (a) R_0 and (b) m parameters in TS.

Then, the harvested energy using the other part of the signal is given by

$$E_r = \eta\rho\left(P_s|h|^2 + \sum_{i=1}^{N} P_i|h_i|^2\right)\frac{1}{2}. \tag{8.193}$$

Again, $T = 1$ and $E\{|s|^2\} = E\{|s_i|^2\} = 1$ have been used for simplicity. The extra energy from the interference is also evident in (8.193). The transmission power of the relay is thus given by

$$P_r = \frac{E_r}{1/2} = \eta\rho\left(P_s|h|^2 + \sum_{i=1}^{N} P_i|h_i|^2\right). \tag{8.194}$$

Using the harvested energy, the received signal at the destination is given as

$$y_d = \sqrt{P_r}agy_r + \sum_{j=1}^{N}\sqrt{Q_j}g_j s_j' + n_{da} + n_{dd} \tag{8.195}$$

where $a = \frac{1}{\sqrt{(1-\rho)P_s|h|^2+2(1-\rho)\sigma_{ra}^2+2\sigma_{rd}^2}}$ is the amplification factor in this case, and all other symbols are the same as before.

Using (8.195), the end-to-end SINR in this case can be derived as

$$\gamma = \frac{\gamma_r' \gamma_d}{\gamma_d + \frac{\left(P_s|h|^2 + 2\sigma_{ra}^2 + \frac{2\sigma_{rd}^2}{1-\rho}\right)/(\eta\rho)}{\left[\sum_{i=1}^{N} P_i|h_i|^2 + 2\sigma_{ra}^2 + \frac{2\sigma_{rd}^2}{1-\rho}\right](P_s|h|^2 + \sum_{i=1}^{N} P_i|h_i|^2)}} \tag{8.196}$$

where $\gamma_r' = \frac{P_s|h|^2}{\sum_{i=1}^{N} P_i|h_i|^2 + 2\sigma_{ra}^2 + 2\sigma_{rd}^2/(1-\rho)}$ is the hop SINR of the source-to-relay link for PS and γ_d is the same as before. Again, if one lets $N = 0$, the case without interference can be obtained. Otherwise, when N increases, more interference is incurred.

Using (8.196), the outage probability for PS in Nakagami-m fading channels was derived in Chen (2016) as

$$\begin{aligned} P_o(\gamma_0) = 1 - &\left(\frac{m_{I1}}{P_{I1}\Omega_{I1}}\right)^{Nm_{I1}} \left(\frac{m_1}{P_s\Omega_1}\right)^{m_1} \left(\frac{m_{I2}}{Q_{I2}\Omega_{I2}}\right)^{Nm_{I2}} \\ &\times \sum_{l=0}^{m_2-1} \sum_{l'=0}^{l} \frac{(m_2/\Omega_2)^l \binom{l'}{l} (2\sigma_{da}^2 + 2\sigma_{dd}^2)^{l-l'} (Nm_{I2} + l' - 1)!}{\Gamma(Nm_{I1})\Gamma(m_1)\Gamma(Nm_{I2})l!} \\ &\times \int_0^{\infty} \int_{\gamma_0 z + 2\gamma_0\sigma_{ra}^2 + 2\gamma_0\sigma_{rd}^2/(1-\rho)}^{\infty} e^{-\frac{m_2(2\sigma_{da}^2 + 2\sigma_{dd}^2)}{\Omega_2} X(y,z) - \frac{m_1}{P_s\Omega_1} y - \frac{m_{I1}}{P_{I1}\Omega_{I1}} z} \\ &\times \frac{[X(y,z)]^l y^{m_1-1} z^{Nm_{I1}-1}}{\left[\frac{m_{I2}}{Q_{I2}\Omega_{I2}} + \frac{m_2 X(y,z)}{\Omega_2}\right]^{Nm_{I2}+l'}} dydz \end{aligned} \tag{8.197}$$

where $X(y,z) = \frac{\gamma_0}{\eta\rho} \frac{y + 2\sigma_{ra}^2 + 2\sigma_{rd}^2/(1-\rho)}{(y+z)[y - \gamma_0 z - 2\gamma_0\sigma_{ra}^2 - 2\gamma_0\sigma_{rd}^2/(1-\rho)]}$ now and other symbols are defined as before. More details on (8.197) are available in Chen (2016). Using (8.197), the achievable rate for delay-constrained applications can be calculated using (8.191).

Figures 8.34 and 8.35 show R for PS versus ρ in a Nakagami-m fading channel with Rayleigh interferer under different conditions. The same parameter settings are used as those in Figures 8.32 and 8.33. Similar observations can be made. Also, the curves for ρ in PS are generally flatter than those in TS, indicating that there are more choices of ρ that give near-optimal performances.

8.7.2 Multi-Hop

We have been studying energy harvesting dual-hop relaying systems so far. However, in some applications, range extension is quite important to provide services for remote nodes. In these applications, multiple relays can be used to form a multi-hop relaying system that can extend the range considerably. Next, we will consider a multi-hop energy harvesting AF relaying system and study how the energy changes with hops. Some of the discussion and derivation can be found in Mao et al. 2015.

Consider a relaying system with one relaying link from the source node to the destination node via several hops. There is no direct link between the source node and the destination node, which is the aim of network coverage extension. All nodes are half-duplex and have a single antenna. The signal from the source node is relayed by multiple nodes in several hops, one node in each hop, until it arrives at the destination

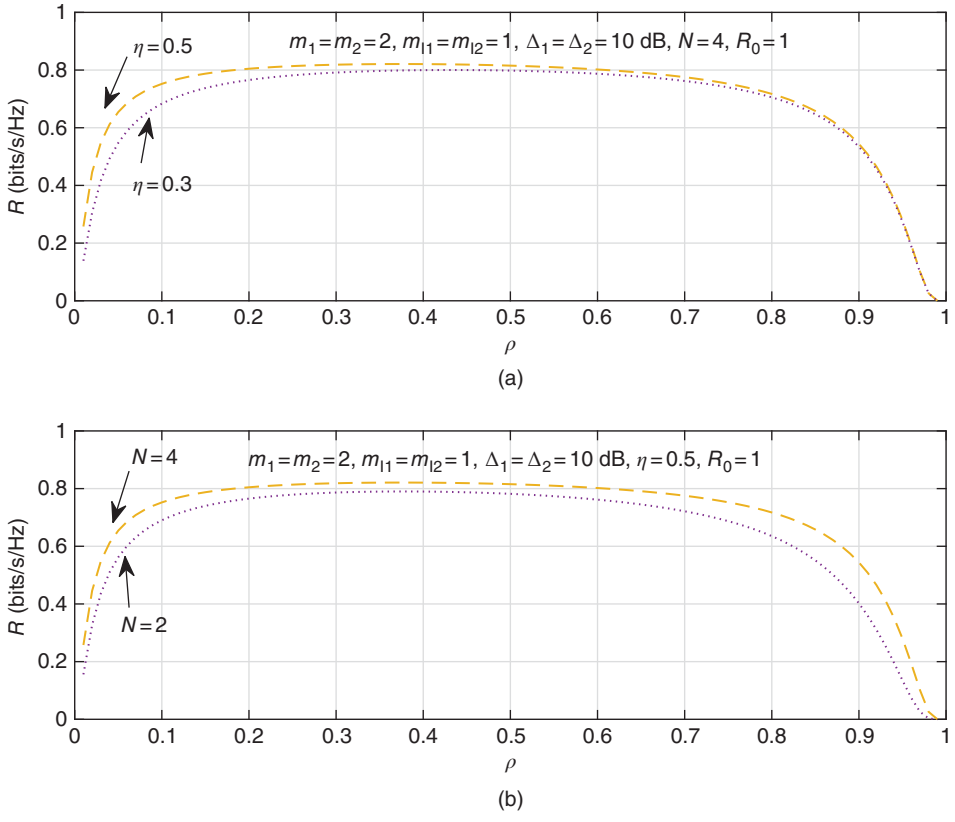

Figure 8.34 R versus ρ for different values of (a) η and (b) N parameters in PS.

node. In each hop, the relaying node first harvests the energy of the signal from the previous hop and the harvested energy is then used to forward the signal to the next hop. Assume that in each hop it takes T seconds to transmit the signal and that the initial transmission power of the source is P_0. In this section, the largest number of hops will be calculated, that is, the hop when the signal dies down due to insufficient energy for forwarding. This calculation depends on the energy harvesting strategies used by the relays. Thus, it is necessary to discuss the TS and PS methods separately.

8.7.2.1 Time Switching

In the TS method, the relay uses a portion of the relaying time to harvest the signal from the source node or the previous hop. Denote α_m as the portion at the mth relay in the mth hop, with $0 \leq \alpha_m \leq 1$ and $m = 1, 2, \cdots$. Thus, among the relaying time T in the mth hop, $\alpha_m T$ will be used to harvest the energy and $(1 - \alpha_m)T$ will be used for forwarding the received signal.

Consider AF first. In the AF protocol, the received signal from the previous hop is amplified and forwarded to the next hop directly. Thus, the received signals at the first relay, the second relay, and the mth relay are given by

$$y_1 = \sqrt{P_0} a_1 s + n_{1a} + n_{1c} \tag{8.198}$$

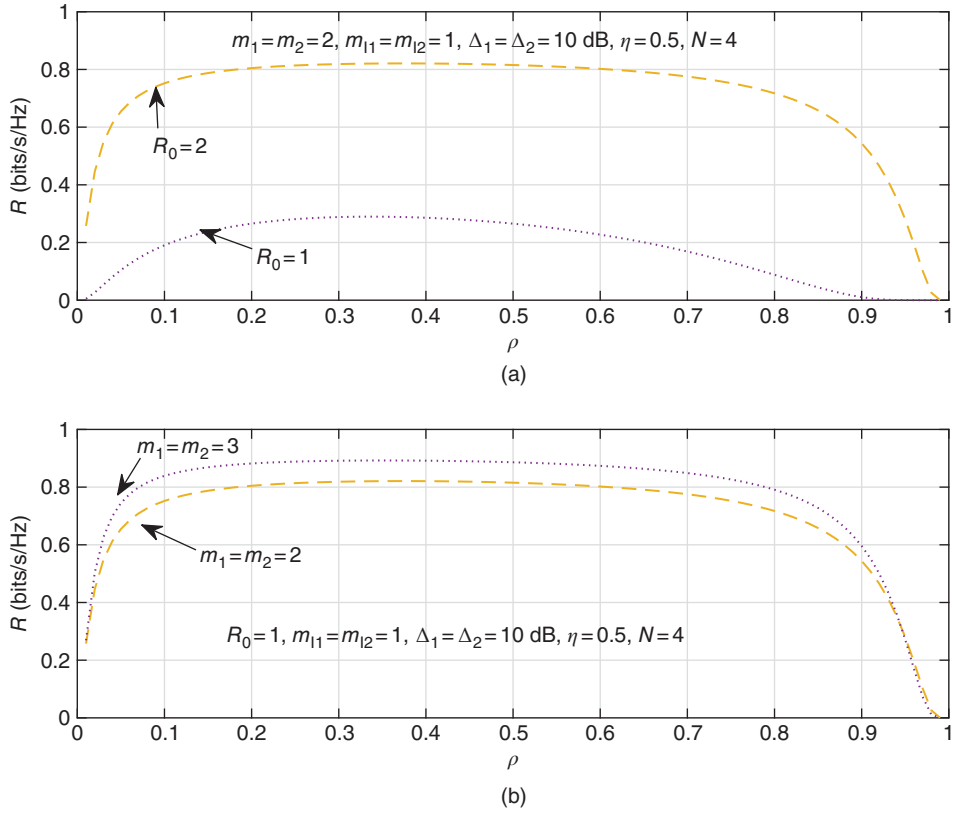

Figure 8.35 R versus ρ for different values of (a) R_0 and (b) m parameters in PS.

$$y_2 = \sqrt{P_1} g_1 a_2 y_1 + n_{2a} + n_{2c} \tag{8.199}$$

$$\vdots$$

$$y_m = \sqrt{P_{m-1}} g_{m-1} a_m y_{m-1} + n_{ma} + n_{mc}, \tag{8.200}$$

respectively, where P_0 is the initial transmission power of the source node, $P_1, \cdots, P_{m-1}$ are the transmission powers of the first until the $(m-1)$th relays that have been harvested from $y_1, \cdots, y_{m-1}$, respectively, $a_1, a_2, \cdots, a_m$ are the channel gains of the first, second, $\cdots$, mth hops, respectively, $g_1, \cdots, g_{m-1}$ are the amplification factors at the first until the $(m-1)$th relays, respectively, s is the transmitted BPSK signal with equal *a priori* probabilities for $s=1$ and $s=-1$, $n_{1a}, n_{2a}, \cdots, n_{ma}$ are the AWGN introduced by the RF fronts at the first relay, the second relay, and the mth relay, respectively, and $n_{1c}, n_{2c}, \cdots, n_{mc}$ are the AWGN introduced in the RF to baseband conversions at the first relay, the second relay, and the mth relay, respectively. Note that we have discussed before that there are two types of noise in energy harvesting relaying, one from the antenna and one from the baseband. Furthermore, assume that the channel gains $a_1, a_2, \cdots, a_m$ are known. Also, assume that $n_{1c}, n_{2c}, \cdots, n_{mc}$ are Gaussian random variables with mean zero and variance $\sigma_{1c}^2, \sigma_{2c}^2, \cdots, \sigma_{mc}^2$, respectively, and $n_{1a}, n_{2a}, \cdots, n_{ma}$ are Gaussian random variables with mean zero and variance

$\sigma_{1a}^2, \sigma_{2a}^2, \cdots, \sigma_{ma}^2$, respectively. Using the iterative relationship, the received signal at the mth relay can be rewritten as

$$y_m = \prod_{i=1}^{m} a_i \prod_{i=1}^{m-1} g_i \prod_{i=0}^{m-1} \sqrt{P_i} s + \sum_{i=1}^{m} \left[\prod_{j=i+1}^{m} a_j \prod_{j=i}^{m-1} g_j \prod_{j=i}^{m-1} \sqrt{P_j} (n_{ia} + n_{ic}) \right]. \tag{8.201}$$

Two types of AF protocol are considered next: fixed-gain; and variable-gain. For fixed-gain AF, the amplification factor is set to $g_i = 1$ for $i = 1, 2, \cdots, m-1$. Other constants can be considered similarly. For variable-gain AF, the amplification factor is set to $g_i = \frac{1}{\sqrt{P_{i-1}|a_i|^2 + \sigma_{ic}^2 + \sigma_{ia}^2}}$ for $i = 1, 2, \cdots, m-1$. Also, in (8.201), if the lower limit of the summation or the product becomes larger than the upper limit of the summation or the product, the sum or the product is assumed to be 1.

The received signals are used in energy harvesting for $\alpha_1 T$, $\alpha_2 T$, and $\alpha_m T$ seconds, respectively, and in relaying for $(1-\alpha_1)T$, $(1-\alpha_2)T$, and $(1-\alpha_m)T$ seconds, respectively. Thus, from (8.198), the energy harvested at the first relay from the transmitted signal of the source node is given by

$$E_{h1} = \eta P_0 a_1^2 \alpha_1 T \tag{8.202}$$

where η is the conversion efficiency of the energy harvester and all other symbols are defined as before. Similarly, the energy harvested at the second relay from the transmitted signal of the first relay is given by

$$E_{h2} = \eta P_1 g_1^2 a_2^2 P_0 a_1^2 \alpha_2 T. \tag{8.203}$$

Finally, the energy harvested at the mth relay from the transmitted signal of the $(m-1)$th relay is given by

$$E_{hm} = \eta \prod_{i=0}^{m-1} P_i \prod_{i=1}^{m-1} g_i^2 \prod_{i=1}^{m} a_i^2 \alpha_m T. \tag{8.204}$$

Since each hop has a relaying time of T, the transmitted power at the first relay, the second relay, and the m-th relay can be calculated as Mao et al. 2015

$$P_1 = \frac{E_{h1}}{T} = \eta P_0 a_1^2 \alpha_1 \tag{8.205a}$$

$$P_2 = \frac{E_{h2}}{T} = \eta P_1 g_1^2 a_2^2 P_0 a_1^2 \alpha_2 \tag{8.205b}$$

$$P_m = \frac{E_{hm}}{T} = \eta \prod_{i=0}^{m-1} P_i \prod_{i=1}^{m-1} g_i^2 \prod_{i=1}^{m} a_i^2 \alpha_m, \tag{8.205c}$$

respectively. Note that these relationships are in fact recurrence relationships. Using 8.205a–8.205c, non-recurrence expressions of the transmission powers can also be obtained by replacing the transmission powers on the right-hand sides of these equations.

One sees that, since $\eta < 1$, $\alpha_1 \leq 1$, and $a_1 < 1$ due to channel attenuation, $E_{h1} = \eta \alpha_1 a_1^2 E_0$ is only a portion of the initial amount of energy transmitted by the

source node as $E_0 = P_0 T$. Also, $E_{h2} = \eta g_1^2 a_2^2 P_0 a_1^2 \alpha_2 E_{h1}$ is only a portion of the harvested energy at the first relay. Thus, the harvested energy at each hop decreases at an accelerated rate when the hop number increases. At some hop, the energy will not be sufficient for transmission. We use the throughput criterion such that

$$R_0 = \log_2(1+\gamma_m)(1-\alpha_m) \tag{8.206}$$

where

$$\gamma_m = \frac{\prod_{i=1}^{m} a_i^2 \prod_{i=1}^{m-1} g_i^2 \prod_{i=1}^{m-1} P_i(1-\alpha_m)T}{\sum_{i=1}^{m}\left[\prod_{j=i+1}^{m} a_j^2 \prod_{j=i}^{m-1} g_j^2 \prod_{j=i}^{m-1} P_j(\sigma_{ia}^2+\sigma_{ic}^2)\right]} \tag{8.207}$$

$m = 1, 2, \cdots$ is the hop index, $(1-\alpha_m)$ in (8.206) takes into account the throughput loss due to energy harvesting time, and $(1-\alpha_m)$ in (8.207) takes into account the transmission time loss due to energy harvesting.

It is of great interest to find the first value of m for which $\log_2(1+\gamma_m)(1-\alpha_m) < R_0$. Before this happens, each hop has a throughput of R_0 such that the TS coefficient α_m can be calculated as Mao et al. 2015

$$\alpha_m = 1 - \frac{(2^{R_0/(1-\alpha_m)} - 1)W}{\prod_{i=1}^{m} a_i^2 \prod_{i=1}^{m-1} g_i^2 \prod_{i=1}^{m-1} P_i T} \tag{8.208}$$

for the mth relay, where $W = \sum_{i=1}^{m}[\prod_{j=i+1}^{m} a_j^2 \prod_{j=i}^{m-1} g_j^2 \prod_{j=i}^{m-1} P_j(\sigma_{ia}^2+\sigma_{ic}^2)]$. This equation does not lead to a closed-form expression of α_m but it can be easily solved using mathematical software.

In the DF protocol, the received signal from the previous hop is first decoded and then the decoded information is forwarded to the next hop. Thus, the received signals at the first relay, the second relay, and the mth relay are given by

$$y_1 = \sqrt{P_0} a_1 s + n_{1a} + n_{1c} \tag{8.209}$$

$$y_2 = \sqrt{P_1} a_2 s_1 + n_{2a} + n_{2c} \tag{8.210}$$

$$\vdots$$

$$y_m = \sqrt{P_{m-1}} a_m s_{m-1} + n_{ma} + n_{mc}, \tag{8.211}$$

respectively, where $s_1 = sgn\{y_1 a_1^*\}, \cdots, s_{m-1} = sgn\{y_{m-1} a_{m-1}^*\}$ are the decoded and forwarded information at the relays, $sgn\{x\} = 1$ when $x > 0$ and $sgn\{x\} = -1$ when $x < 0$ is the signum function, and all other symbols are defined as before. Unlike AF, since $E\{|s_{m-1}|^2\} = 1$, the performance of the mth hop in DF only depends on P_{m-1}, a_m, σ_{ma}^2, and σ_{mc}^2. Next, the largest number of hops, that is, the maximum value of m given an initial amount of energy $E_0 = P_0 T$, will be studied.

For DF, the harvested energy at the first relay can be derived from (8.209) as

$$E_{h1} = \eta P_0 a_1^2 \alpha_1 T. \tag{8.212}$$

Similarly, the harvested energy at the second relay can be derived from (8.210) as

$$E_{h2} = \eta P_1 a_2^2 \alpha_2 T \tag{8.213}$$

and the harvested energy at the mth relay can be derived from (8.211) as

$$E_{hm} = \eta P_{m-1} a_m^2 \alpha_m T. \tag{8.214}$$

Using them, the transmission powers at the first relay, the second relay, and the mth relay, respectively, can be derived as Mao et al. 2015

$$P_1 = \frac{E_{h1}}{T} = \eta P_0 a_1^2 \alpha_1 \tag{8.215a}$$

$$P_2 = \frac{E_{h2}}{T} = \eta P_1 a_2^2 \alpha_2 \tag{8.215b}$$

$$P_m = \frac{E_{hm}}{T} = \eta P_{m-1} a_m^2 \alpha_m. \tag{8.215c}$$

Again, these relationships are recurrent.

Comparing AF with DF, one sees that their energies harvested at the first relay are the same. For the second relay, $E_{h2} = \eta a_2^2 \alpha_2 E_{h1}$ for DF and $E_{h2} = g_1^2 P_0 a_1^2 \eta a_2^2 \alpha_2 E_{h1}$ for AF. Thus, for fixed-gain AF with $g_1 = 1$, the harvested energy for AF is $10\log_{10}(P_0 a_1^2)$ dB more than the harvested energy for DF, implying that fixed-gain AF in this case could support more hops than DF due to more harvested energy. On the other hand, for variable-gain AF with $g_1 = \frac{1}{\sqrt{P_0 a_1^2 + \sigma_{1c}^2 + \sigma_{1a}^2}}$, the harvested energies of AF and DF are almost identical when the SNR of the initial received signal is large such that $P_0 a_1^2 >> \sigma_{1c}^2 + \sigma_{1a}^2$.

Similarly, using the throughput criterion, one has

$$R_0 = \log_2(1 + \gamma_m)(1 - \alpha_m) \tag{8.216}$$

where

$$\gamma_m = \frac{P_{m-1} a_m^2 (1 - \alpha_m) T}{\sigma_{ma}^2 + \sigma_{mc}^2} \tag{8.217}$$

and $m = 1, 2, \cdots$ is the hop index. The TS coefficient α_m can be calculated as Mao et al. 2015

$$\alpha_m = 1 - \frac{(2^{R_0/(1-\alpha_m)} - 1)(\sigma_{ma}^2 + \sigma_{mc}^2)}{P_{m-1} a_m^2 T} \tag{8.218}$$

for the mth relay, until the throughput drops below the threshold as $\log_2(1 + \gamma_m)(1 - \alpha_m) < R_0$, for which the value of m is determined as the largest number of hops supported by the initial energy of E_0.

8.7.2.2 Power Splitting

In the PS method, the relay splits a portion of the received signal power as harvested energy. Denote ρ_m as the splitting factor at the mth relay, with $0 \le \rho_m \le 1$ and $m = 1, 2, \cdots$.

Consider AF first. In this case, the parts of the received signals at the first relay, the second relay, and the mth relay for relaying are given by

$$y_1 = \sqrt{(1 - \rho_1) P_0} a_1 s + \sqrt{1 - \rho_1} n_{1a} + n_{1c} \tag{8.219}$$

$$y_2 = \sqrt{(1 - \rho_2) P_1} g_1 a_2 y_1 + \sqrt{1 - \rho_2} n_{2a} + n_{2c} \tag{8.220}$$

$$\vdots$$

$$y_m = \sqrt{(1 - \rho_m) P_{m-1}} g_{m-1} a_m y_{m-1} + \sqrt{1 - \rho_m} n_{ma} + n_{mc}, \tag{8.221}$$

respectively, for T seconds, where all the symbols are defined as before. Using them, the signal at the mth relay to be relayed is derived as

$$y_m = \prod_{i=0}^{m-1} \sqrt{(1-\rho_{i+1})P_i} \prod_{i=1}^{m} a_i \prod_{i=1}^{m-1} g_i s + \sum_{i=1}^{m} \left[\prod_{j=i}^{m-1} \sqrt{(1-\rho_{j+1})P_j} \cdot \prod_{j=i+1}^{m} a_i \prod_{j=i}^{m-1} g_j((1-\rho_i)n_{ia} + n_{ic}) \right]. \tag{8.222}$$

The same received signals are also used for energy harvesting. Using the harvested energies, the transmission powers at the first relay, the second relay, and the mth relay, respectively, can be calculated as Mao et al. 2015

$$P_1 = \eta P_0 a_1^2 \rho_1 \tag{8.223a}$$

$$P_2 = \eta P_0 P_1 g_1^2 a_1^2 a_2^2 (1-\rho_1)\rho_2 \tag{8.223b}$$

$$P_m = \eta \prod_{i=0}^{m-1} P_i \prod_{i=1}^{m-1} g_i^2 \prod_{i=1}^{m} a_i^2 \prod_{i=1}^{m-1} (1-\rho_i)\rho_m. \tag{8.223c}$$

Comparing these results with those for the TS method, one sees that the harvested power in PS has an additional term of $\prod_{i=1}^{m-1}(1-\rho_i)$. Since this term is smaller than 1 and decreases quickly as m increases, the harvested power using the PS method is much smaller than that using the TS method, under similar conditions. As a result, the largest number of hops using the PS method is much smaller than that using the TS method, which is not desirable for network coverage extension.

Again, applying the throughput per hop restriction, one has

$$R_0 = \log_2(1+\gamma_m) \tag{8.224}$$

where

$$\gamma_m = \frac{\prod_{i=0}^{m-1}(1-\rho_{i+1})P_i \prod_{i=1}^{m} a_i^2 \prod_{i=1}^{m-1} g_i^2 T}{U} \tag{8.225}$$

where $U = \sum_{i=1}^{m}[\prod_{j=i}^{m-1}\sqrt{(1-\rho_{j+1})P_j}\prod_{j=i+1}^{m} a_i^2 \prod_{j=i}^{m-1} g_j^2((1-\rho_i)\sigma_{ia}^2 + \sigma_{ic}^2)]$. The PS splitting factor ρ_m can be calculated as Mao et al. 2015

$$\rho_m = 1 - \frac{(2^{R_0}-1)\sigma_{mc}^2}{\prod_{i=0}^{m-1}(1-\rho_{i+1})P_i \prod_{i=1}^{m} a_i^2 \prod_{i=1}^{m-1} g_i^2 T - W} \tag{8.226}$$

where

$$W = \left\{ \sum_{i=1}^{m-1} \left[\prod_{j=i}^{m-1} \sqrt{(1-\rho_{j+1})P_j} \prod_{j=i+1}^{m} a_i^2 \prod_{j=i}^{m-1} g_j^2((1-\rho_i)\sigma_{ia}^2 + \sigma_{ic}^2) \right] + \sigma_{ma}^2 \right\} (2^{R_0}-1). \tag{8.227}$$

Unlike the TS coefficient α_m, the PS splitting factor ρ_m does have a closed-form expression. However, note that the calculation of ρ_m requires knowledge of $\rho_{m-1}, \cdots, \rho_1$. Thus, this is essentially a recurrence relationship.

For DF, the received signals at the first relay, the second relay, and the mth relay for relaying can be expressed as

$$y_1 = \sqrt{(1-\rho_1)P_0}a_1 s + \sqrt{1-\rho_1}n_{1a} + n_{1c} \tag{8.228}$$

$$y_2 = \sqrt{(1-\rho_2)P_1}a_2 s_1 + \sqrt{1-\rho_2}n_{2a} + n_{2c} \tag{8.229}$$

$$\vdots$$

$$y_m = \sqrt{(1-\rho_m)P_{m-1}}a_m s_{m-1} + \sqrt{1-\rho_m}n_{ma} + n_{mc}, \tag{8.230}$$

respectively, for the whole relaying period T seconds, where all the symbols are defined as before.

Parts of the received signals are also used for energy harvesting. Using the PS method, the transmission powers at the first relay, the second relay, and the mth relay, respectively, can be calculated as Mao et al. 2015

$$P_1 = \eta P_0 a_1^2 \rho_1 \tag{8.231a}$$

$$P_2 = \eta \rho_2 P_1 a_2^2 \tag{8.231b}$$

$$P_m = \eta \rho_m P_{m-1} a_m^2. \tag{8.231c}$$

These values can also be calculated recursively. Then, applying the throughput restriction to each hop, one has

$$R_0 = \log_2(1+\gamma_m) \tag{8.232}$$

where

$$\gamma_m = \frac{(1-\rho_m)P_{m-1}a_m^2 T}{(1-\rho_m)\sigma_{ma}^2 + \sigma_{mc}^2} \tag{8.233}$$

and $m = 1, 2, \cdots$ is the hop index. Using this restriction, the PS splitting factor ρ_m can be calculated as Mao et al. 2015

$$\rho_m = 1 - \frac{(2^{R_0}-1)\sigma_{mc}^2}{P_{m-1}a_m^2 T - \sigma_{ma}^2(2^{R_0}-1)}. \tag{8.234}$$

To summarize, the calculation of the largest number of hops is performed as in the following. For TS, α_m is first calculated, and then P_m and the throughput are calculated for $m = 1, 2, \cdots$. Once the throughput is less than R_0, the calculation stops and the value of m in the previous iteration is decided as the largest number of hops. In the case of PS, ρ_m is first calculated, followed by P_m, both of which will be used to calculate the throughput to find the first value of m that makes the throughput below R_0, for $m = 1, 2, \cdots$.

8.7.2.3 Numerical Examples

In this section, numerical examples will be presented to show the dependence of the largest number of hops on different relaying protocols, different harvesting strategies as well as different system parameters. To do this, in the calculations, the parameters are set as $\sigma_{ma}^2 = \sigma_{mc}^2 = 0.01$ for $m = 1, 2, \cdots$, $a_m^2 = 0.1$ for $m = 1, 2, \cdots$, and $T = 1$. Also, let $\gamma_0 = \frac{a_1^2 P_0 T}{\sigma_{1c}^2 + \sigma_{1a}^2}$ be the initial SNR in the first relay, which is directly related to the initial amount of energy $P_0 T$ from the source node. The effects of R_0, η, and γ_0 are examined.

Tables 8.2–8.6 show the obtained largest numbers of hops in different conditions for different relaying protocols and harvesting strategies. Several observations can be made from these tables.

First, under the same conditions, the value of the largest number of hops generally increases when the initial SNR γ_0 and the conversion efficiency η increase or when the throughput requirement R_0 decreases. This means that one may extend the network coverage by either increasing the amount of energy transferred from the source node and subsequently harvested by all relaying nodes, or improving the efficiency of the energy harvester or reducing the performance requirement. This is expected. Among the three parameters examined, one can also see that the initial SNR γ_0 has the largest impact on the network coverage extension. For example, in Table 8.2, the largest number of hops could have an increase of 5 hops from 2 hops to 7 hops, when γ_0 increases from 10 dB to 30 dB, while for η and R_0, the maximum increase is between 0 and 2 hops when η increases or R_0 decreases. In all the cases, the change of η from 0.3 to 0.5 leads to an increase of 1 hop at most, when $\gamma_0 \leq 25$ dB, indicating that it may not be worth

Table 8.2 The largest number of hops for fixed-gain AF with TS.

	γ_0				
(R_0, η)	**10 dB**	**15 dB**	**20 dB**	**25 dB**	**30 dB**
(1,0.3)	2	2	3	4	5
(1,0.5)	2	2	3	4	7
(2,0.3)	2	2	3	2	4
(2,0.5)	2	2	3	2	6

Table 8.3 The largest number of hops for variable-gain AF with TS.

	γ_0				
(R_0, η)	**10 dB**	**15 dB**	**20 dB**	**25 dB**	**30 dB**
(1,0.3)	2	2	3	3	3
(1,0.5)	2	3	3	3	4
(2,0.3)	2	2	2	3	3
(2,0.5)	2	2	2	3	3

Table 8.4 The largest number of hops for DF with TS.

	γ_0				
(R_0, η)	**10 dB**	**15 dB**	**20 dB**	**25 dB**	**30 dB**
(1,0.3)	2	2	3	3	3
(1,0.5)	2	3	3	3	4
(2,0.3)	2	2	2	3	3
(2,0.5)	2	2	3	3	3

Table 8.5 The largest number of hops for variable-gain or fixed-gain AF with PS.

	γ_0				
(R_0, η)	10 dB	15 dB	20 dB	25 dB	30 dB
(1,0.3)	1	1	1	1	1
(1,0.5)	1	1	1	1	1
(2,0.3)	1	1	1	1	1
(2,0.5)	1	1	1	1	1

Table 8.6 The largest number of hops for DF with PS.

	γ_0				
(R_0, η)	10 dB	15 dB	20 dB	25 dB	30 dB
(1,0.3)	1	1	2	2	2
(1,0.5)	1	2	2	2	3
(2,0.3)	1	1	1	2	2
(2,0.5)	1	1	2	2	2

improving the design of the energy harvester to extend network coverage when the initial amount of energy is low to medium. This is important, as improvement of the energy harvester often requires a considerable amount of time and effort.

Secondly, comparing different relaying protocols, one sees that fixed-gain AF relaying has the largest numbers of hops when the TS method is used. In this case, variable-gain AF relaying and DF have very similar performances. The reason for this is that fixed-gain AF relaying leads to more harvested energies at the relays and therefore can be transferred for more times or more hops while variable-gain AF and DF have similar harvested energies for large SNRs. When the PS method is used, DF relaying has the largest numbers of hops, while variable-gain relaying and fixed-gain AF relaying have similar performances. This can be explained by comparing the harvested power of AF and DF, where one sees that the harvested power of AF is much smaller than that of DF due to the extra term of $\prod_{i=1}^{m-1}(1-\rho_i)$ in the product and thus, the energy transferred from the source node can be exhausted quickly in AF relaying.

Thirdly, comparing the TS method with the PS method, one sees that the TS method can achieve many more hops than the PS method, under similar conditions. This is especially true for AF relaying, where the largest number of hops drops from 7 in Table 8.2 to 1 in Table 8.5, under the same other conditions. This is explained as follows: for the TS method in AF relaying, the powers of the signals for harvesting and for relaying are the same, and only the relaying time is switched. Thus, the first relay can choose to take a small amount of time and therefore harvest a small amount of energy (power is fixed during this), conserving the majority of the energy for later use by the following relays. However, for the PS method in AF relaying, the powers of the signals for harvesting and

relaying are different. Even if the first relay chooses to split a small portion of power for relaying and therefore harvest a small amount of energy (time is fixed during this), with the good intention of passing on the majority of energy for later use by the following relays, according to AF relaying, the first relay is in fact only using a large transmission power (conserved for the following relays) to transmit a very weak signal (due to a small portion of power split) to the next relay. This is as undesirable as using a small transmission power (harvesting most energy from the source node at the first relay) to transmit a strong signal (due to a large portion of power split for the first hop). In both situations, the received power at the next relay will be very small, wasting a huge amount of conserved energy. Thus, the PS method is very ineffective for network coverage extension based on harvesting. If one has to use the PS method due to the hardware requirement, from these tables, DF relaying will be a better option than AF relaying.

In summary, the best way of extending the network coverage using multi-hop relaying with energy harvesting is to use fixed-gain AF relaying combined with the TS method, followed by using variable-gain AF or DF relaying with the TS method, and DF relaying with the PS method. One should avoid using AF with PS to extend the network coverage.

To see how the TS coefficient α_m and the PS splitting factor ρ_m vary with the hop number Figure 8.36 shows them for the case when $\gamma_0 = 30$ dB, $R_0 = 2$, and $\eta = 0.3$. For the PS method, one sees that the splitting factor ρ_1 of the AF relaying is very close to 1, in fact around 0.99, trying to save as much energy as possible for later use in the following hops. However, due to the small splitting factor, the received power at the second relay is scaled down by $1 - \rho_1 \approx 0.01$, leading to a huge loss of energy in effect. Thus, AF relaying combined with PS is not suitable for multi-hop relaying with energy

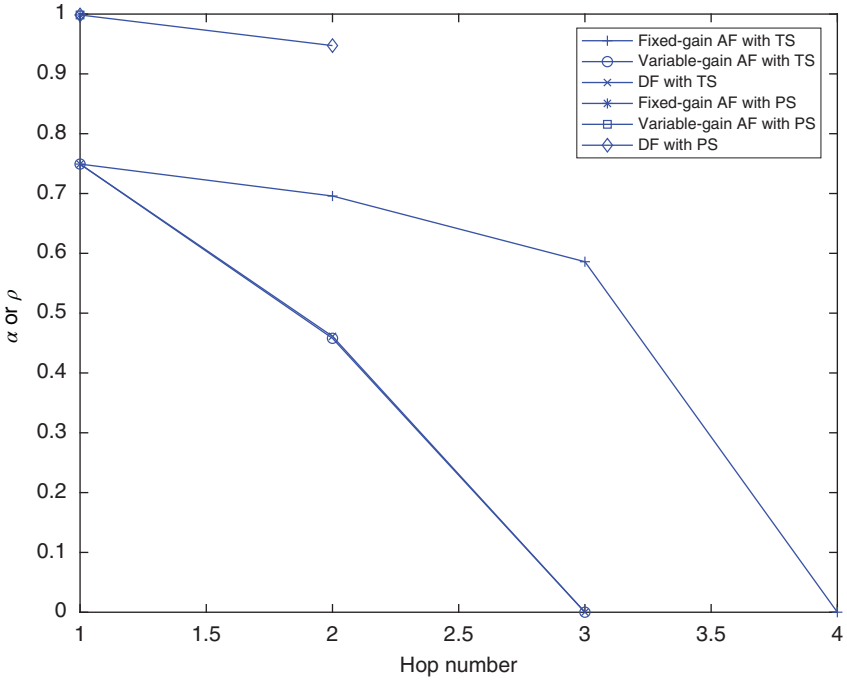

Figure 8.36 The values of α or ρ versus hop number when $\gamma_0 = 30$ dB, $R_0 = 2$, and $\eta = 0.3$.

harvesting. For variable-gain AF relaying and DF relaying, their TS coefficients at the three hops, α_1, α_2 and α_3, are almost identical, which agrees with observations from the tables. For fixed-gain AF relaying, α_1 is around 0.75, α_2 is around 0.7, α_3 is around 0.6, and α_4 is around 0, which decrease at an accelerated rate. In all the TS curves, the TS coefficient goes to 0 when the hop number increases, implying the last hop where all energies should be used for relaying without any energy harvesting to meet the throughput requirement at this hop.

The transmitted power at the first relay (the one after the source node) P_1 is an important indicator of how power decays during energy harvesting relaying, by comparing it with the initial transmitted power of $P_0 = \gamma_0 * (\sigma_{1c}^2 + \sigma_{1a}^2)/a_1^2$ at the source node. Figures 8.37–8.39 show the calculated P_1 versus γ_0 for different values of η and R_0 using the TS method. One sees that P_1 for fixed-gain and variable-gain AF and P_1 for DF using the TS method are identical. This can also be seen from the expressions of those P_1. For each figure, the value of P_1 increases dramatically when γ_0 increases, and in fact γ_0 has the largest impact on P_1. In these figures, η also has a larger impact on P_1 than R_0. At $\gamma_0 = 30$ dB, the initial transmitted power is $P_0 = 200$ and the transmitted power at the first relay is $P_1 = 8.5$. Thus, power decays quickly during relaying and harvesting.

Figure 8.40 shows P_1 versus γ_0 for different values of η and R_0 using fixed-gain AF with PS. Again, P_1 for fixed-gain and variable-gain AF and P_1 for DF using the PS method are identical, as predicted by the derived expressions of P_1, so that P_1 for variable-gain AF and DF are not shown here. From Figure 8.40, the value of P_1 again increases dramatically when γ_0 increases, and in fact γ_0 has the largest impact on P_1. In this case, η also

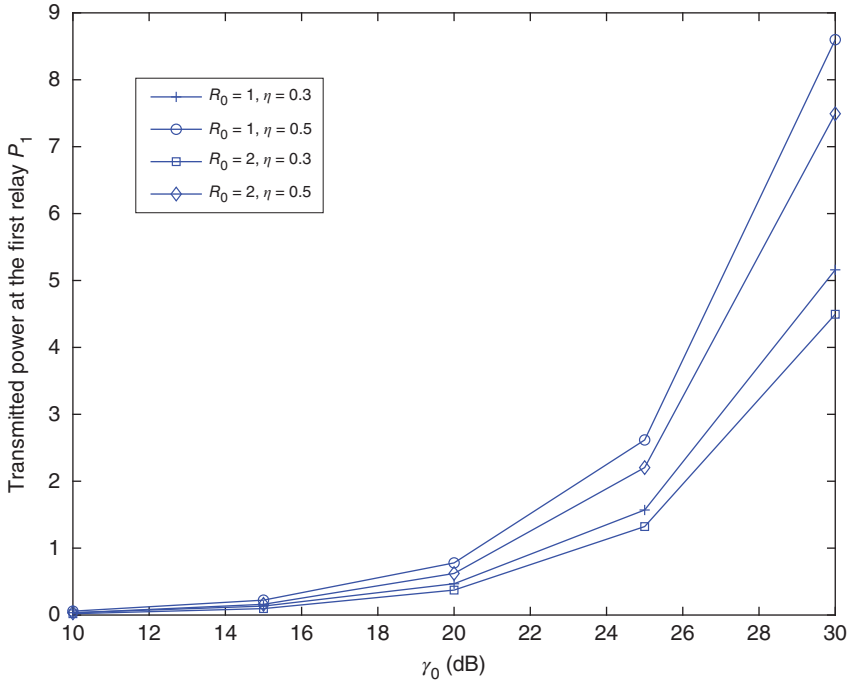

Figure 8.37 P_1 for different values of γ_0, R_0 and η for fixed-gain AF with TS.

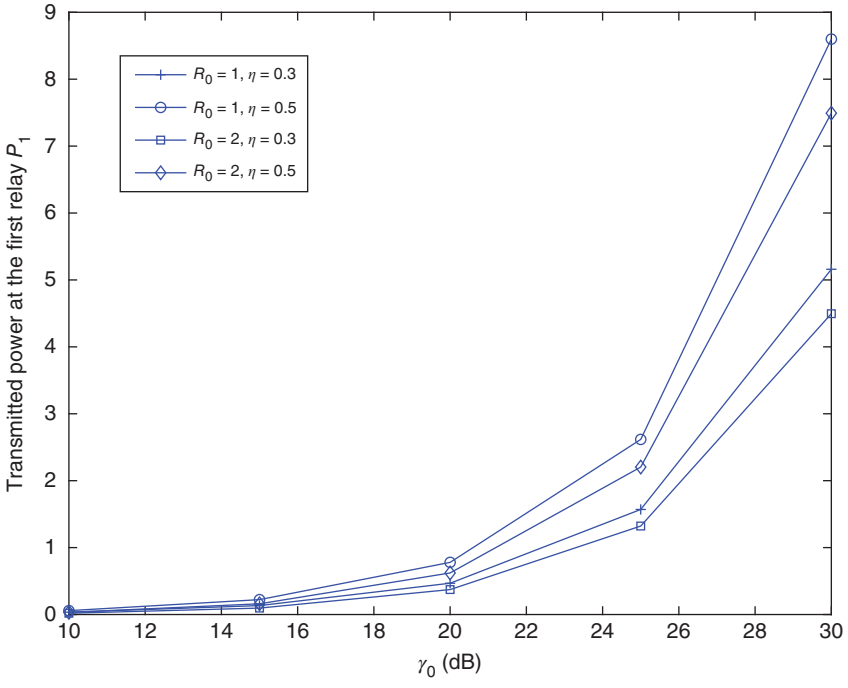

Figure 8.38 P_1 for different values of γ_0, R_0 and η for variable-gain AF with TS.

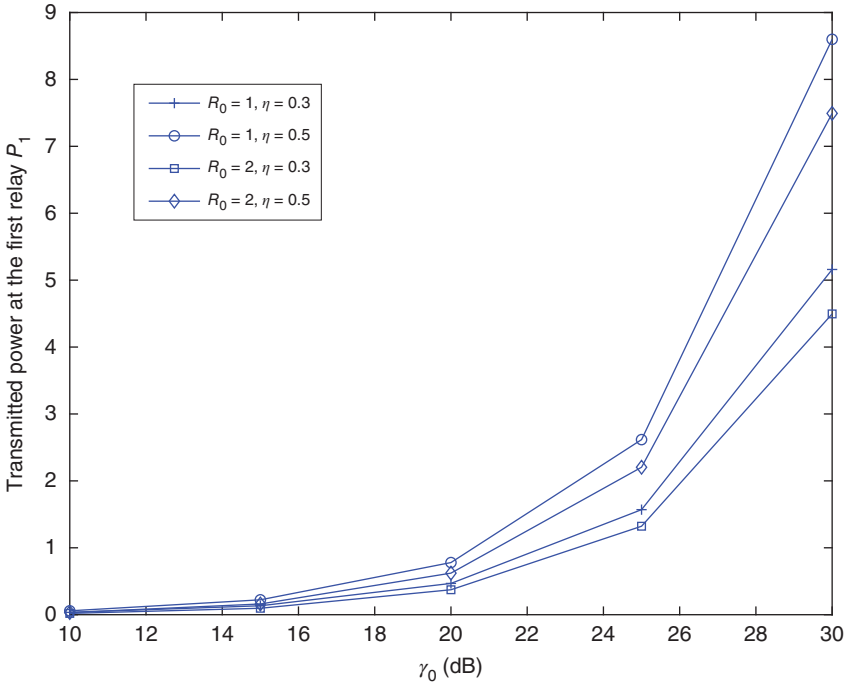

Figure 8.39 P_1 for different values of γ_0, R_0 and η for DF with TS.

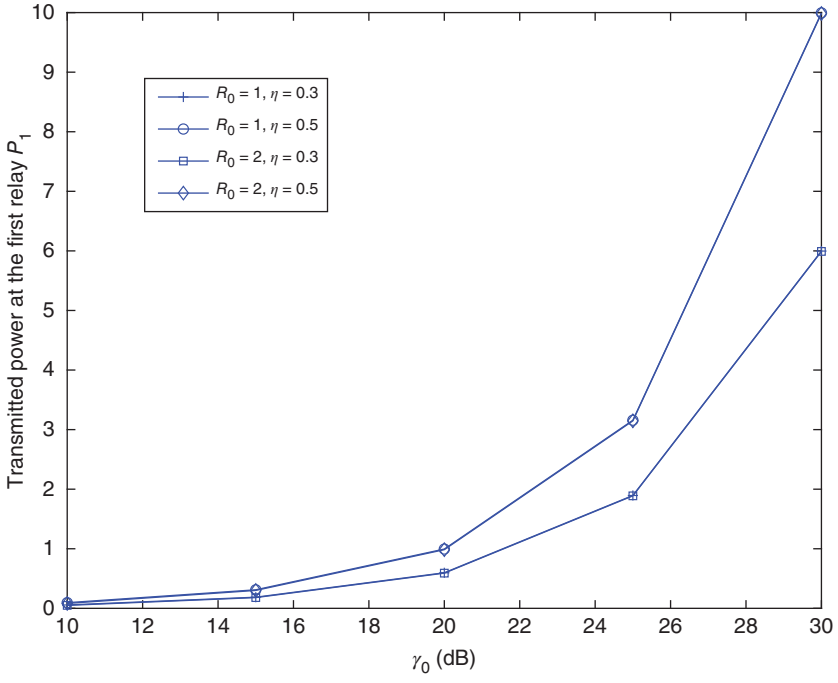

Figure 8.40 P_1 for different values of γ_0, R_0 and η for fixed-gain AF with PS.

has a large impact on P_1. However, the value of R_0 has little impact on P_1, implying that the throughput requirement does not change the received power in the first relay.

Figures 8.41 and 8.42 show α_1 and ρ_1 versus γ_0 for different values of R_0 and η, respectively, for fixed-gain AF. In general, the values of α_1 and ρ_1 increase when the value of γ_0 increases, indicating that more energy will be harvested and transferred to the next hop than is used at the first hop for relaying or decoding, as expected, as once the throughput requirement is met, the first relay should pass on all the remaining energy that increases with γ_0 to the next hop for extended coverage. Interestingly, in this case, the value of η has little impact on α_1 or ρ_1. Comparing Figure 8.41 with Figure 8.42, one sees that the PS factor ρ_1 is relatively high, ranging from 0.82 to nearly 1 in these cases, while the TS coefficient α_1 is relatively low, ranging from 0.32 and 0.86 in these cases. Thus, the PS method harvests more energy at the first relay than the TS method, in the cases considered. Similar graphs for variable-gain AF and DF can also be obtained. They are omitted here.

Figure 8.43 shows how the values of α_m and ρ_m change with m. They decay very quickly and become zero when $m = 3$. Figure 8.44 shows the largest number of hops versus γ_0, where $2\sigma_{ma}^2 = 2\sigma_{md}^2 = 0.01$ and $|g_m|^2 = 0.1$. Also, $\gamma_0 = \frac{|g_1|^2 P_s T}{2\sigma_{1d}^2 + 2\sigma_{1a}^2}$ is the initial SNR, which is directly related to the initial amount of energy $P_s T$ from the source node. For PS, this number is always 1, meaning that PS is not suitable for such multi-hop relaying. For TS, the number increases with γ_0, as expected, as more initial energy allows the signal to go further. This can be explained. For TS in AF, the power for harvesting and for forwarding is the same. Only the time is switched. Thus, the first relay can spend a small amount of

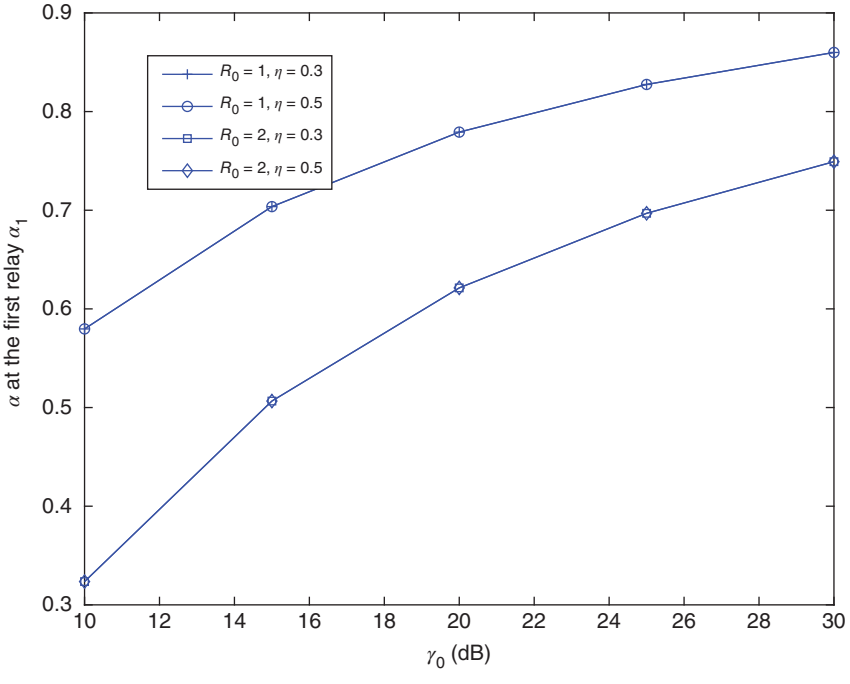

Figure 8.41 α_1 for different values of γ_0, R_0 and η for fixed-gain AF with TS.

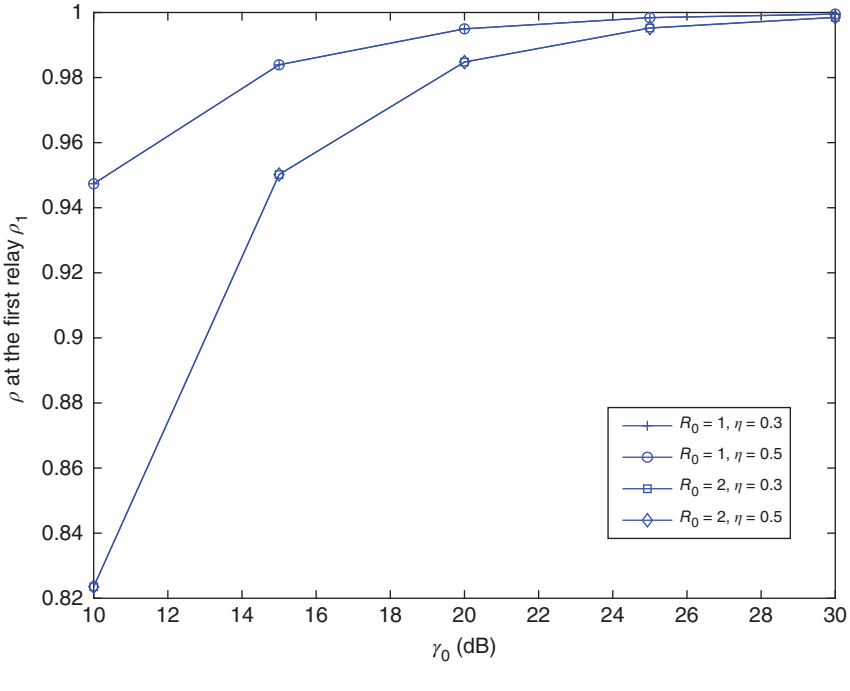

Figure 8.42 ρ_1 for different values of γ_0, R_0 and η for fixed-gain AF with PS.

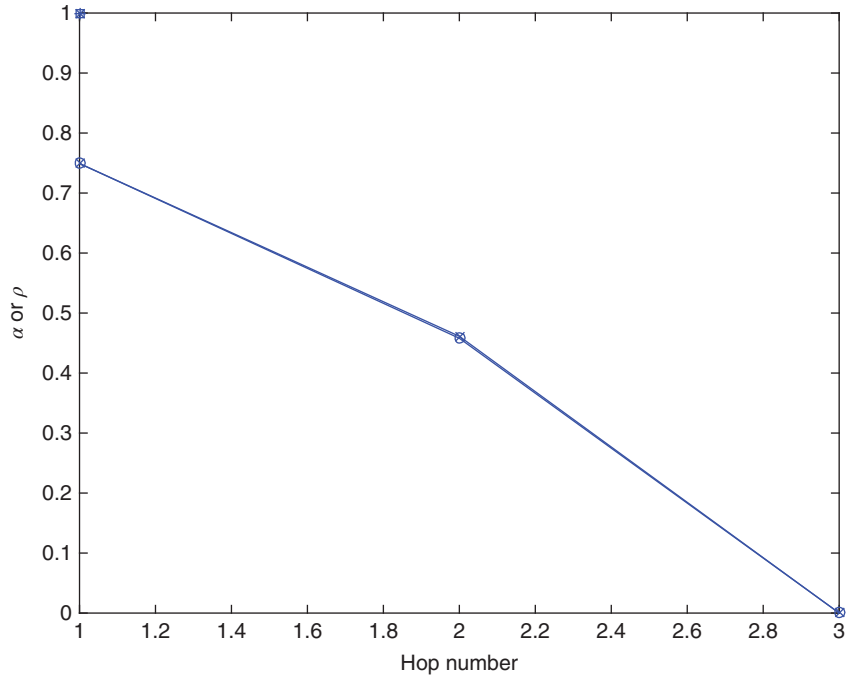

Figure 8.43 Values of α or ρ versus hop number.

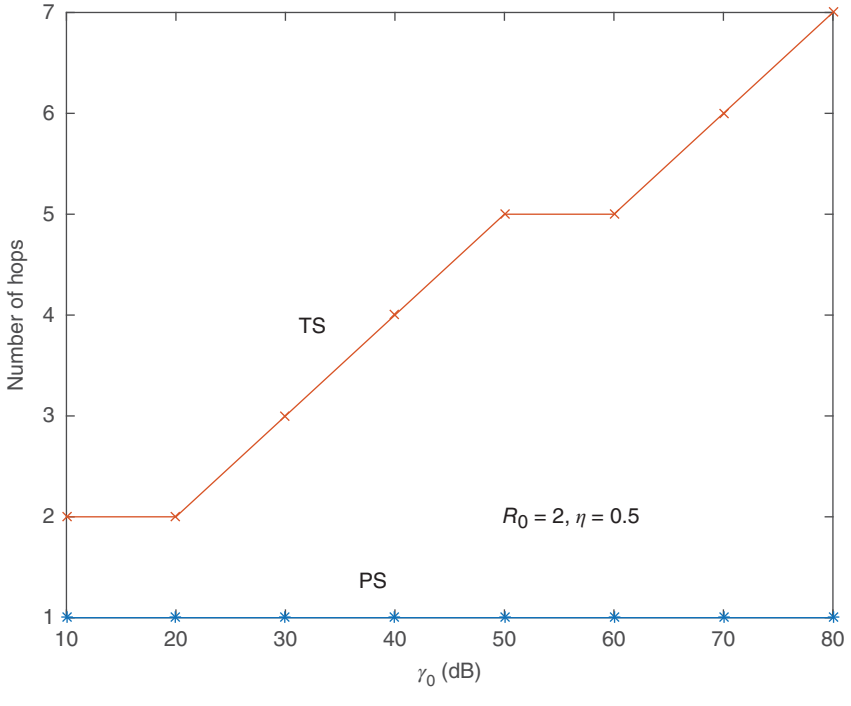

Figure 8.44 Largest number of hops versus γ_0.

time to harvest a small amount of energy (power is fixed in this case), leaving the rest of the energy for harvesting in the following hops. However, for PS in AF, the power for harvesting and forwarding are different. If the first relay splits a small portion of power to harvest a small amount of energy (time is fixed in this case), a strong signal will be forwarded but with weak power. If the first relay splits a large portion for harvesting, a weak signal will be forwarded but with strong power. In both cases, the received signal at the next relay will be very weak. Thus, PS is very ineffective for network coverage extension using energy harvesting.

8.7.3 Others

There are other important issues in energy harvesting relaying. For example, in the above, we have only considered the half-duplex mode. This is a typical operational mode for wireless devices. However, full-duplex has also received a lot of research interest recently. For example, in Zhong et al. (2014), full-duplex relaying was considered. In this study, the relay transmits the signal to the destination at the same time as the source transmits the signal to the relay. Thus, the received signal at the full-duplex relay contains the signal from the source as well as the interference caused by its own transmission. This interference can be partly canceled, as the relay knows its transmitted information. Zhong et al. (2014) then evaluated the performance of this full-duplex relaying system. In Zeng and Zhang (2015a) the source node transmits information to the relay in the first phase. In the second phase, the source transfers power to the relay while the relay forwards the signal to the destination and performs energy harvesting at the same time. Thus, the relay is able to harvest its own transmitted signal. This is called self-energy recycling. In all these radios, to enable transmission and reception at the same time, multiple antennas with different purposes are often used.

Also, we have only considered the use of multiple relays to form a multi-hop link for range extension. Another typical use of multiple relays is virtual antennas that can form multiple dual-hop links for diversity gain. In this case, relay selection can be performed for a simple structure, as discussed in Section 8.2.5. However, relay selection in energy harvesting relaying is slightly different from that in conventional relaying. In energy harvesting relaying, one may use the maximum harvested energy as the selection criterion to maximize the harvested energy at the relay, while conventional relaying normally maximizes the end-to-end or hop SNR. For example, in Michalopoulos et al. (2015), the maximum energy and the maximum SNR criteria were considered in a tradeoff to select the relay that gives both satisfactory capacity and energy transfer. Multiple antennas can also be used at different nodes to further increase the diversity gain (Ben Khelifa et al. 2016; Ben Khelifa and Alouini 2017b).

Finally, the relays considered so far always have fixed locations. Consequently, we have always included the distance-dependent path loss in the average fading power in the above discussion. Sometimes it is also necessary to express the path loss explicitly, for example, for relay placement designs. In this case, the average fading power can be replaced by $\frac{\Omega}{d^v}$, where Ω is the average fading power used before, d is the distance between two nodes, and v is the path loss exponent. In other cases, the nodes could be in motion so that their locations become random. The random location leads to random power loss in the relaying, which could degrade the relaying and harvesting

performance. Ding et al. (2014) evaluated the effect of random location on the relaying performance. These studies require stochastic geometry theories.

8.8 Summary

In this chapter, energy harvesting relaying has been discussed in detail. First, background knowledge in conventional relaying has been introduced. Then, different types of energy harvesting relaying systems have been studied. In particular, we have focused on three important systems where the nodes harvest energy from the ambient environment, from the dedicated power transmitter, as well as systems where the relay harvests energy from the source. Following this, we have examined several important issues in energy harvesting relaying, including interference and multi-hop relaying.

Compared with conventional relaying, energy harvesting relaying is restricted by its energy supply, similar to the designs discussed in Chapter 6, Chapter 7, and other chapters. Thus, most design problems in energy harvesting relaying are related to the restricted energy. In systems where both source and relay harvest energy from the ambient environment, this is reflected by the energy arrival process or the energy causality. In systems where both source and relay harvest energy from the dedicated power transmitter or from each other in the system, this is reflected by the constrained transmission time or transmission power. In these systems, the optimum designs often maximize the achievable rate with respect to these energy, time or power parameters. Based on these designs, one can easily obtain solutions to similar problems where different nodes harvest energy from difference sources, as they can be considered as variants of the problems discussed in this chapter.

Compared with other energy harvesting communications systems, energy harvesting relaying requires at least three nodes and two transmission phases. The connection from one phase to the next phase can then be a problem, as the signal must appear in the first phase before it appears in the second phase. Hence, we have the signal or data causality. Also, the two-hop or multi-hop structures make the design problems more complicated than those in the conventional one-hop structure.

In conclusion, for energy harvesting relaying, the increased number of nodes and the increased number of hops lead to more design problems and make each of the design problems more complicated, but as a promising solution to the energy supply at the relaying node, energy harvesting relaying is seeing more and more applications.